REPORT DOCUMENTATION PAGE

Form Approved
OMB No. 074-0188

1. AGENCY USE ONLY (Leave blank)	2. REPORT DATE	3. REPORT TYPE AND DATES COVERED
	August 2003	Annual (Aug 1, 2002 - Jul 31, 2003)

4. TITLE AND SUBTITLE
Protein Kinase Pathways that Regulate Neuronal Survival and Death

5. FUNDING NUMBERS
DAMD17-99-1-9481

6. AUTHOR(S)
Kim A. Heidenreich, Ph.D.

7. PERFORMING ORGANIZATION NAME(S) AND ADDRESS(ES)
University of Colorado Health Sciences Center
Denver, CO 80291-0238

E-Mail: Kim.heidenreich@uchsc.edu

8. PERFORMING ORGANIZATION REPORT NUMBER

9. SPONSORING / MONITORING AGENCY NAME(S) AND ADDRESS(ES)
U.S. Army Medical Research and Materiel Command
Fort Detrick, Maryland 21702-5012

10. SPONSORING / MONITORING AGENCY REPORT NUMBER

11. SUPPLEMENTARY NOTES
Original contains color plates: ALL DTIC reproductions will be in black and white

12a. DISTRIBUTION / AVAILABILITY STATEMENT
Approved for Public Release; Distribution Unlimited

12b. DISTRIBUTION CODE

13. ABSTRACT (Maximum 200 Words)

Loss of post-mitotic neurons from the adult brain underlies the pathology of neurodegenerative diseases and neurotoxin exposure. Neuronal cell death occurs by two mechanisms: necrosis and apoptosis. Apoptosis is a process whereby developmental cues and environmental stimuli activate a genetic program to implement a series of steps that culminate in cell death. An important aspect of apoptosis is that it can be halted and such interventions may rescue dying neurons. The overall goal of this project is to identify key protein kinases involved in regulating neuronal survival and apoptosis. The aims for the this year of funding as described in the Statement of Work were to: 1) Continue studies on protein kinase cascades that regulate neuronal survival, 2) Modulate the protein kinase cascades regulated by neurotrophic factors and determine the consequence on neuronal survival and death, and 3) Begin studies examining the cross-talk in pro-apoptotic and anti-apoptotic protein kinase signaling cascades. The progress made in these areas has resulted in 4 published manuscripts (plus 2 submitted articles) and 9 abstracts presented at national and international scientific meetings in 2002.

14. SUBJECT TERMS	15. NUMBER OF PAGES
Neurodegeneration, apoptosis, neurons, MEF2, IGF-I, lithium, death receptors, Bim, intrinsic death pathway	82
	16. PRICE CODE

17. SECURITY CLASSIFICATION OF REPORT	18. SECURITY CLASSIFICATION OF THIS PAGE	19. SECURITY CLASSIFICATION OF ABSTRACT	20. LIMITATION OF ABSTRACT
Unclassified	Unclassified	Unclassified	Unlimited

AD_____

Award Number: DAMD17-99-1-9481

TITLE: Protein Kinase Pathways that Regulate Neuronal Survival and Death

PRINCIPAL INVESTIGATOR: Kim A. Heidenreich, Ph.D.

CONTRACTING ORGANIZATION: University of Colorado Health Sciences Center
Denver, Co 80291-0238

REPORT DATE: August 2003

TYPE OF REPORT: Annual

PREPARED FOR: U.S. Army Medical Research and Materiel Command
Fort Detrick, Maryland 21702-5012

Table of Contents

Introduction

Loss of post-mitotic neurons from the adult brain underlies the pathology of neurodegenerative diseases and neurotoxin exposure. Neuronal cell death occurs by two mechanisms: necrosis and apoptosis. Apoptosis is a process whereby developmental cues and environmental stimuli activate a genetic program to implement a series of steps that culminate in cell death. An important aspect of apoptosis is that it can be halted and such interventions may rescue dying neurons. The overall goal of this project is to identify key protein kinases involved in regulating neuronal survival and apoptosis. The aims for the this year of funding as described in the Statement of Work were to: 1) Continue studies on protein kinase cascades that regulate neuronal survival, 2) Modulate the protein kinase cascades regulated by neurotrophic factors and determine the consequence on neuronal survival and death, and 3) Begin studies examining the cross-talk in pro-apoptotic and anti-apoptotic protein kinase signaling cascades. The progress made in these areas, described below, has resulted in 6 published manuscripts, 1 invited chapter, and 16 abstracts presented at national and international scientific meetings.

Task #1. The first task is to identify protein kinase cascades that regulate neuronal survival.

Our previous identified MEF2 as a transcription factor downstream of a depolarization-dependent, calcium-regulated pathway that controls neuronal survival. During this progress report period, we completed a study aimed at determining whether the protein kinase GSK-3b regulates MEF2 in apoptotic neurons. To investigate a potential role for GSK-3b in MEF2D phosphorylation, we examined the effects of lithium, an uncompetitive inhibitor of GSK-3b, on MEF2D in granule neurons induced to undergo apoptosis. Lithium inhibited caspase-3 activation and DNA condensation and fragmentation induced by removal of depolarizing potassium and serum. Lithium suppressed the hyperphosphorylation and caspase-mediated degradation of MEF2D. Moreover, lithium sustained MEF2 DNA binding and transcriptional activity in the absence of depolarization. Unexpectedly, MEF2D hyperphosphorylation was not blocked by either forskolin, insulin-like growth factor-I, or valproate, three mechanistically distinct inhibitors of GSK-3b. These results suggest that lithium targets a novel kinase, different from GSK-3b, that phosphorylates and inhibits the pro-survival function of MEF2D in cerebellar granule neurons. These results were published in the Journal of Neurochemistry (Appendix #1).

The mechanism by which calcium influx regulates MEF2 activity in neurons is complex and involves multiple effector proteins that modulate MEF2 activity. In the last year we demonstrated that depolarization-mediated MEF2 activity and granule neuron survival are compromised by overexpression of the MEF2 transcriptional repressor histone deacetylase-5 (HDAC5). Furthermore, induction of apoptosis by removal of depolarizing extracellular potassium induced rapid cytoplasm-to-nuclear

translocation of endogenous HDAC5. This effect was mimicked by addition of the calcium/calmodulin-dependent protein kinase (CaMK) inhibitor KN93 to depolarizing medium. Removal of depolarization or KN93 addition increased the mobility of HDAC5 on polyacrylamide gels, consistent with its dephosphorylation. Moreover, HDAC5 co-precipitated with MEF2D under these conditions. Induction of HDAC5 nuclear translocation by KN93 resulted in a marked loss of MEF2 transcriptional activity. MEF2 inactivation was followed by caspase-3 activation, microtubule disruption, and chromatin fragmentation. To selectively decrease CaMKII activity, cerebellar granule neurons were incubated with a fluorescein-labeled, phosphorothioate antisense oligonucleotide to CaMKIIa. Antisense to CaMKIIa decreased CaMKIIa protein expression and induced nuclear shuttling of HDAC5 in granule neurons maintained in depolarizing medium. Selectivity of the CaMKIIa antisense was demonstrated by its lack of effect on CaMKIV-mediated cAMP-response element binding protein phosphorylation. Finally, antisense to CaMKIIa induced caspase-3 activation and apoptosis, whereas a missense control oligonucleotide had no effect on neuronal survival. These results indicate that depolarization-mediated calcium influx acts through CaMKII to inhibit function of the MEF2 repressor HDAC5, thereby sustaining high MEF2 activity in cerebellar granule neurons maintained under depolarizing conditions. This work is currently in press in the Journal of Biochemistry (Appendix2).

Task #2 The second task is to determine whether activation or inhibition of the neurotrophin-regulated kinases is necessary or sufficient to influence neuronal survival.

Cerebellar granule neurons depend on insulin-like growth factor-I (IGF-I) for their survival. Studies in the last year have indicated that IGF-I promotes neuronal survival by suppressing key elements of the intrinsic (mitochondrial) death pathway. IGF-I blocked activation of the executioner caspase-3 and the intrinsic initiator caspase-9 in primary cerebellar granule neurons deprived of serum and depolarizing potassium. IGF-I inhibited cytochrome C release from mitochondria and prevented its redistribution to neuronal processes. The effects of IGF-I on cytochrome C release were not mediated by blockade of the mitochondrial permeability transition pore since IGF-I failed to inhibit mitochondrial swelling or depolarization. In contrast, IGF-I blocked induction of the BH3-only Bcl-2 family member, Bim, a mediator of Bax-dependent cytochrome C release. The suppression of Bim expression by IGF-I did not involve inhibition of the c-Jun transcription factor. Instead, IGF-I prevented activation of the forkhead family member, FKHRL1, another transcriptional regulator of Bim. Finally, adenoviral-mediated expression of dominant-negative AKT activated FKHRL1 and induced expression of Bim. These data suggest that IGF-I signaling via AKT promotes survival of cerebellar granule neurons by blocking the FKHRL1-dependent transcription of Bim, a principal effector of the intrinsic death signaling cascade. These results were published in The Journal of Neuroscience (Appendix3).

Recent studies in the lab have revealed that the prosurvival transcription factor MEF2 is another target for IGF-I in cerebellar granule neurons. We have previously reported that the transcription factors MEF2A and MEF2D are hyperphosphorylated and degraded when granule neurons undergo apoptosis. Recent studies in the lab using electrophoretic mobility shift assays (EMSAs) have shown that IGF does not prevent loss of MEF2D DNA binding but does inhibit its degradation. Since degradation of MEF2 proteins appears to be mediated by caspases, fututre studies will examine which caspase(s) is inhibited by IGF-I.

Task #3 The third task is to determine whether there is cross-talk between pro-apoptotic and anti-apoptotic signaling pathways.

In the past year, we have discovered a novel programmed death pathway in Purkinje neurons. Under the same conditions that induce apoptosis of granule neurons, the Purkinje neurons die by a slower programmed mechanism that involves activation of autophagy. We demonstrated that the death process activated in cerebellar Purkinje neurons following trophic factor withdrawal is autophagic by several methods. The abundant cytoplasmic vacuoles that form in degenerating Purkinje neurons stain with lysosensor blue, a pH-sensitive dye that only fluoresces in acidic cellular compartments, and monodansylcadaverine, an autofluorescent drug that specifically accumulates in autophagic vacuoles. Also, in collaboration with Dr. Charleen Chu at the University of Pittsburg, we were able to demonstrate the appearance of multiple-membrane autophagic vacuoles in degenerating Purkinje neurons by transmission electron microscopy. In addition, a method for quantifying the degree of Purkinje neuron vacuolation was developed based on the size distribution of lysosensor-positive Purkinje vacuoles.

We were also able to demonstrate that death receptor signaling is involved in the regulation of Purkinje autophagy and death. Adenoviral dominant-negative FADD infection prevented the death and vacuolation of Purkinje neurons induced by trophic factor withdrawal. The addition of exogenous death ligand, TNFa, was able to induce death and vacuolation in Purkinje neurons. However, we were unable to find evidence implicating TNFa as the mediator of death during trophic factor withdrawal as soluble death receptor-Fc proteins, ligand-neutralizing antibodies and chemical inhibitors of the TNFa synthesis pathway did not increase the survival of Purkinje neurons undergoing trophic factor withdrawal.

The p75 neurotrophin receptor is implicated in mediating many diverse neuronal processes including cell cycle arrest, neurite extension, neuronal survival and neuronal death. p75ntr is highly expressed by Purkinje neurons during development and following axotomy of adult neurons. Nerve growth factor (NGF), one of the neurotrophin ligands for p75ntr is required for proper development and survival of many types of neurons both *in vivo* and *in vitro*, including Purkinje neurons. Since p75ntr is also a member of the death receptor family, we wished to examine if it was involved in the autophagic

death of Purkinje neurons. Exogenous NGF increased survival and decreased vacuolation of Purkinje neurons undergoing trophic factor withdrawal. Conversely, NGF-neutralizing antibodies decreased survival and induced vacuolation of Purkinje neurons. Antisense to p75ntr had two effects on the cells in the culture. In cells maintained in complete media, antisense to p75ntr decreased the survival of both Purkinje and granule neurons. However, the antisense increased survival and delayed the onset of vacuolation of Purkinje neurons following trophic factor withdrawal. These results are consistent with a model in which liganded p75ntr signals survival and unliganded p75ntr may engage an alternate pathway that signals death. These results are in the process of being submitted to Neuron.

KEY RESEARCH ACCOMPLISHMENTS

Our key research accomplishments over the last year lie in several areas. One is identifying protein kinases and phosphatases that regulate transcription factors controlling neuronal survival and death. We have also examined the intrinsic and extrinsic death machinery in cerebellar neurons and the protein kinases that impact on the death process. Perhaps, the most exciting finding over the last year is the discovery that different types of neurons use distinct molecular mechanisms to die. While granule neurons die by a classic apoptotic pathway when deprived of trophic support, Purkinje neurons in the same cultures die by an autophagic pathway. Interestingly, the morphology of autophagic death seen in our cultures closely resembles the morphology of neurons seen in a variety of neurodegenerative diseases postautopsy.

Reportable Outcomes

Manuscripts (2002-2003)

1. Allen, MP, DA Linseman, H Udo, M Xu, B Varnum, ER Kandel, **KA Heidenreich**, and ME Wierman. A novel mechanism for GnRH neuron migration involving Gas6/Ark signaling to p38 MAP kinase. Mol. Cell. Biol. 22 (2): 599-613, 2002.

2. Linseman, DA, ML McClure, RJ Bouchard, TA Laessig, D Brenner, and **KA Heidenreich**. Suppression of death receptor signaling in cerebellar Purkinje neurons protects neighboring granule neurons form apoptosis. J. Biol. Chem 277:24546-24553, 2002.

3. Linseman, DA, RA Phelps, RJ Bouchard, TA Laessig, SS Le, and **KA Heidenreich**. Insulin-like growth factor-I blocks Bim induction and intrinsic death signaling in cerebellar granule neurons. J. Neuroscience 22: 9287-9297, 2002.

4. Allen, MP, M Xu, DA Linseman, JE Pawlowski, GM Bokoch, **KA Heidenreich**, and ME Wierman Adhesion related kinase (ARK) repression of gonadotropin releasing hormone (GnRH) gene expression requires Rac activation of the extracellular signal-regulated kinase (ERK) pathway. J. Biol. Chem. 277: 38133-38140, 2002.

5. Linseman, DA, BJ Cornejo, SS Le, MK Meintzer,, TA Laessig , RJ Bouchard, and **KA Heidenreich.** A novel mechanism for lithium neuroprotection involving suppression of myocyte enhancer factor 2D hyperphosphorylation and degradation. J.Neurochem.. 85: 1488-1499, 2003.

6. **Heidenreich KA**. Molecular Mechanisms of Neuronal Cell Death. In Parkinson's Disease, Annals of the New York Academy of Sciences, vol.991, 237-250, 2003.

7. Linseman, DA, CM Bartley, SS Le, TA Laessig , RJ Bouchard, MK Meintzer, M Li, and **KA Heidenreich.** Inactivation of the MEF2 repressor HDAC5 by endogenous CAMKII promotes depolarization-mediated neuronal survival. J. Biol. Chem., in press.

Abstracts (2002-2003)

1. Linseman, DA, ML McClure, RA Phelps, RJ Bouchard, TA Laessig, SS Le, F Ahmadi, and **KA Heidenreich**. Extrinsic and intrinsic death signaling in cerebellar neuronal apoptosis: the IGF-I connection. 8th International Conference on Neural Transplantation and Repair, Keystone, CO 2002.

2. Jones, SM, MK Meintzer, CR Freed, **KA Heidenreich**, and Zawada, WM. SC68376, a novel inhibitor of p38 MAP kinase rescues rat and human dopaminergic neurons from apoptotic cell death. 8th International Conference on Neural Transplantation and Repair, Keystone, CO 2002

3. Ahmadi, F., S. Doolin, NR Zahniser, MP McGrogan, **KA Heidenreich**, and MW Zawada. Effects of serum withdrawal and MPP+ on the HNT-neurons. 8th International Conference on Neural Transplantation and Repair, Keystone, CO 2002.

4. Linseman, DA, RA Phelps, RJ Bouchard, TA Laessig, SS Le, F Ahmadi, and **KA Heidenreich.** IGF-I inhibits Bim induction and the intrinsic death signaling cascade in cerebellar granule neurons. Keystone Symposium, Mitochondria and Pathogenesis, Copper, CO 2002.

5. McClure, ML, DA Linseman, RJ Bouchard, TA Laessig, FA Ahmadi, and **KA Heidenreich**, Suppression of death receptor signaling in cerebellar Purkinje neurons protects neighboring granule neurons from apoptosis via an IGF-I dependent mechanism. The Endocrine Society's 84th Annual Meeting, 2002.

6. Linseman, DA, RA Phelps, RJ Bouchard, TA Laessig, SS Le, and **KA Heidenreich**. Insulin-like growth factor-I rescues cerebellar granule cerebellar neurons from apoptosis by blocking Bim induction and mitochondrial death signaling. The Endocrine Society's 84th Annual Meeting, 2002.

7. McClure ML, D A Linseman, R Bouchard, T A Laessig, M K Meintzer, S S Le and **K A Heidenreich**. Identification of an autophagic death pathway in cerebellar Purkinje neurons downstream of death receptor signaling.. Society for Neuroscience 2002.

8. Ahmadi, F., DA Linseman, RJ Bouchard, S Jones, CR Freed, **KA Heidenreich**, and MW Zawada. Rotenone induces death of primary dopamine neurons by a caspase-dependent mechanism. Soc. for Neuroscience Annual meeting, 2002.

9. Linseman, DA, CM Bartley, MK Meintzer, SS Le, TA Laessig, RJ Bouchard, and **KA Heidenreich.** Ca2+/Calmodulin-dependent Protein kinase II Promotes Neuronal Survival by Inhibiting HDAC Repression of MED2D. The American Society for Cell Biology, 2002.

10. Linseman, DA, RA Phelps, TA Laessig, MK Meintzer, RJ Bouchard, SS Le, and **KA Heidenreich**. Bim induction and Bax translocation to mitochondria: key events in neuronal apoptosis that are targeted by neurotrophic factors. Keystone Symposium, Molecular mechanisms of Apoptosis, 2003.

11. Linseman DA, RA Phelps, TA Laessig, MK Meintzer, RJ Bouchard, SS Le, and **KA Heidenreich.** IGF-I blocks neuronal apoptosis by inhibiting Bim induction and Bax translocation to mitochondria. Gordon Research Conference, Insulin-like Growth Factors in Physiology and Disease, 2003.

12. Precht, TA, RA Phelps, DA Linseman, BD Butts, RJ Bouchard, SS Le, TA Laessig, and **KA Heidenreich**. Bax translocation to mitochondria is triggered by permeability transition pore opening in cerebellar granule neurons undergoing apoptosis. Society for Neuroscience 2003.

13. Le, SS, RJ Bouchard, TA Laessig, BD Butts, RA Phelps, **KA Heidenreich**, and DA Linseman. Inhibition of Rac GTPase induces Bim and activates a mitochondrial apoptotic casacade in cerebellar granule neurons. Society for Neuroscience 2003.

14. Butts, BD, DA Linseman, TA Precht, RA Phelps, TA Laessig, RJ Bouchard, SS Le, KL Tyler, **KA Heidenreich**. Glygogen synthase kinase –3b promotes Bax translocation to mitochondria during apoptosis of cerebellar granule neurons. Society for Neuroscience 2003.

15. Linseman, DA, CM Bartley, SS Le, TA Laessig, RJ Bouchard, and **KA Heidenreich**. CamKII promotes cerebellar granule cell survival by blocking HDAC repression of MEF2 transcriptional activity. Society for Neuroscience 2003.

16. McClure ML, DA Linseman, CT Chu, RJ Bouchard, TA Laessig, SS Le, and **KA Heidenreich**. Neurotrophins and death receptors regulate autophagic death in cerebellar Purkinje neurons. Society for Neuroscience 2003.

Invited talks

2002	Plenary talk, New York Academy of Science Symposium " PD: Life Cycle of the Dopamine Neuron", Princeton, N.J.
2003	Chairperson and Invited Speaker, Gordon Conference on Insulin-like Growth Factors, Ventura, CA

Conclusions

The scope of research over the last year has been to continue experiments outlined in Task#1, Task#2, and Task #3 of our original research proposal. Towards this goal, we have identified a number protein kinase cascades and effectors that regulate neuronal survival and apoptosis. In cultured rat cerebellar granule neurons, a good model for studying apoptosis in primary differentiated neurons, we have studied various aspects of 2 different pathways that regulate neuronal survival, an IGF-I–regulated protein kinase pathway involving PI-3 kinase and Akt and a Ca++ sensitive pathway regulating the activity of a family of transcription factors (MEF2) that signal survival. We will continue to examine other components of the intrinsic death pathway, i.e. Bax and determine how they interact to promote cell death. Experiments are

also planned to continue studying the regulation of MEF2s in neurons and identify the genes that are transcriptionally modified by this family of transcription factors.

Appendices: 3 MANUSCRIPTS attached
6 ABSTRACTS attached

Journal of Neurochemistry, 2003, **85**, 1488–1499 doi:10.1046/j.1471-4159.2003.01790.x

A myocyte enhancer factor 2D (MEF2D) kinase activated during neuronal apoptosis is a novel target inhibited by lithium

Daniel A. Linseman, Brandon J. Cornejo, Shoshona S. Le, Mary Kay Meintzer, Tracey A. Laessig, Ron J. Bouchard and Kim A. Heidenreich

Department of Pharmacology, University of Colorado Health Sciences Center and the Denver Veterans Affairs Medical Center, Denver, Colorado, USA

Abstract

Depolarization promotes the survival of cerebellar granule neurons via activation of the transcription factor myocyte enhancer factor 2D (MEF2D). Removal of depolarization induces hyperphosphorylation of MEF2D on serine/threonine residues, resulting in its decreased DNA binding and susceptibility to caspases. The subsequent loss of MEF2-dependent gene transcription contributes to the apoptosis of granule neurons. The kinase(s) that phosphorylates MEF2D during apoptosis is currently unknown. The serine/threonine kinase, glycogen synthase kinase-3β (GSK-3β), plays a pro-apoptotic role in granule neurons. To investigate a potential role for GSK-3β in MEF2D phosphorylation, we examined the effects of lithium, a non-competitive inhibitor of GSK-3β, on MEF2D activity in cultured cerebellar granule neurons. Lithium inhibited caspase-3 activation and chromatin condensation in granule neurons induced to undergo apoptosis by removal of depolarizing potassium and serum. Concurrently, lithium suppressed the hyperphosphorylation and caspase-mediated degradation of MEF2D. Moreover, lithium sustained MEF2 DNA binding and transcriptional activity in the absence of depolarization. Lithium also attenuated MEF2D hyperphosphorylation and apoptosis induced by calcineurin inhibition under depolarizing conditions, a GSK-3β-independent model of neuronal death. In contrast to lithium, MEF2D hyperphosphorylation was not inhibited by forskolin, insulin-like growth factor-I, or valproate, three mechanistically distinct inhibitors of GSK-3β. These results demonstrate that the kinase that phosphorylates and inhibits the pro-survival function of MEF2D in cerebellar granule neurons is a novel lithium target distinct from GSK-3β.

Keywords: apoptosis, cerebellar granule neuron, glycogen synthase kinase, lithium, MEF2 transcription factor, phosphorylation.

J. Neurochem. (2003) **85**, 1488–1499.

Apoptosis is a programmed form of cell death executed via the cleavage of critical cellular proteins by the caspase family of cysteine proteases (Shi 2002). Neuronal apoptosis is a highly regulated process that plays a key role in the normal development of the CNS (Nijhawan *et al.* 2000; Roth and D'Sa 2001). Aberrant neuronal apoptosis often occurs during adulthood and is thought to contribute to the development and progression of debilitating neurodegenerative diseases including Alzheimer's, Parkinson's, Huntington's, and Creutzfeldt–Jakob disease (Honig and Rosenberg 2000; Andersen 2001; Kawashima *et al.* 2001). In addition, significant apoptosis of transplanted neural tissue is one of the major impediments to neurotranplantation as a potential treatment for neurodegenerative disease (Schierle *et al.* 1999). Elucidation of the cellular signaling pathways that regulate neuronal survival and apoptosis is necessary to develop useful therapeutics to combat neurodegenerative disorders

Received January 22, 2003; revised manuscript received March 4, 2003; accepted March 5, 2003.

Address correspondence and reprint requests to Dr Kim A. Heidenreich, University of Colorado Health Sciences Center, Department of Pharmacology (C236), 4200 E. Ninth Ave., Denver, CO 80262, USA. E-mail: Kim.Heidenreich@UCHSC.edu

Abbreviations used: BSA, bovine serum albumin; CGN, cerebellar granule neuron; CK-2, casein kinase-2; CREB, cAMP response element binding protein; CyA, cyclosporin A; DAPI, 4,6-diamidino-2-phenylindole; EMSA, electrophoretic mobility shift assay; GSK-3β, glycogen synthase kinase-3β; HMC, high molecular weight protein–DNA complex; IGF-I, insulin-like growth factor-I; LMC, low molecular weight protein–DNA complex; MADS, MCM1-agamous-deficiens-serum response factor; MAPKAPK-2, mitogen-activated protein kinase-activated protein kinase-2; MEF2, myocyte enhancer factor 2; PBS, phosphate-buffered saline; PI3K, phosphatidylinositol 3-kinase; PKA, protein kinase A; PRAK, p38-regulated/activated protein kinase; SDS–PAGE, sodium dodecyl sulfate–polyacrylamide gel electrophoresis; VPA, sodium valproate.

and to enhance the survival of donor neurons following transplantation.

Primary cultures of cerebellar granule neurons (CGNs) isolated from early postnatal rats are a well-characterized *in vitro* model for investigating neuronal apoptosis. CGNs require both serum-derived growth factors and depolarization-mediated calcium influx for their survival and die by apoptosis when deprived of this trophic support (D'Mello *et al.* 1993; Atabay *et al.* 1996). Recently, a transcription-dependent mechanism was identified for the pro-survival effects of depolarization in CGNs. Depolarization activates a calcium-sensitive pathway that enhances the DNA binding and activity of the myocyte enhancer factor 2 (MEF2) transcription factors (Mao *et al.* 1999).

The mammalian MEF2 family is made up of four distinct isoforms (MEF2A, B, C and D) (McKinsey *et al.* 2002). The MEF2 proteins are members of the MADS (MCM1-agamous-deficiens-serum response factor) family of transcription factors (Shore and Sharrocks 1995). MEF2 genes were originally identified in cells of skeletal, cardiac, and smooth muscle lineages and play a key role in the myogenic differentiation of these tissues (Black and Olson 1998). In the CNS, the expression of MEF2 proteins is associated temporally and spatially with the initiation of post-mitotic neuronal maturation (Lyons *et al.* 1995). For example, the maturation of cerebral cortical neurons *in vivo* is associated with an enhanced expression of MEF2C (Leifer *et al.* 1993). Similarly, development and differentiation of the internal granule cell layer of the cerebellum involves the co-ordinated up-regulation of MEF2A and MEF2D (Lin *et al.* 1996). *In vitro* studies further support an essential role for MEF2 proteins in promoting neuronal survival. Transfection of primary cerebral cortical neurons with a dominant-interfering mutant of MEF2C induces apoptosis of these cells, whereas expression of a constitutively active MEF2 mutant significantly attenuates apoptosis of CGNs following removal of depolarizing potassium (Mao *et al.* 1999). Thus, MEF2 proteins are critical for the survival and differentiation of post-mitotic neurons *in vitro* and *in vivo*.

Recently, we identified two specific MEF2 isoforms, MEF2D and MEF2A, as substrates for caspase-dependent cleavage during the apoptosis of CGNs (Li *et al.* 2001). Following the removal of depolarizing potassium, MEF2D and MEF2A are rapidly hyperphosphorylated on serine/threonine residues. This hyperphosphorylation is followed by decreased DNA binding and cleavage by caspases to fragments that dissociate the NH_2-terminal DNA binding domain from the C-terminal transactivation domain. The NH_2-terminal MEF2 fragments in turn act as dominant-interfering transcription factors by inhibiting the DNA binding of full-length MEF2 proteins. The loss of MEF2 DNA binding, and the formation of truncated MEF2 fragments that have the potential to act as dominant-negative transcription factors, results in a marked decrease in MEF2-dependent transcription of putative pro-survival genes that contributes to neuronal apoptosis (Li *et al.* 2001; Okamoto *et al.* 2002).

In the above cascade of events, the initiating signal is the hyperphosphorylation of MEF2D and MEF2A on serine/threonine residues induced by removal of the depolarization stimulus. The phosphorylation that occurs on these proteins during apoptosis is functionally distinct from phosphorylation events that have previously been reported to enhance MEF2 transcriptional activity (e.g. via ERK5 or p38 MAP kinase) (Han *et al.* 1997; Kato *et al.* 1997). In fact, the hyperphosphorylation observed on MEF2D and MEF2A under non-depolarizing (apoptotic) conditions in CGNs results in a loss of MEF2 transcriptional activity (Li *et al.* 2001). Identification of the kinase(s) that phosphorylates MEF2 proteins during neuronal apoptosis is critical to understanding the regulation of these transcription factors.

Recently, we showed that the serine/threonine kinase, glycogen synthase kinase-3β (GSK-3β), is involved in the apoptotic death of CGNs (Li *et al.* 2000). In the current study, we found that lithium, a known inhibitor of GSK-3β (Klein and Melton 1996; Stambolic *et al.* 1996) that has previously been documented to protect CGNs from apoptosis (D'Mello *et al.* 1994; Grignon *et al.* 1996; Li *et al.* 2000; Mora *et al.* 2001), significantly attenuated the hyperphosphorylation of MEF2D and MEF2A. Lithium prevented the caspase-mediated degradation of MEF2D and sustained MEF2 DNA binding and transcriptional activity under non-depolarizing conditions. Surprisingly, the inhibitory effect of lithium on the hyperphosphorylation of MEF2D could be dissociated from inhibition of GSK-3β activity. These data suggest that lithium inhibits a distinct kinase that phosphorylates MEF2 proteins and blocks their pro-survival function during neuronal apoptosis.

Experimental procedures

Materials

Monoclonal antibody to MEF2D raised against a peptide corresponding to amino acids 346–511 of mouse MEF2D was purchased from Transduction Laboratories (Lexington, KY, USA). The MEF2A antibody is a rabbit polyclonal raised against a peptide corresponding to amino acids 487–507 of human MEF2A purchased from Santa Cruz Biotechnology (Santa Cruz, CA, USA). According to the manufacturer, this antibody may cross-react with MEF2D. Polyclonal antibody to Tau phosphorylated on Ser404 was also purchased from Santa Cruz Biotechnology. Polyclonal antibodies to total GSK-3β and GSK-3β phosphorylated on Ser9 and rabbit polyclonal antibody to active caspase-3 (for western blotting) were from Cell Signaling Technologies (Beverly, MA, USA). Rabbit polyclonal antibody to active caspase-3 (for immunocytochemistry) was from Promega Corporation (Madison, WI, USA). DAPI (4,6-diamidino-2-phenylindole), Hoechst dye 33258, lithium chloride, and valproic acid (2-propylpentanoic acid, sodium salt) were purchased from Sigma (St Louis, MO, USA). Wortmannin, H89,

cyclosporin A, and forskolin were obtained from Calbiochem (San Diego, CA, USA). Insulin-like growth factor-I (recombinant, human) was provided by Margarita Quiroga (Chiron Corporation, Emeryville, CA, USA). The pGL2-MEF2-luc reporter plasmid was provided by Dr Saadi Khochbin (INSERM, France). Both the β-galactosidase enzyme assay system and the luciferase assay system were purchased from Promega. FITC-conjugated anti-rabbit and Cy3-conjugated anti-mouse secondary antibodies were from Jackson Immunoresearch Laboratories (Westgrove, PA, USA). Horseradish peroxidase-conjugated secondary antibodies and reagents for enhanced chemiluminescence were from Amersham Pharmacia Biotech (Arlington Heights, IL, USA).

Neuronal cell culture

Rat CGNs were prepared from 7- to 8-day-old Sprague Dawley rat pups (15–19 g) as described previously (Li *et al.* 2000). Neurons were plated at a density of 2.0×10^6 cells/mL in Basal Modified Eagle's (BME) medium containing 10% fetal bovine serum, 25 mM KCl, 2 mM L-glutamine, and penicillin (100 U/mL)/streptomycin (100 μg/mL). Cytosine arabinoside (10 μM) was added to the culture medium 24 h after plating to limit the growth of non-neuronal cells. Using this protocol, greater than 95% of the cultured cells were CGNs. In general, transient transfections were performed on day 5 or 6 in culture and experiments were conducted after 7 days in culture. Apoptosis was induced by removing the serum and reducing the extracellular potassium from 25 mM to 5 mM. Control cultures were maintained in medium supplemented with serum and 25 mM KCl. Alternatively, apoptosis was induced by addition of the calcineurin protein phosphatase inhibitor, cyclosporin A, in serum-free medium containing depolarizing (25 mM) potassium.

Quantification of apoptosis

Following induction of apoptosis, cells were fixed with 4% paraformaldehyde and nuclei were stained with Hoechst dye. Cells were considered apoptotic if their nuclei were condensed and/or fragmented. In general, approximately 500 cells from two fields of a 35-mm well were counted. Data are presented as a percentage of cells in a given treatment group that were scored as apoptotic. Quantification of apoptosis was performed in triplicate.

Immunocytochemistry

Cerebellar cultures were plated on polyethyleneimine-coated glass cover slips at a density of $\sim 1.0 \times 10^5$ cells per cover slip. Seven days after plating, cells were induced to undergo apoptosis in low potassium, serum-free conditions in either the absence or presence of LiCl (20 mM). After treatment, cells were fixed with 4% paraformaldehyde and then permeabilized and blocked in phosphate-buffered saline (PBS, pH 7.4) containing 0.2% Triton-X-100 and 5% BSA. Cells were then incubated overnight at 4°C with mouse-anti-MEF2D (1 : 1000) and rabbit-anti-caspase-3 (active fragment, 1 : 250) diluted in PBS containing 0.2% Triton-X-100 and 2% BSA. The primary antibodies were aspirated and cells were washed five times with PBS. Cells were then incubated with the appropriate Cy3-conjugated and FITC-conjugated secondary antibodies (1 : 500) and DAPI for 1 h at room temperature (22°C). The cells were then washed five more times with PBS and coverslips were adhered to glass slides in mounting medium (0.1% *p*-phenylenediamine in 75% glycerol in PBS). Fluorescence imaging was performed on a Zeiss Axioplan 2 microscope equipped with a Cooke Sensicam deep-cooled CCD camera and images were analyzed and subjected to digital deconvolution using the Slidebook software program (Intelligent Imaging Innovations Inc., Denver, CO, USA).

Western blot analysis

Following incubation for the indicated times and with the reagents specified in the text, the culture medium was aspirated, cells were washed once with 2 mL of ice-cold PBS, placed on ice and scraped into lysis buffer (200 μL/35-mm well) containing 20 mM HEPES (pH 7.4), 1% Triton X-100, 50 mM NaCl, 1 mM EGTA, 5 mM β-glycerophosphate, 30 mM sodium pyrophosphate, 100 μM sodium orthovanadate, 1 mM phenylmethylsulfonyl fluoride, 10 μg/mL leupeptin, and 10 μg/mL aprotinin. Cell debris was removed by centrifugation at 6000 *g* for 3 min and the protein concentration of the supernatant was determined using a commercially available protein assay kit (Pierce Chemical Co., Rockford, IL, USA). Aliquots (~150 μg) of supernatant protein were diluted to a final concentration of 1 × sodium dodecyl sulfate-polyacrylamide gel electrophoresis sample buffer, boiled for 5 min, and electrophoresed through 7.5 or 15% polyacrylamide gels. Proteins were transferred to polyvinylidene difluoride membranes (Millipore Corp., Bedford, MA, USA) and processed for western blot analysis. Non-specific binding sites were blocked in PBS (pH 7.4) containing 0.1% Tween 20 (PBS-T) and 1% BSA for 1 h at room temperature. Primary antibodies were diluted in blocking solution and incubated with the membranes for 1 h. Excess primary antibody was removed by washing the membranes three times in PBS-T. The blots were then incubated with the appropriate horseradish peroxidase-conjugated secondary antibody diluted in PBS-T for 1 h and were subsequently washed three times in PBS-T. Immunoreactive proteins were detected by enhanced chemiluminescence. Autoluminograms shown are representative of from two to four independent experiments.

Preparation of nuclear extracts and electrophoretic mobility shift assays (EMSAs)

CGNs were detached from the dish by scraping into buffer and nuclei were released by Dounce homogenization. Nuclear proteins were extracted, dialyzed, and the protein content quantified exactly as described previously (Li *et al.* 2001). Nuclear extracts (10 μg) were incubated with double-stranded ^{32}P-end labeled oligonucleotides corresponding to the muscle creatine kinase MEF2 site or to a mutant oligonucleotide, as previously described (Li *et al.* 2001). Following incubation, the protein–DNA complexes were analyzed on 5% non-denaturing polyacrylamide gels containing 3% glycerol and 0.25 × TBE (90 M Tris borate, 1 mM EDTA). After electrophoresis, the gels were dried and exposed to film at −70°C.

Transfection assays and reporter gene expression

CGNs were transiently transfected using a calcium phosphate coprecipitation method described previously (Li *et al.* 2000). Cells were transfected with 1 μg of MEF2-luciferase expression plasmid (pGL2-MEF2-luc) and 1 μg of pCMV-β-gal as an internal control for transfection efficiency. The total amount of DNA for each transfection was kept constant. Following transfection, neurons were kept in conditioned medium for 2 h. The medium was then changed

to either high potassium, serum-containing medium or low potassium, serum-free medium, each in the absence or presence of LiCl (20 mM). Alternatively, cells were switched to serum-free depolarizing medium in the absence or presence of cyclosporin A. After an additional 2–4-h incubation, cell extracts were prepared using reporter lysis buffer and the activities of luciferase and β-galactosidase were measured with the respective enzyme assay system kits (Promega).

Data analysis

Results shown represent the means ± SEM for the number (n) of independent experiments performed. Statistical differences between the means of unpaired sets of data were evaluated using either a Student's t-test or one-way ANOVA followed by a *post-hoc* Dunnett's-test. A p-value of < 0.05 was considered statistically significant.

Results

Lithium rescues CGNs from apoptosis and inhibits the activation of caspase-3

CGNs maintained in the presence of serum and a depolarizing concentration of potassium (25 mM) contained nuclei that were large and intact, as demonstrated by DAPI staining (Fig. 1a). The acute removal of serum in combination with

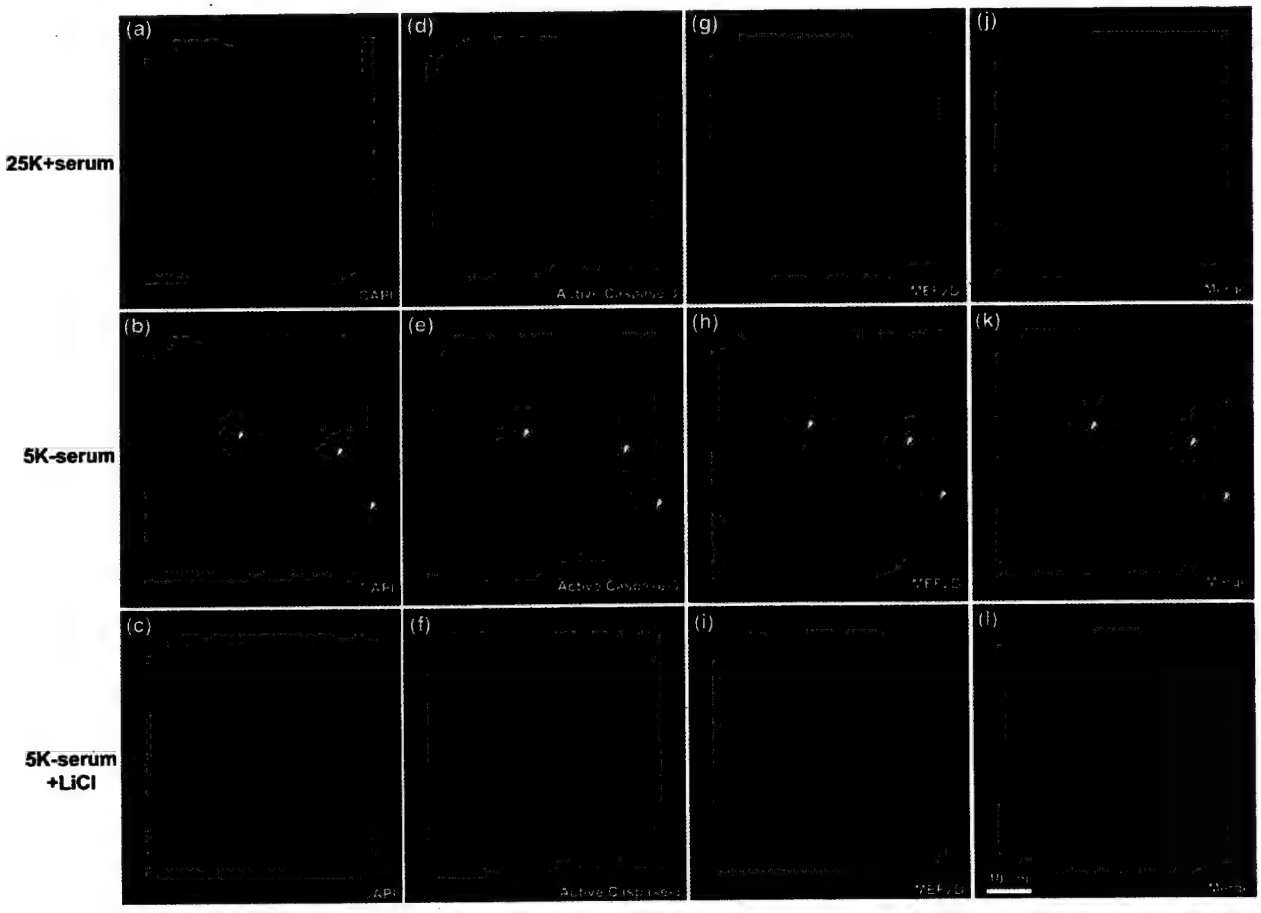

Fig. 1 Lithium inhibits CGN apoptosis and blocks caspase-3 activation and degradation of MEF2D. CGNs were incubated for 6 h in either control (25K + serum) or apoptotic (5K – serum) medium ± LiCl (20 mM). Following incubation, cells were fixed in 4% paraformaldehyde, permeabilized with 0.2% Triton-X-100 and blocked in 5% BSA. CGNs were incubated with primary antibodies to active caspase-3 (rabbit polyclonal) and MEF2D (mouse monoclonal). Following removal of excess primary antibodies, CGNs were then incubated with FITC-conjugated anti-rabbit and Cy3-conjugated anti-mouse secondary antibodies and DAPI. Fluorescent images were captured using a 63X oil objective. The images shown are representative of results obtained from two independent experiments. Scale bar = 10 μm. (a–c) DAPI staining of CGN nuclei with condensed and fragmented nuclei indicated by the arrows in (b). (d–f) Active caspase-3 was only detectable in CGNs incubated in apoptotic medium in the absence of LiCl. The most intense caspase-3 staining was observed in cells containing fragmented nuclei (see arrows in e). (g–i) MEF2D immunoreactivity was restricted to the nuclear compartment in CGNs maintained in either control medium or in apoptotic medium containing LiCl. In contrast, CGNs showing fragmented nuclei displayed MEF2D staining that was substantially decreased in intensity (compared with cells with intact nuclei) and was localized to the cytoplasm (see arrows in h). (j–l) Merged images showing the co-localization of active caspase-3 and MEF2D in CGNs containing fragmented nuclei (indicated by the arrows in k).

lowering of the extracellular potassium concentration to 5 mM (trophic factor withdrawal) for 6 h resulted in significant chromatin condensation and fragmentation in CGNs, consistent with induction of apoptosis (Fig. 1b). Addition of LiCl (20 mM) to trophic factor-deprived CGN cultures essentially abolished the induction of apoptosis (Fig. 1c). Quantification of the effects of increasing concentrations of LiCl on the formation of apoptotic nuclei observed at 24 h after trophic factor withdrawal, demonstrated a dose-dependent protective effect of lithium, with complete protection observed at a concentration of 20 mM (Fig. 2a). In agreement with numerous previous findings (D'Mello *et al.* 1994; Grignon *et al.* 1996; Li *et al.* 2000; Mora *et al.* 2001), these data confirm that lithium is effective at rescuing CGNs from apoptosis.

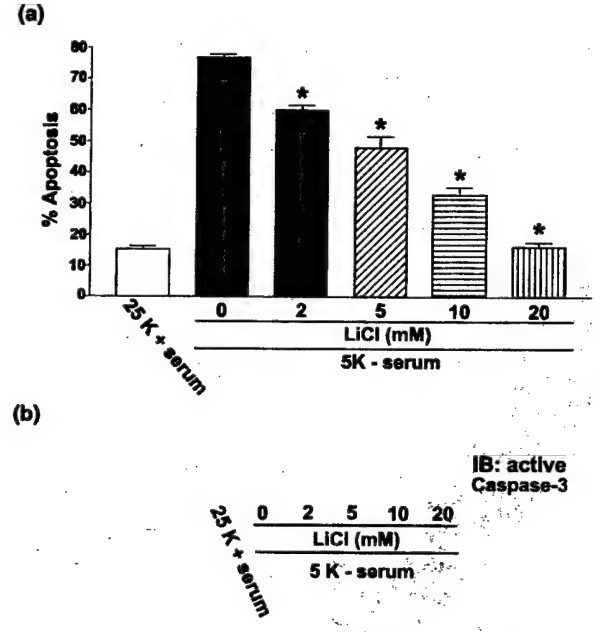

Fig. 2 Dose-dependence of lithium effects on CGN apoptosis and caspase-3 activation. (a) CGNs were incubated for 24 h in either control (25K + serum) or apoptotic (5K – serum) medium in the presence of increasing concentrations of LiCl. Following incubation, cells were fixed in 4% paraformaldehyde and nuclei were stained with Hoechst dye. Approximately 500 cells from at least two fields of a culture dish were scored for apoptosis from each condition. CGNs were considered apoptotic if their nuclei were condensed and/or fragmented. The data shown represent the means ± SEM for three independent experiments, each performed in triplicate. *Significantly different from the (5K – serum) condition in the absence of lithium ($p < 0.05$). (b) CGNs were incubated as described in (a) for 6 h and detergent-soluble cell lysates were electrophoresed on 15% polyacrylamide gels. Proteins were transferred to PVDF membranes and immunoblotted (IB) with a polyclonal antibody that specifically recognizes the active (cleaved) form of caspase-3, as described in Experimental procedures. The blot shown is representative of three separate experiments.

Apoptotic cell death is carried out by the caspase family of cysteine proteases (Shi 2002). Caspase-3 is an executioner caspase, activated following cleavage by initiator caspases (caspase-8 or –9), that has been implicated in the apoptosis of CGNs (Eldadah *et al.* 2000). CGNs maintained in medium containing serum and depolarizing potassium displayed very little active caspase-3 detectable by either immunocytochemistry (Fig. 1d) or immunoblotting (Fig. 2b, first lane) using antibodies that specifically recognize the cleaved form of the caspase. In contrast, trophic factor withdrawal for 6 h induced a marked activation of caspase-3 as shown immunocytochemically (Fig. 1e) and by western blotting (Fig. 2b, second lane). As previously reported (Mora *et al.* 2001), inclusion of LiCl during trophic factor withdrawal significantly attenuated the activation of caspase-3 (Fig. 1f) in a dose-dependent manner (Fig. 2b). Thus, consistent with its ability to decrease chromatin condensation and fragmentation, lithium concomitantly suppresses caspase activation in CGNs deprived of trophic support.

Lithium attenuates the hyperphosphorylation and degradation of MEF2D

Next, we examined the effects of LiCl on the hyperphosphorylation of MEF2D and MEF2A that occurs in CGNs undergoing apoptosis (Li *et al.* 2001). As shown in Fig. 3, immunoblotting CGN lysates revealed a marked upward shift in the electrophoretic mobility of MEF2D following the removal of trophic factors (Fig. 3a, compare the first and second lanes). We previously showed that this mobility shift is indicative of the hyperphosphorylation of MEF2D on serine/threonine residues, as it can be reversed by incubating the cell lysates with calf intestinal alkaline phosphatase (Li *et al.* 2001). Inclusion of LiCl at concentrations from 2 to 20 mM dose-dependently attenuated the hyperphosphorylation of MEF2D (Fig. 3a). In addition to the effect on MEF2D, LiCl (20 mM) also significantly blunted the hyperphosphorylation of MEF2A (Fig. 3b).

During neuronal apoptosis, MEF2D is a substrate for caspase-mediated cleavage (Li *et al.* 2001; Okamoto *et al.* 2002). Immunocytochemical analysis of CGNs demonstrated that MEF2D was localized exclusively to the nuclear compartment in cells maintained in the presence of serum and depolarization (Fig. 1g). Trophic factor withdrawal resulted in a decrease of MEF2D immunoreactivity in CGNs displaying active caspases and nuclear fragmentation (Fig. 1h). The reduction in the intensity of MEF2D staining was significantly blocked by lithium (Fig. 1i). Consistent with a caspase-dependent mechanism for MEF2D degradation, MEF2D appeared to colocalize with active caspases in trophic factor-deprived CGNs (Fig. 1k). Collectively, the above results demonstrate that lithium effectively inhibits both the hyperphosphorylation and caspase-mediated degradation of MEF2D that occur during CGN apoptosis.

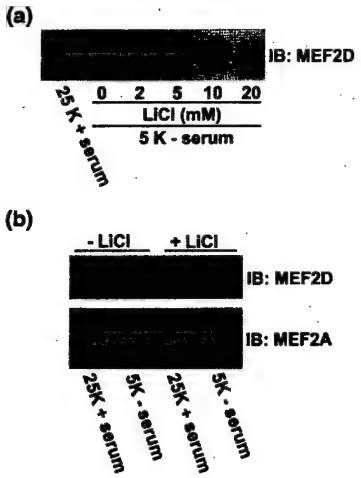

Fig. 3 Lithium attenuates the hyperphosphorylation of MEF2D and MEF2A induced following removal of depolarizing potassium and serum. (a) CGNs were incubated for 4 h in either control (25K + serum) or apoptotic (5K – serum) medium in the presence of increasing concentrations of LiCl. Following incubation, cell lysates were electrophoresed on 7.5% polyacrylamide gels and immunoblotted (IB) with a monoclonal antibody that specifically recognizes MEF2D, as described in Experimental procedures. (b) CGNs were incubated for 4 h in either control or apoptotic medium ± LiCl (20 mM). Cell lysates were subjected to sodium dodecyl sulfate – polyacrylamide gel electrophoresis (SDS–PAGE) and immunoblotted for either MEF2D or MEF2A. Note that the polyclonal antibody to MEF2A also cross-reacts with MEF2D, evident by the apparent doublet. The blots shown are each illustrative of three independent experiments.

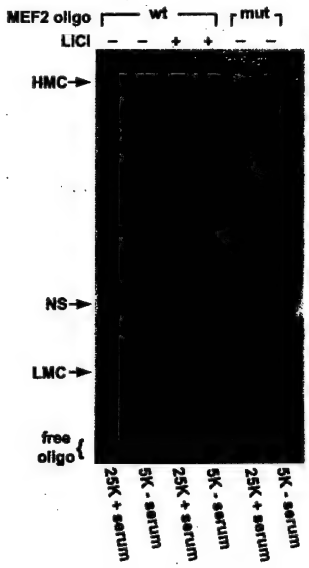

Fig. 4 Lithium prevents the loss of MEF2 DNA binding and blocks formation of truncated NH2-terminal MEF2 fragments in CGNs switched to medium lacking depolarizing potassium and serum. CGNs were incubated in either control (25K + serum) or apoptotic (5K – serum) medium ± LiCl (20 mM) for 4 h. Nuclear extracts were prepared and gel mobility shift assays were performed using either a double-stranded ^{32}P-labeled consensus (wild-type, wt) or mutant (mut) MEF2 oligonucleotide, as described in Experimental procedures. HMC, high molecular weight protein–DNA complex; LMC, low molecular weight protein–DNA complex; NS, non-specific protein–DNA complex. The HMC represents DNA binding by full length MEF2 proteins. The LMC represents DNA binding by truncated NH2-terminal MEF2 fragments (see Results). The gel shown is representative of two independent experiments that produced similar results.

Lithium sustains MEF2 DNA binding and inhibits formation of truncated NH_2-terminal MEF2 fragments

The hyperphosphorylation of MEF2 proteins results in decreased binding to DNA detectable by electrophoretic mobility shift assay (EMSA). As we previously reported (Li *et al.* 2001), nuclear extracts obtained from CGNs incubated in the presence of serum and depolarizing potassium contained a single specific high molecular weight protein–DNA complex (HMC) recognized by a wild-type MEF2 double-stranded oligonucleotide (Fig. 4, first lane). Removal of serum and depolarizing potassium for 4 h induced a decrease in the HMC, indicative of a relative loss of DNA binding by full-length MEF2 proteins (Fig. 4, second lane). Trophic factor withdrawal also promoted the appearance of a new low molecular weight protein–DNA complex (LMC) (Fig. 4, second lane) consisting of truncated MEF2 fragments that contain the NH_2-terminal DNA binding domain but lack the C-terminal transcriptional activation domain. We and others have previously shown that these NH2-terminal MEF2 fragments are generated via caspase-dependent cleavage of the full length MEF2 proteins, and have the potential to act as dominant-interfering transcription factors (Li *et al.* 2001; Okamoto *et al.* 2002). Inclusion of LiCl (20 mM) in apoptotic medium prevented both the decrease in DNA binding of full-length MEF2 proteins (i.e., loss of the HMC) and formation of the NH_2-terminal MEF2 fragments (i.e., appearance of the LMC) (Fig. 4, third and fourth lanes). Neither the HMC nor the LMC was detected using a mutant MEF2 oligonucleotide (Fig. 4, fifth and sixth lanes). These results show that lithium sustains MEF2 DNA binding and concurrently suppresses the formation of caspase-generated, dominant-negative MEF2 fragments in CGNs deprived of depolarization and serum.

Lithium preserves MEF2-dependent transcriptional activity in trophic factor-deprived CGNs

We utilized transient transfection of a luciferase reporter plasmid containing two MEF2 consensus sites followed by the luciferase reporter gene to measure the transcriptional activity of MEF2 proteins in CGNs. CGNs maintained in the presence of serum and depolarizing potassium exhibited high endogenous MEF2-dependent transcriptional activity. As shown in Fig. 5, trophic factor withdrawal for 2 h induced a marked (~60%) reduction in MEF2-driven luciferase activity. Consistent with the ability of lithium to attenuate the

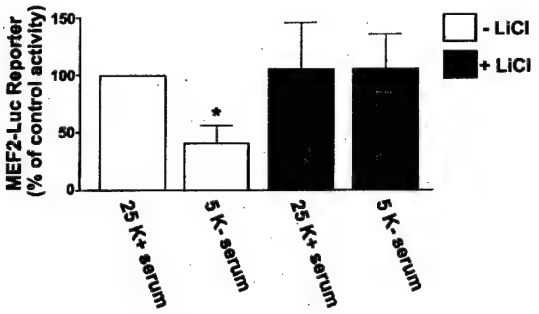

Fig. 5 Lithium sustains MEF2-dependent transcriptional activity in CGNs incubated in apoptotic medium. CGNs were transiently co-transfected with a MEF2-responsive luciferase reporter plasmid (pGL2-MEF2-Luc) and pCMV-β-gal. Two hours post-transfection, CGNs were incubated for a further 2 h in either control (25K + serum) or apoptotic (5K – serum) medium ± LiCl (20 mM). Following incubation, luciferase and β-galactosidase activities were assayed as described in Experimental procedures. Luciferase activity was normalized for transfection efficiency by dividing by the β-galactosidase activity. The normalized MEF2-Luc reporter activity obtained for CGNs incubated in control medium in the absence of lithium was set at 100% and all other values were calculated relative to the control. The data represent the means ± SEM. for three separate experiments, each performed in duplicate. *Significantly different from the (25K + serum) condition in the absence of lithium ($p < 0.05$).

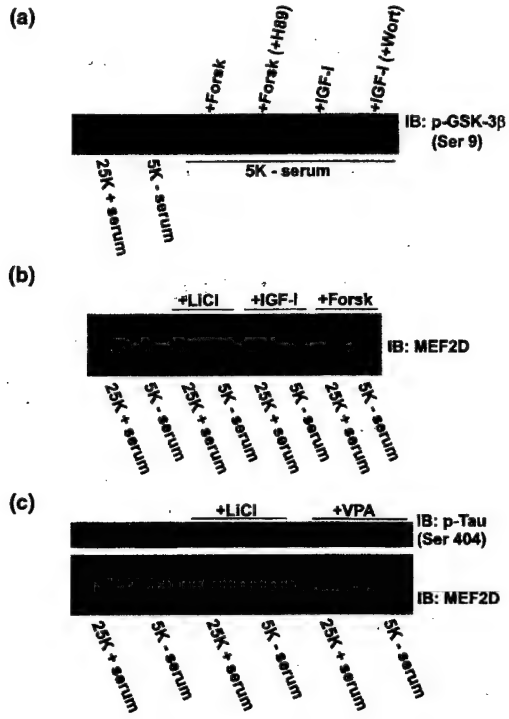

Fig. 6 Distinct inhibitors of GSK-3β do not mimic the inhibitory effects of lithium on MEF2D hyperphosphorylation. (a) CGNs were incubated for 4 h in either control (25K + serum) or apoptotic (5K – serum) medium alone or containing either forskolin (Forsk, 10 μM) ± H89 (10 μM) or insulin-like growth factor-I (IGF-I, 200 ng/mL) ± wortmannin (Wort, 100 nM). Following incubation, cell lysates from each treatment condition containing equal amounts of protein were subjected to SDS–PAGE on 10% polyacrylamide gels. Proteins were transferred to PVDF membranes and immunoblotted (IB) with a polyclonal antibody that specifically recognizes (*inactive*) GSK-3β phosphorylated on Ser9 (p-GSK-3β). (b) CGNs were incubated for 4 h in either control or apoptotic medium alone or containing either LiCl (20 mM), IGF-I (200 ng/mL), or Forsk (10 μM). Cell lysates were then western blotted for MEF2D, as described in Experimental procedures. (c) Cells were incubated for 4 h in either control or apoptotic medium alone or containing either LiCl (20 mM) or sodium valproate (VPA, 20 mM). Protein extracts were then immunoblotted for the GSK-3β substrate Tau phosphorylated on Ser404 (p-Tau, upper panel) and MEF2D (lower panel). The blots shown are each representative of results obtained in three separate experiments.

hyperphosphorylation and degradation of MEF2 proteins and to sustain MEF2 DNA binding, addition of LiCl (20 mM) prevented the loss of MEF2-dependent transcriptional activity in CGNs incubated in apoptotic medium. Thus, lithium sustains activity of the pro-survival MEF2 transcription factors in trophic factor-deprived CGNs.

The ability of lithium to block the hyperphosphorylation of MEF2D is not mimicked by distinct inhibitors of GSK-3β

One of the principal anti-apoptotic actions of lithium is inhibition of the serine/threonine kinase GSK-3β (Klein and Melton 1996; Stambolic *et al.* 1996), a protein that we previously implicated in the apoptosis of CGNs (Li *et al.* 2000). GSK-3β also plays a role in the apoptosis of primary cortical and sympathetic neurons (Crowder and Freeman 2000; Hetman *et al.* 2000). Moreover, in neuroblastoma cells GSK-3β translocates to the nucleus during apoptosis, consistent with a role for this kinase in the phosphorylation of nuclear substrates (Bijur and Jope 2001). To determine if the inhibitory effects of lithium on the hyperphosphorylation of MEF2D were mediated by its ability to blunt GSK-3β activity, we investigated the effects of three mechanistically distinct inhibitors of GSK-3β on MEF2D phosphorylation. We recently showed that activation of protein kinase A (PKA) is neuroprotective in CGNs through phosphorylation of an inhibitory serine residue (Ser9) on GSK-3β (Li *et al.* 2000). In agreement with this finding, forskolin, a direct activator of adenylyl cyclase, prevented the dephosphorylation (activation) of GSK-3β that occurs following trophic factor withdrawal in CGNs (Fig. 6a, first through third lanes). The phosphorylation of GSK-3β on Ser9 induced by forskolin was prevented by the PKA inhibitor H89 (Fig. 6a, fourth lane). Serine 9 on GSK-3β is also a consensus phosphorylation site for the antiapoptotic kinase AKT that is activated downstream of growth factor signaling in a phosphatidylinositol 3-kinase (PI3K)-dependent manner (van Weeren *et al.* 1998). Consistent with this, addition of insulin-like growth factor-I (IGF-I), a known survival factor

for CGNs (D'Mello *et al.* 1993; Linseman *et al.* 2002), induced phosphorylation (inactivation) of GSK-3β, an effect that was blocked by the PI3K inhibitor wortmannin (Fig. 6a, fifth and sixth lanes). Although both forskolin and IGF-I significantly induced phosphorylation of GSK-3β on Ser9, indicative of its inactivation, neither had any discernible effect on the hyperphosphorylation of MEF2D following trophic factor withdrawal from CGNs (Fig. 6b). Finally, incubation of CGNs with either lithium or sodium valproate (VPA, 20 mM), another recognized inhibitor of GSK-3β (Chen *et al.* 1999) that protects CGNs from apoptosis (Mora *et al.* 1999; Li *et al.* 2000), completely blocked phosphorylation of the GSK-3β substrate Tau (Utton *et al.* 1997) induced following trophic factor withdrawal (Fig. 6c, upper blot). However, VPA had no significant effect on the hyperphosphorylation of MEF2D observed under these conditions (Fig. 6c, lower blot). These results indicate that the inhibitory effects of lithium on MEF2D hyperphosphorylation can be dissociated from its ability to inhibit the pro-apoptotic kinase GSK-3β, suggesting the presence of an additional kinase target for lithium in CGNs.

Lithium blocks MEF2D hyperphosphorylation and apoptosis induced by calcineurin inhibition – a GSK-3β-independent model of CGN death

As trophic factor withdrawal results in both the activation of GSK-3β (Li *et al.* 2000) and the hyperphosphorylation of MEF2 proteins (Li *et al.* 2001) in CGNs, the relative contribution of lithium's effects on each of these signaling pathways to its pro-survival action is unclear. To strengthen the conclusion that inhibition of MEF2D hyperphosphorylation significantly contributes to lithium's neuroprotective action, we examined a different paradigm of CGN apoptosis. Previous work has shown that MEF2 DNA binding and transcriptional activity depend on depolarization-mediated activation of the calcium-regulated protein phosphatase calcineurin (Mao and Wiedmann 1999). In agreement with these findings, we observed that incubation of CGNs in depolarizing (25 mM KCl) medium containing the calcineurin inhibitor, cyclosporin A (CyA), resulted in the hyperphosphorylation of MEF2D (Fig. 7a, *compare first and fourth lanes*), loss of MEF2 transcriptional activity (Fig. 7b), and significant apoptosis (Fig. 7d, *open bars*). In contrast to trophic factor withdrawal (see Fig. 6a, *first and second lanes*), incubation with CyA under depolarizing conditions failed to activate GSK-3β (measured by dephosphorylation of the inhibitory residue Ser9, Fig. 7e, *compare first and second lanes*). This latter result was expected as GSK-3β has previously been shown to be regulated by a distinct protein phosphatase, PP2A (Mora *et al.* 2002). Thus, calcineurin inhibition in the presence of depolarizing potassium is a MEF2 phosphorylation-dependent, but GSK-3β-independent, model of CGN apoptosis. Lithium significantly blocked the hyperphosphorylation of MEF2D (Fig. 7a, *compare fourth and fifth lanes*), loss of MEF2 transcriptional activity (Fig. 7c), and apoptosis (Fig. 7d) induced by addition of CyA, strongly suggesting that inhibition of MEF2 hyperphosphorylation is a novel pro-survival action of lithium in CGNs.

Discussion

The effectiveness of lithium as a therapy for bipolar disorder is well documented (Muller-Oerlinghausen *et al.* 2002). However, the ability of lithium to act as a neuroprotective agent has only recently gained attention. Previous studies have demonstrated that lithium inhibits neuronal apoptosis *in vitro* induced by trophic factor withdrawal (D'Mello *et al.* 1994; Grignon *et al.* 1996; Li *et al.* 2000; Mora *et al.* 2001), excitotoxicity (Nonaka *et al.* 1998a; Chen and Chuang 1999), neurotoxin exposure (Nonaka *et al.* 1998b; Maggirwar *et al.* 1999), beta-amyloid (Alvarez *et al.* 1999), and ceramide (Centeno *et al.* 1998). Moreover, lithium inhibits hippocampal neuronal death induced by *in vivo* exposure to the neurotoxin aluminum (Ghribi *et al.* 2002). Lithium has also been shown to enhance the survival of chick ciliary ganglion neurons during embryonic development (Ikonomov *et al.* 2000). The above results demonstrate that lithium provides neuroprotection both *in vitro* and *in vivo*.

Although lithium is a known inhibitor of the pro-apoptotic serine/threonine kinase, GSK-3β (Klein and Melton 1996; Stambolic *et al.* 1996), relatively few studies have concluded that lithium provides neuroprotection via this mechanism (Maggirwar *et al.* 1999; Bijur *et al.* 2000; Li *et al.* 2000). Several alternative mechanisms have also been proposed. For example, lithium has recently been shown to inhibit a serine/threonine phosphatase that dephosphorylates (inactivates) the pro-survival kinase AKT (Mora *et al.* 2001, 2002). It is noteworthy however, that a principal target of AKT is GSK-3β (van Weeren *et al.* 1998), and therefore, the net result of this effect of lithium may inevitably involve inhibition of GSK-3β activity. In addition, lithium has been shown to up-regulate the expression of the anti-apoptotic Bcl-2 protein (Chen and Chuang 1999; Manji *et al.* 2000) and to decrease expression of the pro-apoptotic proteins, p53 and Bax (Chen and Chaung 1999). These latter effects are only observed after chronic (several days) treatment with lithium. In the current study, we investigated the neuroprotective mechanism of lithium in primary cultures of rat CGNs. Specifically, we analyzed the effects of lithium on the apoptotic processing of MEF2 proteins, transcription factors that are critical for CGN survival (Mao *et al.* 1999). In agreement with previous results showing that CGNs matured *in vitro* are protected from apoptosis by lithium (D'Mello *et al.* 1994; Grignon *et al.* 1996; Li *et al.* 2000; Mora *et al.* 2001), we found that acute addition of lithium effectively inhibits CGN apoptosis and caspase activation induced by removal of depolarizing potassium and serum. Moreover, our data reveal

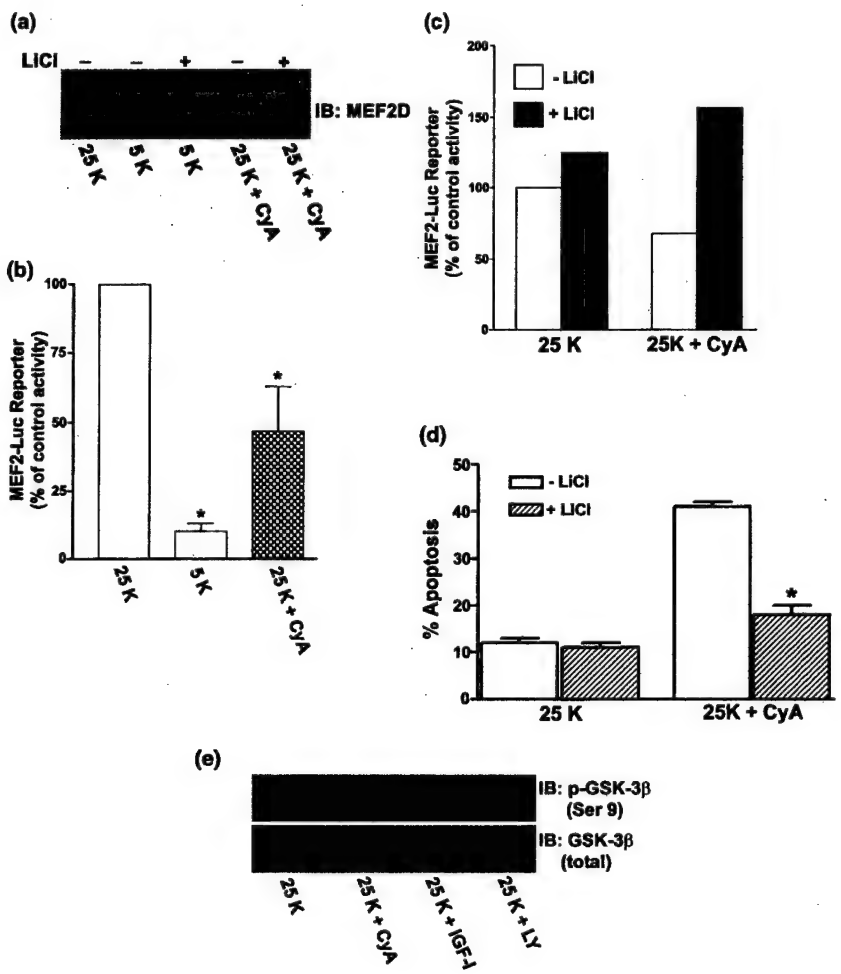

Fig. 7 Incubation with the calcineurin phosphatase inhibitor, cyclosporin A (CyA), under depolarizing conditions induces lithium-sensitive MEF2D hyperphosphorylation, loss of MEF2 transcriptional activity and apoptosis in the absence of GSK-3β activation. (a) CGNs were incubated for 4 h in serum-free medium containing either 25 mM KCl (25K), 5 mM KCl (5K), or 25 mM KCl + 10 μM CyA (25K + CyA) in the absence or presence of LiCl (20 mM). Following incubation, cell lysates were immunoblotted (IB) for MEF2D, as described in Experimental procedures. (b) CGNs were transiently co-transfected with a MEF2-responsive luciferase reporter plasmid (pGL2-MEF2-Luc) and pCMV-β-gal. Following transfection, cells were incubated for 4 h as described in (a) and luciferase and β-galactosidase activities were assayed and normalized as described in Experimental procedures. *Significantly different from the 25K control ($p < 0.05$). (c) Cells were transfected as described in (b) and were subsequently incubated in either 25K or 25K + CyA in the absence or presence of LiCl (20 mM). Luciferase and β-galactosidase activities were assayed and the results shown represent the mean values of triplicate samples from a single experiment. (d) CGNs were incubated for 24 h in either 25K medium alone or containing CyA (10 μM). Cells were stained with Hoechst dye and apoptosis was quantified as described in Experimental procedures. *Significantly different from 25K + CyA in the absence of lithium ($p < 0.05$). (e) CGNs were incubated for 4 h in the absence or presence of CyA. Cell lysates were probed for GSK-3β phosphorylated on Ser9 (upper panel) and total GSK-3β (lower panel). When the phospho-specific GSK-3β signal was normalized for the total GSK-3β, no significant change in phosphorylation state was observed with the addition of CyA. IGF-I and the PI3K inhibitor, LY294002 (LY), are included as positive and negative controls for GSK-3β phosphorylation on Ser9, respectively.

a novel mechanism for the pro-survival effects of lithium in CGNs that involves preservation of MEF2 transcriptional activity.

We show that lithium inhibits the hyperphosphorylation of MEF2D and MEF2A induced by trophic factor withdrawal in CGNs. Consistent with previous observations that hyperphosphorylation of MEF2 proteins leads to a decrease in their DNA binding (Mao and Wiedmann 1999; Li *et al.* 2001), we also show that lithium sustains MEF2 DNA binding and MEF2 transcriptional activity in trophic factor-deprived CGNs. In addition, lithium blocks the caspase-dependent formation of NH_2-terminal MEF2 fragments that have the potential to act as dominant-interfering transcription factors (Li *et al.* 2001; Okamoto *et al.* 2002). The relative contribution of MEF2 hyperphosphorylation versus MEF2 degradation to the induction of CGN apoptosis is presently

unclear. The ability of lithium to block the hyperphosphorylation of MEF2 proteins suggests that it acts very early in the apoptotic cascade as hyperphosphorylation of MEF2 precedes loss of DNA binding or transcriptional activity and caspase-mediated degradation of MEF2 proteins (Li *et al.* 2001). The latter likely leads to a more prolonged inhibition of MEF2 activity as the fragments formed have the potential to compete with newly synthesized full-length MEF2 proteins for DNA binding. However, it appears that hyperphosphorylation of MEF2 proteins may be the initiating event that ultimately leads to loss of MEF2 activity and apoptosis. This is the first report to demonstrate that lithium preserves the activity of MEF2 transcription factors in neurons subjected to an apoptotic stimulus. The fact that a constitutively active MEF2 mutant has previously been shown to protect CGNs from apoptosis (Mao *et al.* 1999) supports our conclusion that the effects of lithium on MEF2 proteins described above play an important role in the neuroprotective mechanism of this cation.

A likely target for the action of lithium in CGNs is the kinase that phosphorylates MEF2D and MEF2A during apoptosis. We initially examined the effects of lithium on phosphorylation of MEF2 proteins in CGNs because lithium is an established inhibitor of GSK-3β (Klein and Melton 1996; Stambolic *et al.* 1996), a serine/threonine kinase that is involved in the apoptosis of CGNs (Li *et al.* 2000). However, many of the results obtained in the present study argue against a role for GSK-3β in phosphorylating MEF2 proteins during CGN apoptosis. Firstly, forskolin and IGF-I, agents that promote the phosphorylation of GSK-3β on the inhibitory Ser9 via either PKA or AKT kinase activation, respectively (van Weeren *et al.* 1998; Li *et al.* 2000), had no significant effect on the hyperphosphorylation of MEF2D. Secondly, another compound known to inhibit GSK-3β, VPA (Chen *et al.* 1999), significantly blocked phosphorylation of the GSK-3β substrate Tau, but had no discernible effect on the hyperphosphorylation of MEF2D. Thirdly, MEF2D hyperphosphorylation was induced in depolarizing medium by addition of the calcineurin phosphatase inhibitor, CyA, conditions under which GSK-3β activity was not further stimulated. These results suggest that the kinase that phosphorylates MEF2D and inhibits DNA binding of MEF2 proteins during apoptosis of CGNs is a novel lithium target that is distinct from GSK-3β. This finding is in contrast to the ability of lithium to stimulate DNA binding of the transcription factor cAMP response element binding protein (CREB), an effect that is mediated via inhibition of GSK-3β (Grimes and Jope 2001). Collectively, these observations indicate that the potential for lithium to inhibit multiple pro-apoptotic signals, including GSK-3β and the kinase that phosphorylates MEF2 proteins, likely contributes to its effectiveness as a neuroprotective agent. In particular, the finding that lithium inhibits MEF2D hyperphosphorylation and apoptosis induced by calcineurin inhibition, a GSK-3β-independent model of CGN death, strongly supports the conclusion that inhibition of a MEF2 kinase is a novel anti-apoptotic action of lithium in neurons.

Finally, although lithium is commonly regarded as a highly selective inhibitor of GSK-3β (Klein and Melton 1996; Stambolic *et al.* 1996; Woodgett 2001), it is clear that it inhibits the function of other enzymes as well. For example, lithium is an established inhibitor of the inositol monophosphatase (Phiel and Klein 2001), and this effect may be involved in its efficacy in bipolar disorder (Atack *et al.* 1995). Recently, lithium has been suggested to inhibit activation of the protein serine/threonine phosphatase, PP2A, which is involved in the regulation of AKT activity (Mora *et al.* 2002). In regards to other potential kinases that may be inhibited by lithium, a recent screen against a relatively large panel of possible kinase targets showed that lithium (10 mM) inhibited GSK-3β most potently, but also decreased the activities of three other serine/threonine kinases tested, including casein kinase-2 (CK-2), mitogen-activated protein kinase-activated protein kinase-2 (MAPKAPK-2), and p38-regulated/activated protein kinase (PRAK) (Davies *et al.* 2000). Interestingly, CK-2 has previously been shown to phosphorylate MEF2C; however, this phosphorylation enhanced MEF2C binding to DNA (Molkentin *et al.* 1996). The potential of either MAPKAPK-2 or PRAK to phosphorylate the MEF2 proteins has not yet been examined. Thus, identification of the lithium-sensitive kinase that phosphorylates MEF2D and MEF2A in CGNs during apoptosis will require further investigation.

In conclusion, we have demonstrated that lithium inhibits the hyperphosphorylation and caspase-dependent degradation of MEF2 transcription factors and maintains their DNA binding and activity in CGNs deprived of depolarizing potassium and serum. These effects of lithium are mediated via the inhibition of a serine/threonine kinase, distinct from GSK-3β, that phosphorylates MEF2 proteins and inhibits their pro-survival function. These data identify the regulation of MEF2 transcriptional activity as a novel mechanism underlying the neuroprotective effects of lithium.

Acknowledgements

This work was supported by Department of Veterans Affairs Merit Awards (to KAH and DAL), a Department of Defense Grant DAMD17-99-1-9481 (to KAH), an NIH Grant NS38619–01A1 (to KAH), and a VA Research Enhancement Award Program (to KAH and DAL). The authors acknowledge Mingtao Li and Xiaomin Wang for technical support.

References

Alvarez G., Munoz-Montano J. R., Satrustegui J., Avila J., Bogonez E. and Diaz-Nido J. (1999) Lithium protects cultured neurons against beta-amyloid-induced neurodegeneration. *FEBS Lett.* **453**, 260–264.

Andersen J. K. (2001) Does neuronal loss in Parkinson's Disease involve programmed cell death? *Bioessays* **23**, 640–646.

Atabay C., Cagnoli C. M., Kharlamov E., Ikonomovic M. D. and Manev H. (1996) Removal of serum from primary cultures of cerebellar granule neurons induces oxidative stress and DNA fragmentation: protection with antioxidants and glutamate receptor antagonists. *J. Neurosci. Res.* **43**, 465–475.

Atack J. R., Broughton H. B. and Pollack S. J. (1995) Inositol monophosphatase – a putative target for Li^+ in the treatment of bipolar disorder. *Trends Neurosci.* **18**, 343–349.

Bijur G. N. and Jope R. S. (2001) Pro-apoptotic stimuli induce nuclear accumulation of glycogen synthase kinase-3 beta. *J. Biol. Chem.* **276**, 37436–37442.

Bijur G. N., De Sarno P. and Jope R. S. (2000) Glycogen synthase kinase-3beta facilitates staurosporine- and heat shock-induced apoptosis. Protection by lithium. *J. Biol. Chem.* **275**, 7583–7590.

Black B. L. and Olson E. N. (1998) Transcriptional control of muscle development by myocyte enhancer factor-2 (MEF2) proteins. *Annu. Rev. Cell Dev. Biol.* **14**, 167–196.

Centeno F., Mora A., Fuentes J. M., Soler G. and Claro E. (1998) Partial lithium-associated protection against apoptosis induced by C2-ceramide in cerebellar granule neurons. *Neuroreport* **9**, 4199–4203.

Chen G., Huang L. D., Jiang Y. M. and Manji H. K. (1999) The mood-stabilizing agent valproate inhibits the activity of glycogen synthase kinase-3. *J. Neurochem.* **72**, 1327–1330.

Chen R. W. and Chuang D. M. (1999) Long-term lithium treatment suppresses p53 and Bax expression but increases Bcl-2 expression. A prominent role in neuroprotection against excitotoxicity. *J. Biol. Chem.* **274**, 6039–6042.

Crowder R. J. and Freeman R. S. (2000) Glycogen synthase kinase-3 beta activity is critical for neuronal death caused by inhibiting phosphatidylinositol 3-kinase or Akt but not for death caused by nerve growth factor withdrawal. *J. Biol. Chem.* **275**, 34266–34271.

D'Mello S. R., Galli C., Ciotti T. and Calissano P. (1993) Induction of apoptosis in cerebellar granule neurons by low potassium: inhibition of death by insulin-like growth factor I and cAMP. *Proc. Natl Acad. Sci. USA* **90**, 10989–10993.

D'Mello S. R., Anelli R. and Calissano P. (1994) Lithium induces apoptosis in immature cerebellar granule cells but promotes survival of mature neurons. *Exp. Cell Res.* **211**, 332–338.

Davies S. P., Reddy H., Caivano M. and Cohen P. (2000) Specificity and mechanism of action of some commonly used protein kinase inhibitors. *Biochem. J.* **351**, 95–105.

Eldadah B. A., Ren R. F. and Faden A. I. (2000) Ribozyme-mediated inhibition of caspase-3 protects cerebellar granule cells from apoptosis induced by serum-potassium deprivation. *J. Neurosci.* **20**, 179–186.

Ghribi O., Herman M. M., Spaulding N. K. and Savory J. (2002) Lithium inhibits aluminum-induced apoptosis in rabbit hippocampus by preventing cytochrome c translocation, Bcl-2 decrease, Bax elevation and caspase-3 activation. *J. Neurochem.* **82**, 137–145.

Grignon S., Levy N., Couraud F. and Bruguerolle B. (1996) Tyrosine kinase inhibitors and cycloheximide inhibit Li+ protection of cerebellar granule neurons switched to non-depolarizing medium. *Eur. J. Pharmacol.* **315**, 111–114.

Grimes C. A. and Jope R. S. (2001) CREB DNA binding activity is inhibited by glycogen synthase kinase-3 beta and facilitated by lithium. *J. Neurochem.* **78**, 1219–1232.

Han J., Jiang Y., Li Z., Kravchenko V. V. and Ulevitch R. J. (1997) Activation of the transcription factor MEF2C by the MAP kinase p38 in inflammation. *Nature* **386**, 296–299.

Hetman M., Cavanaugh J. E., Kimelman D. and Xia Z. (2000) Role of glycogen synthase kinase-3 beta in neuronal apoptosis induced by trophic withdrawal. *J. Neurosci.* **20**, 2567–2574.

Honig L. S. and Rosenberg R. N. (2000) Apoptosis and neurologic disease. *Am. J. Med.* **108**, 317–330.

Ikonomov O. C., Petrov T., Soden K., Shisheva A. and Manji H. K. (2000) Lithium treatment in ovo: effects on embryonic heart rate, natural death of ciliary ganglion neurons, and brain expression of a highly conserved chicken homologue of human MTG8/ETO. *Brain Res. Dev. Brain Res.* **123**, 13–24.

Kato Y., Kravchenko V. V., Tapping R. I., Han J., Ulevitch R. J. and Lee J. D. (1997) BMK1/ERK5 regulates serum-induced early gene expression through transcription factor MEF2C. *EMBO J.* **16**, 7054–7066.

Kawashima T., Doh-ura K., Ogomori K. and Iwaki T. (2001) Apoptotic bodies in the cerebellum of Japanese patients with Creutzfeldt-Jakob disease. *Pathol. Int.* **51**, 140–144.

Klein P. S. and Melton D. A. (1996) A molecular mechanism for the effect of lithium on development. *Proc. Natl Acad. Sci. USA* **93**, 8455–8459.

Leifer D., Krainc D., Yu Y. T., McDermott J., Breitbart R. E., Heng J., Neve R. L., Kosofsky B., Nadal-Ginard B. and Lipton S. A. (1993) MEF2C, a MADS/MEF2-family transcription factor expressed in a laminar distribution in cerebral cortex. *Proc. Natl Acad. Sci. USA* **90**, 1546–1550.

Li M., Wang X., Meintzer M. K., Laessig T., Birnbaum M. J. and Heidenreich K. A. (2000) Cyclic AMP promotes neuronal survival by phosphorylation of glycogen synthase kinase 3 beta. *Mol. Cell Biol.* **20**, 9356–9363.

Li M., Linseman D. A., Allen M. P., Meintzer M. K., Wang X., Laessig T., Wierman M. E. and Heidenreich K. A. (2001) Myocyte enhancer factor 2A and 2D undergo phosphorylation and caspase-mediated degradation during apoptosis of rat cerebellar granule neurons. *J. Neurosci.* **21**, 6544–6552.

Lin X., Shah S. and Bulleit R. F. (1996) The expression of MEF2 genes is implicated in CNS neuronal differentiation. *Brain Res. Mol. Brain Res.* **42**, 307–316.

Linseman D. A., Phelps R. A., Bouchard R. J., Le S. S., Laessig T. A., McClure M. L. and Heidenreich K. A. (2002) Insulin-like growth factor-I blocks Bcl-2 interacting mediator of cell death (Bim) induction and intrinsic death signaling in cerebellar granule neurons. *J. Neurosci.* **22**, 9287–9297.

Lyons G. E., Micales B. K., Schwarz J., Martin J. F. and Olson E. N. (1995) Expression of MEF2 genes in the mouse central nervous system suggests a role in neuronal maturation. *J. Neurosci.* **15**, 5727–5738.

Maggirwar S. B., Tong N., Ramirez S., Gelbard H. A. and Dewhurst S. (1999) HIV-1 Tat-mediated activation of glycogen synthase kinase-3beta contributes to Tat-mediated neurotoxicity. *J. Neurochem.* **73**, 578–586.

Manji H. K., Moore G. J. and Chen G. (2000) Lithium up-regulates the cytoprotective protein Bcl-2 in the CNS *in vivo*: a role for neurotrophic and neuroprotective effects in manic-depressive illness. *J. Clin. Psychiatry* **61**, 82–96.

Mao Z. and Wiedmann M. (1999) Calcineurin enhances MEF2 DNA binding activity in calcium-dependent survival of cerebellar granular neurons. *J. Biol. Chem.* **274**, 31102–31107.

Mao Z., Bonni A., Xia F., Nadal-Vicens M. and Greenberg M. E. (1999) Neuronal activity-dependent cell survival mediated by transcription factor MEF2. *Science* **286**, 785–790.

McKinsey T. A., Zhang C. L. and Olson E. N. (2002) MEF2: a calcium-dependent regulator of cell division, differentiation and death. *Trends Biochem. Sci.* **27**, 40–47.

Molkentin J. D., Li L. and Olson E. N. (1996) Phosphorylation of the MADS-Box transcription factor MEF2C enhances its DNA binding activity. *J. Biol. Chem.* **271**, 17199–17204.

Mora A., Gonzalez-Polo R. A., Fuentes J. M., Soler G. and Centeno F. (1999) Different mechanisms of protection against apoptosis by valproate and Li+. *Eur. J. Biochem.* **266**, 886–891.

Mora A., Sabio G., Gonzalez-Polo R. A., Cuenda A., Alessi D. R., Alonso J. C., Fuentes J. M., Soler G. and Centeno F. (2001) Lithium inhibits caspase 3 activation and dephosphorylation of PKB and GSK3 induced by K^+ deprivation in cerebellar granule cells. *J. Neurochem.* **78**, 199–206.

Mora A., Sabio G., Risco A. M., Cuenda A., Alonso J. C., Soler G. and Centeno F. (2002) Lithium blocks the PKB and GSK3 dephosphorylation induced by ceramide through protein phosphatase-2A. *Cell Signal.* **14**, 557–562.

Muller-Oerlinghausen B., Berghofer A. and Bauer M. (2002) Bipolar disorder. *Lancet* **359**, 241–247.

Nijhawan D., Honarpour N. and Wang X. (2000) Apoptosis in neural development and disease. *Annu. Rev. Neurosci.* **23**, 73–87.

Nonaka S., Hough C. J. and Chuang D. M. (1998a) Chronic lithium treatment robustly protects neurons in the central nervous system against excitotoxicity by inhibiting N-methyl-D-aspartate receptor-mediated calcium influx. *Proc. Natl Acad. Sci. USA* **95**, 2642–2647.

Nonaka S., Katsube N. and Chuang D. M. (1998b) Lithium protects rat cerebellar granule cells against apoptosis induced by anticonvulsants, phenytoin and carbamazepine. *J. Pharmacol. Exp. Ther.* **286**, 539–547.

Okamoto S., Li Z., Ju C., Scholzke M. N., Mathews E., Cui J., Salvesen G. S., Bossy-Wetzel E. and Lipton S. A. (2002) Dominant-interfering forms of MEF2 generated by caspase cleavage contribute to NMDA-induced neuronal apoptosis. *Proc. Natl Acad. Sci. USA* **99**, 3974–3979.

Phiel C. J. and Klein P. S. (2001) Molecular targets of lithium action. *Annu. Rev. Pharmacol. Toxicol.* **41**, 789–813.

Roth K. A. and D'Sa C. (2001) Apoptosis and brain development. *Ment. Retard. Dev. Disabil. Res. Rev.* **7**, 261–266.

Schierle G. S., Hansson O., Leist M., Nicotera P., Widner H. and Brundin P. (1999) Caspase inhibition reduces apoptosis and increases survival of nigral transplants. *Nat. Med.* **5**, 97–100.

Shi Y. (2002) Mechanisms of caspase activation and inhibition during apoptosis. *Mol. Cell* **9**, 459–470.

Shore P. and Sharrocks A. D. (1995) The MADS-box family of transcription factors. *Eur. J. Biochem.* **229**, 1–13.

Stambolic V., Ruel L. and Woodgett J. R. (1996) Lithium inhibits glycogen synthase kinase-3 activity and mimics wingless signaling in intact cells. *Curr. Biol.* **6**, 1664–1668.

Utton M. A., Vandecandelaere A., Wagner U., Reynolds C. H., Gibb G. M., Miller C. C., Bayley P. M. and Anderton B. H. (1997) Phosphorylation of tau by glycogen synthase kinase 3beta affects the ability of tau to promote microtubule self-assembly. *Biochem. J.* **323**, 741–747.

van Weeren P. C., de Bruyn K. M., de Vries-Smits A. M., van Lint J. and Burgering B. M. (1998) Essential role for protein kinase B (PKB) in insulin-induced glycogen synthase kinase 3 inactivation. Characterization of dominant-negative mutant of PKB. *J. Biol. Chem.* **273**, 13150–13156.

Woodgett J. R. (2001) Judging a protein by more than its name: GSK-3. *Sci. STKE* **2001**, RE12.

JBC Papers in Press. Published on August 1, 2003 as Manuscript M307245200

Inactivation of the Myocyte Enhancer Factor-2 Repressor Histone Deacetylase-5 by Endogenous Ca^{2+}/calmodulin-dependent Kinase II Promotes Depolarization-mediated Cerebellar Granule Neuron Survival

Daniel A. Linseman, Christopher M. Bartley, Shoshona S. Le, Tracey A. Laessig, Ron J. Bouchard, Mary Kay Meintzer, Mingtao Li, and Kim A. Heidenreich†

Department of Pharmacology, University of Colorado Health Sciences Center and the Denver Veterans Affairs Medical Center, Denver, Colorado 80262

†To whom correspondence should be addressed: Kim A. Heidenreich, Ph.D.
University of Colorado
Health Sciences Center
Department of Pharmacology (C236)
4200 East Ninth Avenue
Denver, CO 80262
Tel.: (303)-399-8020 (ext. 3891)
Fax: (303)-393-5271
E-mail: Kim.Heidenreich@UCHSC.edu

Running Title: CaMKII Blocks HDAC5 Repression of MEF2 Activity in CGNs

Cerebellar granule neuron (CGN) survival depends on activity of the myocyte enhancer factor-2 (MEF2) transcription factors. Neuronal MEF2 activity is regulated by depolarization via a mechanism that is presently unclear. Here, we show that depolarization-mediated MEF2 activity and CGN survival are compromised by overexpression of the MEF2 repressor histone deacetylase-5 (HDAC5). Furthermore, removal of depolarization induced rapid cytoplasm-to-nuclear translocation of endogenous HDAC5. This effect was mimicked by addition of the calcium/calmodulin-dependent kinase (CaMK) inhibitor KN93 to depolarizing medium. Removal of depolarization or KN93 addition resulted in dephosphorylation of HDAC5 and its co-precipitation with MEF2D. HDAC5 nuclear translocation triggered by KN93 induced a marked loss of MEF2 activity and subsequent apoptosis. To selectively decrease CaMKII, CGNs were incubated with an antisense oligonucleotide to CaMKIIα. This antisense decreased CaMKIIα expression and induced nuclear shuttling of HDAC5 in CGNs maintained in depolarizing medium. Selectivity of the CaMKIIα antisense was demonstrated by its lack of effect on CaMKIV-mediated CREB phosphorylation. Finally, antisense to CaMKIIα induced caspase-3 activation and apoptosis, whereas a missense control oligonucleotide had no effect on CGN survival. These results indicate that depolarization-mediated calcium influx acts through CaMKII to inhibit HDAC5, thereby sustaining high MEF2 activity in CGNs maintained under depolarizing conditions.

INTRODUCTION

Myocyte enhancer factor-2 (MEF2) transcription factors were originally identified in cells of skeletal, cardiac and smooth muscle lineages (1-4). In muscle, activity of MEF2 proteins is modulated by calcium-regulated signals that ultimately drive myogenic differentiation (5, 6). MEF2 proteins also play a critical role in the differentiation and survival of neurons in the developing central nervous system [CNS] (2, 7-11). In particular, MEF2 function is essential for activity-dependent neuronal survival mediated through the formation of proper synaptic contacts during CNS development (12).

In early postnatal cerebellum, transcripts for two mammalian MEF2 isoforms, MEF2A and MEF2D, are markedly increased in parallel with enhanced expression of the $GABA_A$ receptor $\alpha 6$ subunit, a marker for differentiation of mature cerebellar granule neurons [CGNs] (9). Similarly, primary cultures of CGNs, that require medium containing depolarizing extracellular potassium for their survival (13), demonstrate high levels of endogenous MEF2A and MEF2D proteins and MEF2 transcriptional activity. We have previously reported that MEF2A and MEF2D are phosphorylated and subsequently cleaved by caspases in CGNs that are deprived of depolarizing potassium (14). The resulting loss of MEF2 transcriptional activity contributes to CGN apoptosis under these conditions. Likewise, Gaudilliere et al. (15) recently showed that downregulation of MEF2A using RNA interference significantly compromises depolarization-mediated survival of CGNs. Thus, MEF2 proteins transduce activity-dependent calcium signals into an essential pro-survival pathway in CGNs.

The precise mechanism(s) by which calcium influx regulates MEF2 activity in CGNs is presently unclear. Previous work in muscle indicates that activity of the calcium/calmodulin-

dependent, serine/threonine phosphatase, calcineurin, is required for MEF2 function (16). Similarly, calcineurin positively regulates MEF2 DNA binding and transcriptional activity in CGNs (17). In muscle, calcineurin modulation of MEF2 activity is integrated with regulation by a pathway involving calcium/calmodulin-dependent protein kinase (CaMK) activity (5). Muscle MEF2 activity is repressed by interaction with class II histone deacetylases [HDACs] (18-20). Overexpression of constitutively-active CaMK isoforms I and IV in muscle and non-muscle cells (eg., COS or NIH3T3 fibroblasts) promotes serine phosphorylation of HDACs. Phosphorylation of HDACs induces their nuclear export and promotes their association with cytosolic scaffolding proteins of the 14-3-3 family, ultimately resulting in derepression of MEF2 activity (21). Although these overexpression studies suggest a role for CaMK regulation of HDAC function in muscle, the endogenous CaMK isoform involved has yet to be identified. Moreover, a role for endogenous CaMK activity in modulating MEF2 function in neurons has not yet been investigated.

Here, we show that depolarization-mediated MEF2 activity and CGN survival are compromised by overexpression of the class II HDAC, HDAC5. Moreover, removal of depolarizing potassium or addition of a CaMK inhibitor induces nuclear translocation of endogenous HDAC5, loss of MEF2 activity, and CGN apoptosis. Finally, antisense-mediated downregulation of CaMKIIα expression is sufficient to drive nuclear translocation of HDAC5 and induce CGN apoptosis under depolarizing conditions. These results demonstrate that CaMK-mediated inhibition of HDAC function plays a significant role in the calcium regulation of MEF2 activity and survival in CGNs. In addition, these data are the first to identify an endogenous CaMK isoform (CaMKII) that regulates HDAC function.

EXPERIMENTAL PROCEDURES

Materials-A truncated mutant of MEF2A lacking the C-terminal transcriptional activation domain, pcDNA3.1-MEF2A131, was kindly provided by Dr. Ron Prywes (Columbia University, NY). Empty pcDNA3.1 vector was obtained from Invitrogen (Grand Island, NY). Adenoviral green fluorescent protein (Ad-GFP) was a gift from Dr. Jerry Schaack (University of Colorado Health Sciences Center, Denver, CO). The pGL2-MEF2-luciferase reporter plasmid and HA-tagged HDAC5 and HDAC4 were provided by Dr. Saadi Khochbin (INSERM, France). Hoecsht dye number 33258, 4',6-diamidino-2-phenylindole (DAPI), monoclonal antibody to the Flag epitope, and monoclonal antibody to beta-tubulin were from Sigma (St. Louis, MO). Monoclonal antibody to the HA epitope and rabbit polyclonal antibodies to phospho-CREB (Ser133), HDAC4, and HDAC5 for immunocytochemistry were obtained from Cell Signaling Technologies (Beverly, MA). Rabbit polyclonal antibody to active (cleaved) caspase-3 was from Promega (Madison, WI). Monoclonal antibody to MEF2D for immunocytochemistry and western blotting was purchased from Transduction Laboratories (Lexington, KY). Monoclonal antibody to CaMKIIα for immunocytochemistry was from Chemicon (Temecula, CA). According to the manufacturer, this antibody may show some cross-reactivity with CaMKIIδ or γ subunits. FITC- and Cy3-conjugated secondary antibodies for immunofluorescence were from Jackson Immunoresearch Laboratories (West Grove, PA). Rabbit polyclonal antibody to MEF2 for immunoprecipitation, rabbit polyclonal antibody to HDAC5 for western blotting, and protein A/G-agarose were obtained from Santa Cruz Biotechnology (Santa Cruz, CA). Horseradish peroxidase-linked secondary antibodies and reagents for enhanced chemiluminescence detection were purchased from Amersham Biosciences (Piscataway, NJ). KN93, KN62, phosphorothioate 18 mer antisense oligonucleotide complementary to CaMKIIα subunit mRNA nucleotides 33-50

(unlabeled and FITC-labeled), and an unlabeled, scrambled, missense control oligonucleotide were from Calbiochem (La Jolla, CA). According to the manufacturer, this antisense construct is highly specific for the α subunit of CaMKII and does not affect CaMKIIβ expression.

Cell Culture-Rat CGNs were isolated from 7-day-old Sprague-Dawley rat pups (15-19g) as described previously (22). Briefly, neurons were plated on 35-mm diameter plastic dishes coated with poly-L-lysine at a density of $2.0x10^6$ cells/ml in basal modified Eagle's medium containing 10% fetal bovine serum, 25 mM KCl, 2 mM L-glutamine, and penicillin (100 units/ml)/ streptomycin (100 μg/ml) (Life Technologies, Grand Island, NY). Cytosine arabinoside (10 μM) was added to the culture medium 24 h after plating to limit the growth of non-neuronal cells. Using this protocol, the cultures were approximately 95% pure for granule neurons. In general, experiments were performed after 7 days in culture.

Preparation of Adenoviral Dominant-negative MEF2 and Adenoviral Infection-pcDNA3.1-MEF2A131 was tagged on the C-terminus with the Flag epitope by polymerase chain reaction. The resulting Flag-tagged construct was cloned into shuttle vector and Ad-Flag-MEF2A131 was prepared using the Ad-Easy adenovirus expression kit according to the manufacturer's instructions (Quantum Biotechnologies Inc., Canada). Recombinant adenoviruses were purified by cesium chloride gradient ultracentrifugation. The viral titer was determined by measuring the absorbance at 260 nm (where 1.0 absorbance units=$1x10^{12}$ particles/ml) and infectious particles were verified by plaque assay. Ad-GFP or Ad-Flag-MEF2A131 were added to CGN cultures on day 4 at a multiplicity of infection (m.o.i.) of 100. On day 7 (72 h post-infection), CGN apoptosis was assessed in GFP-positive or Flag-immunoreactive cells by DAPI staining.

Quantification of Apoptosis-Apoptosis was assessed by fixing CGNs in 4% paraformaldehyde and staining nuclei with either Hoechst dye (non-permeabilized cells) or DAPI (permeabilized

cells for immunocytochemistry). Cells were considered apoptotic if their nuclei were either condensed or fragmented. In general, approximately 500 cells from at least two fields of a 35-mm well were counted. For immunocytochemical studies where cells were plated on glass coverslips, approximately 100-200 cells from two-three coverslips per treatment group were counted. Data are presented as the percentage of cells in a given treatment group which were scored as apoptotic. Experiments were performed on cells isolated from at least three independent preparations.

Immunocytochemistry-CGNs were cultured on polyethyleneimine-coated glass cover slips at a density of approximately $2.5x10^5$ cells per coverslip. Following incubation as described in Results, cells were fixed in 4% paraformaldehyde and were then permeabilized and blocked in PBS (pH 7.4) containing 0.2% Triton X-100 and 5% BSA. Cells were then incubated for approximately 16 h at 4°C with primary antibody diluted in PBS containing 0.2% Triton X-100 and 2% BSA. The primary antibody was aspirated and the cells were washed five times with PBS. The cells were then incubated with either Cy3-conjugated or FITC-conjugated secondary antibodies and DAPI for 1 h at room temperature. CGNs were then washed five more times with PBS and coverslips were adhered to glass slides in mounting medium (0.1% *p*-phenylenediamine in 75% glycerol in PBS). Fluorescent images were captured using a 63X oil immersion objective on a Zeiss Axioplan 2 microscope equipped with a Cooke Sensicam deep-cooled CCD camera and a Slidebook software analysis program for digital deconvolution (Intelligent Imaging Innovations Inc., Denver, CO).

Preparation of CGN Cell Extracts-After incubation for the indicated times and with the reagents specified in Results, the culture medium was aspirated; the cells were washed once with 2 ml of ice-cold PBS, pH 7.4, placed on ice, and scraped into lysis buffer (200µl/35-mm well)

containing 20 mM HEPES (pH 7.4), 1% Triton X-100, 50 mM NaCl, 1 mM EGTA, 5 mM β-glycerophosphate, 30 mM sodium pyrophosphate, 100 μM sodium orthovanadate, 1 mM phenylmethylsulfonyl fluoride, 10 μg/ml leupeptin, and 10 μg/ml aprotinin. Cell debris was removed by centrifugation at 6,000 x g for 3 min and the protein concentration of the supernatant was determined using a commercially available protein assay kit (Pierce, Rockford, IL). Aliquots (~150 μg) of supernatant protein were diluted to a final concentration of 1X SDS-PAGE sample buffer, boiled for 5 min, and electrophoresed through 7.5% polyacrylamide gels. Proteins were transferred to polyvinylidene difluoride (PVDF) membranes (Millipore, Bedford, MA) and processed for immunoblot analysis.

Western Blot Analysis-Nonspecific binding sites were blocked in PBS (pH 7.4) containing 0.1% Tween 20 (PBS-T) and 1% BSA for 1 h at room temperature. Primary antibodies were diluted in blocking solution and incubated with the membranes for 1 h. Excess primary antibody was removed by washing the membranes three times in PBS-T. The blots were then incubated with the appropriate horseradish peroxidase-conjugated secondary antibody diluted in PBS-T for 1 h and were subsequently washed three times in PBS-T. Immunoreactive proteins were detected by enhanced chemiluminescence. Autoluminograms shown are representative of at least three independent experiments.

Immunoprecipitation of MEF2D-CGN lysates were prepared as described above, except in lysis buffer containing 0.1% Triton X-100. Four μg of polyclonal antibody against MEF2D was added to 500 μl of lysate (approximately 1 μg/μl CGN protein concentration), and samples were mixed for 16 h at 4°C by continuous inversion. Agarose-conjugated protein A/G (40 μl) was added and samples were mixed for a further 4 h. Immune complexes were pelleted, washed three times with lysis buffer containing 0.1% Triton X-100, and boiled in 1X SDS-PAGE sample

buffer. Immune complexes were resolved on 7.5% polyacrylamide gels, transferred to PVDF, and immunoblotted for MEF2D and HDAC5.

CGN Transfection and Reporter Gene Expression-CGNs were transiently transfected using a calcium phosphate co-precipitation method described previously (14). Cells were co-transfected with 1 μg of MEF2-luciferase expression plasmid (pGL2-MEF2-luc), 1 μg of pCMV-β-gal as an internal control for transfection efficiency, and 2 μg of either pcDNA3.1, MEF2A131, or HA-tagged HDAC5. The total amount of DNA for each transfection was kept constant. Following transfection, neurons were placed in conditioned medium and the medium was subsequently changed to serum-free containing either 25 mM KCl or 5 mM KCl. After incubation, cell extracts were prepared using reporter lysis buffer and the activities of luciferase and β-galactosidase were measured with the respective enzyme assay system kits (Promega).

Incubation with Antisense Oligonucleotides to CaMKIIα-Phosphorothioate, FITC-labeled or unlabeled, antisense oligonucleotides to CaMKIIα, or a scrambled missense control oligonucleotide, were added directly to the culture medium (each at a final concentration of 1 μM), as was previously described for primary hippocampal neuronal cultures (23). Following incubation for 8 to 24 h, cells were processed for immunocytochemical analysis and/or quantification of apoptosis, as described in the Results.

Data Analysis-The results shown represent the means ± SEM for the number (*n*) of independent experiments that were performed. Statistical differences between the means of unpaired sets of data were evaluated by one-way ANOVA, followed by a *post hoc* Dunnett's test. A p value of <0.01 was considered statistically significant.

RESULTS

Adenoviral Expression of a Dominant-negative MEF2 Mutant Blocks Depolarization-mediated Survival of CGNs-In CGNs co-transfected with a MEF2-luciferase reporter (24) and empty pcDNA3.1 vector, removal of the depolarization stimulus resulted in a dramatic loss of MEF2 activity (14±2% of control, $p<0.01$, Fig. 1*A*). This effect was mimicked under depolarizing conditions by co-transfection with a truncated, dominant-negative form of MEF2 (MEF2A131) that lacks the transcriptional activation domain. Expression of MEF2A131 decreased endogenous MEF2 activity in the presence of depolarization to 39±6% ($p<0.01$) of that observed in cells transfected with empty vector (Fig. 1*A*). Thus, dominant-negative MEF2 competes with endogenous MEF2 transcription factors for DNA binding, resulting in a loss of endogenous MEF2 activity.

Previous studies showing that MEF2 transcription factors are critical for CGN survival utilized either transient transfection protocols of MEF2 mutants (12, 14) or, more recently, RNA interference methodology to knock down expression of MEF2 proteins (15). One limitation of each of these approaches is that only a small percentage (usually <5%) of the CGNs are transfected. As a means of interfering with MEF2 activity in a larger, and possibly more representative, percentage of the CGN culture, we prepared a Flag epitope-tagged MEF2A131 and expressed this construct in adenovirus. CGNs maintained in depolarizing medium were then infected with either adenovirus expressing green fluorescent protein (Ad-GFP, to serve as a control for adenoviral infection) or expressing the Flag-tagged dominant-negative MEF2 (Ad-Flag-MEF2A131). Each adenovirus was infected into the cells at a m.o.i. of 100 (equivalent to 10,000 infectious particles per cell). At this titer, the relative infection efficiency observed over

three independent experiments was approximately 35% for Ad-Flag-MEF2A131. Following infection, cells were incubated for 72 h and MEF2A131-expressing cells were identified by immunocytochemistry with a monoclonal anti-Flag and a Cy3-conjugated secondary antibody. GFP-positive cells were detected by fluorescence under a FITC filter. Apoptosis was quantified by staining nuclei with DAPI and counting the percentage of GFP-positive or Flag-MEF2A131-positive cells containing condensed and/or fragmented chromatin. As shown in Fig. 1*B*, infection with Ad-GFP did not result in significant CGN apoptosis (2±1%), whereas cells expressing the Flag-MEF2A131 demonstrated massive apoptosis (89±7%), even in the presence of depolarization. In agreement with previous work (12, 14, 15), our results using an adenoviral dominant-negative MEF2 mutant demonstrate that MEF2 transcriptional activity is a critical component of depolarization-mediated survival signaling in CGNs.

Overexpression of the MEF2 Repressor HDAC5 Induces CGN Apoptosis in Depolarizing Medium-The activity of MEF2 transcription factors is repressed in skeletal, cardiac, and smooth muscle by members of the class II family of HDACs including HDAC4, 5, 7 and 9 (reviewed in 6). Consistent with a potential role for HDAC regulation of MEF2 activity in CGNs, overexpression of HA-tagged HDAC5 significantly decreased MEF2-driven luciferase activity (56±6% of the empty vector control, $p<0.01$) in cells cultured in the presence of depolarizing potassium (Fig. 2*A*). As a result of the loss in endogenous MEF2 activity, overexpression of HDAC5 induced significant CGN apoptosis (42±1% compared to 17±1% in cells transfected with empty vector, $p<0.01$, Fig. 2*B*). Similar results were obtained following transfection with another class II family member, HDAC4 (data not shown). Thus, depolarization-mediated MEF2 activity and CGN survival are compromised by overexpression of HDAC transcriptional repressors.

Removal of Depolarizing Potassium or CaMK Inhibition Induces Cytoplasm-to-Nuclear Translocation of Endogenous HDAC5-We next examined the subcellular localization of endogenous HDAC5 and MEF2D in CGNs maintained in either depolarizing or non-depolarizing medium. Cells cultured in the presence of depolarizing extracellular potassium demonstrated immunocytochemical localization of HDAC5 in the cytoplasm with little to no immunoreactivity observed in nuclei. In contrast, MEF2D was localized exclusively to nuclei, and therefore, there was essentially no overlapping staining for MEF2D and HDAC5 in control CGNs (Fig. 3, *left panels*). Removal of depolarizing potassium for 4 h induced a dramatic cytoplasm-to-nuclear translocation of endogenous HDAC5, resulting in significant overlap of MEF2D and HDAC5 staining (Fig. 3, *middle panels*).

Previous work in skeletal and cardiac muscle has shown that the subcellular localization of class II HDACs during muscle differentiation can be regulated by CaMK activity (19, 20). Overexpression of either constitutively-active CaMKI or CaMKIV induced phosphorylation of two serine residues (Ser259 and Ser498 in HDAC5) resulting in docking of HDACs to cytoplasmic scaffolding proteins of the 14-3-3 family (21). In this manner, CaMK-mediated phosphorylation of HDACs results in their nuclear exclusion, allowing for derepression of MEF2 activity that is required for muscle differentiation. To examine if depolarization maintains HDAC5 in the cytoplasm of CGNs via endogenous CaMK activity, cells were incubated in depolarizing medium containing the CaMK inhibitor KN93. Inclusion of KN93 mimicked the effect of removing the depolarization stimulus, resulting in nuclear translocation of HDAC5 and its co-localization with MEF2D (Fig. 3, *right panels*). In a similar manner, either removal of the depolarization stimulus or addition of KN93 also induced the nuclear translocation of HDAC4 in

CGNs (data not shown). These data suggest that depolarization promotes the nuclear exclusion of HDAC5 and 4 via the activity of an endogenous CaMK.

CaMK Inhibition Results in Dephosphorylation of HDAC5 and Its Association with MEF2D- To evaluate the phosphorylation status of endogenous HDAC5 in CGNs, we examined the electrophoretic mobility of HDAC5 on SDS-polyacrylamide gels. In cell lysates obtained from CGNs maintained in depolarizing medium, HDAC5 appeared as a broad band or doublet on western blots (Fig. 4*A*, *first lane*). Removal of depolarizing potassium (Fig. 4*A*, *second lane*) or addition of the CaMK inhibitor, KN93 (Fig. 4*A*, *third lane*), increased the electrophoretic mobility of HDAC5 and resulted in the disappearance of the upper band of the doublet, indicative of a loss of the phosphorylated HDAC5 species. These results suggest that a CaMK activated by depolarization in CGNs regulates the phosphorylation status of HDAC5.

To determine if the dephosphorylation and nuclear translocation of HDAC5 induced by removal of the depolarization stimulus or CaMK inhibition permits its direct interaction with nuclear MEF2 proteins, we performed co-immunoprecipitation experiments. MEF2D immune complexes isolated from CGNs maintained in depolarizing medium did not contain any detectable HDAC5 (Fig. 4*B*, *first lane*). This finding is consistent with the immunocytochemical data shown in Fig. 3 that demonstrated little co-localization of MEF2D and HDAC5 under control conditions. In contrast, MEF2D isolated from cells incubated in either non-depolarizing medium or in the presence of KN93 co-precipitated with HDAC5 (Fig. 4*B*, *second and third lanes*). Note that the electrophoretic mobility of MEF2D was significantly retarded in cells cultured in non-depolarizing medium, consistent with its hyperphosphorylation under these conditions as we have previously reported (14, 25). Interestingly, CaMK inhibition also resulted in some decreased mobility of MEF2D, suggesting that HDAC5 association with MEF2D may

alter the accessibility of MEF2D to phosphatases (eg., calcineurin). Collectively, these data suggest that inhibition of CaMK activity in CGNs promotes the dephosphorylation and nuclear translocation of HDAC5, ultimately resulting in its co-association with MEF2 transcription factors.

CaMK Inhibition Blocks Depolarization-mediated MEF2 Activity and Survival of CGNs-To determine the functional consequences of HDAC5 nuclear translocation and its interaction with MEF2D, we next examined the effects of CaMK inhibition on MEF2 transcriptional activity and CGN survival. Incubation of CGNs with the CaMK inhibitors, KN93 or KN62, induced a marked decrease in endogenous MEF2 activity measured with a MEF2-driven luciferase reporter gene (Fig. 5*A*). Moreover, CaMK inhibition induced significant CGN apoptosis in the presence of depolarizing potassium (Fig. 5*B*). Apoptosis induced by KN93 was characterized morphologically by substantial chromatin fragmentation, microtubule disruption, and caspase-3 activation (Fig. 5*C*). These results demonstrate that inhibition of endogenous CaMK activity is sufficient to induce nuclear translocation of the MEF2 repressor, HDAC5, resulting in a loss of MEF2 activity and induction of CGN apoptosis.

Antisense to CaMKIIα Induces Nuclear Translocation of HDAC5-Previous work in skeletal muscle describing the regulation of HDAC localization by CaMK activity has relied on overexpression of various CaMK isoforms (19). To date, identification of the endogenous CaMK isozyme(s) involved in HDAC regulation has not been reported. The CaMK enzyme family is made up of several distinct isoforms, including CaMK I, II and IV, with four distinct genes (α, β, δ, γ) coding for members of the CaMKII subfamily (26). Of the many CaMK isozymes identified, only CaMKIIα is exclusively expressed in the brain (27). The CaMK inhibitors, KN93 and KN62, lack isozyme-specificity and have been shown to inhibit the

activities of CaMKI, II and IV (28, 29). To selectively evaluate a role for CaMKII in regulating the subcellular localization of HDAC5 in CGNs, cells were incubated with a CaMKIIα-specific antisense oligonucleotide. This antisense construct has previously been reported to reduce CaMKIIα expression and induce epileptiform activity in primary cultured hippocampal neurons (23).

Addition of 1 μM of a FITC-labeled, phosphorothioate antisense oligonucleotide to CaMKIIα to CGN cultures for 8 h resulted in a marked reduction in CaMKIIα immunoreactivity in cells expressing the FITC-antisense when compared to cells in the same field that did not take up the antisense construct (Fig. 6*A*). In general, approximately 25% of the CGNs took up the FITC-labeled CaMKIIα antisense following 8 to 24 h of incubation at a concentration of 1 μM. Granule neurons expressing the FITC-CaMKIIα antisense demonstrated a dramatic redistribution of endogenous HDAC5 from the cytosol to the nucleus, even when maintained in depolarizing medium (Fig. 6*B*). In contrast, cells in the same field that did not express the antisense showed HDAC5 localization that was extensively cytoplasmic. These results indicate that the endogenous CaMKII isozyme regulates depolarization-mediated cytoplasmic localization of HDAC5 in CGNs.

Antisense to CaMKIIα Does Not Affect CaMKIV-dependent Phosphorylation of CREB-To confirm the selectivity of the CaMKIIα antisense, we examined its effects on phosphorylation of the CaMKIV substrate, cAMP-response element binding protein (CREB). A recent study demonstrated that CaMKIV activity promotes depolarization-mediated CGN survival via phosphorylation of CREB on the activating Ser133 (30). As shown in Fig. 7*A* (*upper panels*), CREB phosphorylation on Ser133 was high in CGNs maintained in depolarizing medium. Addition of the CaMK inhibitor, KN93, resulted in a complete loss of CREB phosphorylation

(Fig. 7*A*, *lower panels*). This latter result is consistent with the relative non-selectivity of KN93 for the various isoforms of CaMK (28, 29). In contrast, the FITC-labeled antisense to CaMKIIα had no significant effect on CREB phosphorylation after 8 h of incubation (Fig. 7*B*, *compare the CREB phosphorylation in FITC-positive cells to that in antisense-negative cells*), a time point at which it caused significant nuclear translocation of HDAC5 (see Fig. 6*B*). These results demonstrate the selectivity of the CaMKIIα antisense. In addition, they suggest that CaMKII regulation of HDAC localization is an alternative calcium-dependent pathway to CaMKIV/CREB for mediating CGN survival.

Antisense to CaMKIIα Induces Caspase-3 Activation and Apoptosis of CGNs-To determine the extent of CGN apoptosis induced by antisense treatment, we quantified the number of cells with condensed and/or fragmented nuclei in cultures incubated with either the CaMKIIα antisense or a missense control oligonucleotide. Because the missense oligonucleotide was not fluorescently labeled, an unlabeled antisense was utilized in these experiments. The overall basal apoptosis of control CGN cultures maintained in depolarizing medium measured 9±1% (n=3 experiments, performed in triplicate) on day 8 *in vitro*. On day 7 *in vitro*, cells were exposed to either the CaMKIIα antisense or a control missense oligonucleotide for 24 h, each at a final concentration of 1 μM. CGN cultures incubated with the antisense to CaMKIIα demonstrated an overall apoptosis of 33±11% (n=3), whereas cells treated with the missense construct showed apoptosis comparable to the untreated controls (8±1%, n=3). These results demonstrate that the scrambled missense had no discernible effect on CGN survival when added at the same concentration as the antisense construct.

As mentioned previously, in a given experiment approximately 25% of the entire culture took up the FITC-labeled antisense. Therefore, the overall apoptosis observed in CGN cultures

incubated with the unlabeled antisense was consistent with near complete apoptosis of the antisense-positive cells. To verify this result, we quantitated the fraction of FITC-positive cells that were apoptotic following a 24 h incubation with 1 μM of the FITC-labeled CaMKIIα antisense. Greater than 95% of the FITC-positive (antisense-positive) CGNs were apoptotic under these conditions, as assessed by nuclear morphology. In agreement with these findings, essentially every cell that accumulated the FITC-labeled antisense to CaMKIIα for 24 h demonstrated substantial immunoreactivity for active (cleaved) caspase-3, whereas surrounding antisense-negative cells in the same field were devoid of active caspase-3 staining (Fig. 8). Thus, antisense-mediated depletion of CaMKIIα inhibits depolarization-dependent survival signaling and induces CGN apoptosis.

DISCUSSION

MEF2 proteins are members of the MADS (MCM1-agamous-deficiens-serum response factor) family of transcription factors (31-33). The mammalian MEF2 family consists of four distinct genes (A, B, C, D) that each code for multiple splice variants (31, 34). MEF2 proteins play a key role in the differentiation and survival of neurons during CNS development. The expression of MEF2 proteins in the developing CNS is regulated temporally and spatially in an isoform-specific manner, and coincides with neuronal maturation. For example, cerebral cortical neuron development is associated with changes in the expression of MEF2C (35-37), whereas CGN maturation is coupled to enhanced expression of MEF2A and MEF2D (9). Their differential tissue distribution suggests that MEF2 proteins may be regulated in an isoform-specific manner. Indeed this is the case in CGNs where MEF2A and MEF2D are phosphorylated and ultimately cleaved by caspases following removal of depolarizing potassium, whereas MEF2B and MEF2C are not modified in this manner (14). These findings indicate that signal transduction pathways which regulate MEF2 activity display both tissue-specific and isoform-specific properties.

To date, the modulation of MEF2 activity by calcium-regulated signals has largely been studied in muscle cells in which MEF2 proteins act as key regulators of myogenic differentiation (5, 6). Given that distinct MEF2 isoforms can be regulated differently, even within the same cell (14), it is unknown if signaling pathways that modulate MEF2 proteins in muscle will necessarily translate directly into neurons. Moreover, MEF2 regulation in muscle has been investigated during either myogenic differentiation (38-40) or hypertrophy (41-43). In contrast, a principal function of MEF2 proteins in neurons is to promote activity-dependent cell survival

(12, 15). The signaling pathways that are invoked during muscle differentiation or hypertrophy may be different from those generated in neurons by activity-dependent calcium influx.

Despite these important differences, at least two signaling pathways have been implicated in MEF2 regulation in both muscle and neurons. First, the stress-activated protein kinase, p38 MAP kinase, stimulates MEF2 activity in hypertrophic muscle (41, 44) and in CGNs responding to depolarization (12). Second, the phosphatase, calcineurin, positively regulates MEF2 activity in both muscle cells (16, 45, 46) and CGNs (17). In muscle, p38 MAP kinase and calcineurin cooperate with CaMK to maximally activate MEF2 transcriptional activity (5, 47).

CaMK-mediated regulation of MEF2 activity in muscle has been proposed to occur primarily by an indirect mechanism. Class II HDAC proteins act as endogenous repressors of MEF2 transcriptional activity by directly interacting with MEF2 proteins in the nucleus (40). Overexpression of active CaMK I or IV derepresses MEF2 activity in muscle by phosphorylating HDACs and promoting their nuclear export (18, 19). CaMK-mediated phosphorylation of HDACs on specific serine residues promotes HDAC binding to cytosolic scaffolding proteins of the 14-3-3 family, resulting in sequestration of HDACs in the cytoplasm (21, 48). In the present study, we demonstrate that *endogenous* CaMKII plays a key role in CGNs to exclude HDACs from the nucleus, and in turn, to derepress MEF2 activity and promote cell survival.

We initially confirmed an essential role for MEF2 activity in CGN survival by demonstrating that adenoviral infection of a truncated, dominant-interfering mutant of MEF2 (MEF2A131) is sufficient to induce apoptosis of CGNs that are maintained in depolarizing medium. To examine a potential role for HDACs in the regulation of MEF2 activity in CGNs, the effects of overexpressing the class II HDAC, HDAC5, on MEF2 activity and CGN survival were assessed.

Transient transfection of CGNs with HDAC5 induced a significant loss of endogenous MEF2 transcriptional activity and substantial apoptosis under depolarizing conditions.

To directly investigate the involvement of endogenous HDAC5 in regulating MEF2 activity, we next analyzed the subcellular localization of MEF2D and HDAC5 in CGNs. As expected, the transcription factor MEF2D was exclusively nuclear under all conditions tested. In contrast, endogenous HDAC5 was extensively cytoplasmic in CGNs cultured in depolarizing medium. Either removal of the depolarization stimulus or addition of the CaMK inhibitor, KN93, induced a marked translocation of HDAC5 into the nucleus where it co-localized with MEF2D. While this paper was in preparation, Chawla et al. (49) described a partial inhibition of HDAC5 nuclear export in hippocampal neurons following incubation with a similar CaMK inhibitor, KN62. However, these authors did not examine the effects of CaMK inhibition on MEF2 activity or neuronal survival downstream of HDAC shuttling. In the current study performed in CGNs, the nuclear translocation of HDAC5 was associated with its enhanced mobility on polyacrylamide gels (consistent with its dephosphorylation) and its co-precipitation with MEF2D. Collectively, these data indicate that depolarization-mediated calcium influx stimulates the activity of an endogenous CaMK that, in turn, phosphorylates HDAC5 and inhibits its nuclear localization.

The ultimate consequence of removing the depolarization stimulus from cerebellar cultures is the apoptotic death of CGNs (13, 50). Loss of MEF2 transcriptional activity precedes CGN death under non-depolarizing conditions and apoptosis can be attenuated by expression of a constitutively-active MEF2 mutant (12, 14). Previous work suggests a role for CaMK activity in depolarization-mediated survival of CGNs (51). In agreement with this, addition of the CaMK inhibitors, KN93 or KN62, to CGNs maintained in depolarizing medium mimicked the loss of MEF2 activity and induction of CGN apoptosis that normally occur under non-depolarizing

conditions. The ability of CaMK inhibitors to induce the nuclear translocation of HDAC5 and the consequent loss of MEF2 activity suggests that an endogenous CaMK isozyme(s) actively derepresses MEF2-dependent transcription of putative pro-survival genes in CGNs maintained in depolarizing medium.

The regulation of HDAC localization by CaMK in muscle and other non-neuronal cells has been analyzed primarily by overexpression of various CaMK isoforms, including constitutively-active mutants of CaMKI and IV (19, 48). Thus far, the endogenous CaMK isozyme(s) involved in HDAC regulation has not been identified. CaMKIIα is a brain-specific CaMK isozyme best known for its role in hippocampal long term potentiation, a cellular model of learning and memory (52). However, CaMKIIα is also expressed in cerebellum (53), where it has been implicated in CGN neurite outgrowth (51, 54). Since the CaMK inhibitors, KN93 and KN62, lack isozyme selectivity (28, 29), we utilized an antisense strategy to specifically interfere with CaMKII signaling in CGNs.

Recently, direct addition of a phosphorothioate antisense oligonucleotide to CaMKIIα to primary hippocampal neurons was shown to substantially decrease CaMKIIα expression *in vitro* (23). We found that addition of an identical FITC-labeled CaMKIIα antisense oligonucleotide to CGN cultures maintained in depolarizing medium resulted in a marked loss of CaMKIIα immunoreactivity and nuclear translocation of HDAC5. In contrast, this antisense construct had no discernible effect on phosphorylation of the CaMKIV substrate, CREB, demonstrating the specificity of the oligonucleotide for CaMKII. Finally, antisense to CaMKIIα induced caspase-3 activation and apoptosis, whereas a scrambled missense control oligonucleotide had no effect on CGN survival. Collectively, these results indicate that CaMKII is an important endogenous regulator of HDAC5 localization and MEF2-mediated survival of CGNs.

Our data implicating CaMKII in neuronal survival support previous findings suggesting that reductions in CaMKII activity contribute to neuronal death induced by excitotoxicity or ischemia *in vitro* and *in vivo* (55-58). Since loss of MEF2 activity has recently been implicated in excitotoxic and ischemic neuronal death (59), it will be interesting to determine if nuclear localization of HDAC5 (or other class II family members) is also detected in these conditions. One implication of this would be that HDAC repression may act in a coordinated manner with caspase-mediated degradation of MEF2 proteins to deplete MEF2 activity during neuronal apoptosis (14, 59).

In summary, data in the present study establish a principal role for endogenous CaMKII in the modulation of HDAC5 localization in CGNs. By phosphorylating HDAC5, CaMKII excludes this transcriptional repressor from the nucleus and prevents it from interacting with MEF2D. In this manner, CaMKII works in a coordinated fashion with other signaling molecules, such as calcineurin, to maximize MEF2-dependent transcription of putative pro-survival genes. These results add further insight into the complexities of MEF2 regulation in neurons and suggest that multiple calcium-regulated pathways act in concert to modulate the function of these important transcription factors during CNS development.

Acknowledgments-This work was supported by Department of Veterans Affairs Merit Awards (K.A.H. and D.A.L.), a Department of Defense Grant DAMD17-99-1-9481 (K.A.H.), an NIH Grant NS38619-01A1 (K.A.H.), and a Department of Veterans Affairs Research Enhancement Award Program (K.A.H. and D.A.L.).

REFERENCES

1. Breitbart, R. E., Liang, C. S., Smoot, L. B., Laheru, D. A., Mahdavi, V., and Nadal-Ginard, B. (1993) *Development* **118,** 1095-1106
2. McDermott, J. C., Cardoso, M. C., Yu, Y. T., Andres, V., Leifer, D., Krainc, D., Lipton, S. A., and Nadal-Ginard, B. (1993) *Mol. Cell. Biol.* **13,** 2564-2577
3. Edmondson, D. G., Lyons, G. E., Martin, J. F., and Olson, E. N. (1994) *Development* **120,** 1251-1263
4. Firulli, A. B., Miano, J. M., Bi, W., Johnson, A. D., Casscells, W., Olson, E. N., and Schwarz, J. J. (1996) *Circ. Res.* **78,** 196-204
5. Wu, H., Naya, F. J., McKinsey, T. A., Mercer, B., Shelton, J. M., Chin, E. R., Simard, A. R., Michel, R. N., Bassel-Duby, R., Olson, E. N., and Williams, R. S. (2000) *EMBO J.* **19,** 1963-1973
6. McKinsey, T. A., Zhang, C. L., and Olson, E. N. (2002) *Trends Biochem. Sci.* **27,** 40-47
7. Ikeshima, H., Imai, S., Shimoda, K., Hata, J., and Takano, T. (1995) *Neurosci. Lett.* **200,** 117-120
8. Lyons, G. E., Micales, B. K., Schwarz, J., Martin, J. F., and Olson, E. N. (1995) *J. Neurosci.* **15,** 5727-5738
9. Lin, X., Shah, S., and Bulleit, R. F. (1996) *Brain Res. Mol. Brain Res.* **42,** 307-316
10. Krainc, D., Bai, G., Okamoto, S., Carles, M., Kusiak, J. W., Brent, R. N., and Lipton, S. A. (1998) *J. Biol. Chem.* **273,** 26218-26224
11. Okamoto, S., Krainc, D., Sherman, K., and Lipton, S. A. (2000) *Proc. Natl. Acad. Sci. USA* **97,** 7561-7566

12. Mao, Z., Bonni, A., Xia, F., Nadal-Vicens, M., and Greenberg, M. E. (1999) *Science* **286,** 785-790

13. D'Mello, S. R., Galli, C., Ciotti, T., and Calissano, P. (1993) *Proc. Natl. Acad. Sci. USA* **90,** 10989-10993

14. Li, M., Linseman, D. A., Allen, M. P., Meintzer, M. K., Wang, X., Laessig, T., Wierman, M. E., and Heidenreich, K. A. (2001) *J. Neurosci.* **21,** 6544-6552

15. Guadilliere, B., Shi, Y., and Bonni, A. (2002) *J. Biol. Chem.* **277,** 46442-46446

16. Wu, H., Rothermel, B., Kanatous, S., Rosenberg, P., Naya, F. J., Shelton, J. M., Hutcheson, K. A., DiMaio, J. M., Olson, E. N., Bassel-Duby, R., and Williams, R. S. (2001) *EMBO J.* **20,** 6414-6423

17. Mao, Z., and Wiedmann, M. (1999) *J. Biol. Chem.* **274,** 31102-31107

18. Lu, J., McKinsey, T. A., Nicol, R. L., and Olson, E. N. (2000) *Proc. Natl. Acad. Sci. USA* **97,** 4070-4075

19. McKinsey, T. A., Zhang, C. L., Lu, J., and Olson, E. N. (2000) *Nature* **408,** 106-111

20. Dressel, U., Bailey, P. J., Wang, S. C., Downes, M., Evans, R. M., and Muscat, G. E. (2001) *J. Biol. Chem.* **276,** 17007-17013

21. McKinsey, T. A., Zhang, C. L., and Olson, E. N. (2000) *Proc. Natl. Acad. Sci. USA* **97,** 14400-14405

22. Li, M., Wang, X., Meintzer, M. K., Laessig, T., Birnbaum, M. J., and Heidenreich, K. A. (2000) *Mol. Cell. Biol.* **20,** 9356-9363

23. Churn, S. B., Sombati, S., Jakoi, E. R., Sievert, L., and DeLorenzo, R. J. (2000) *Proc. Natl. Acad. Sci. USA* **97,** 5604-5609

24. Lemercier, C., Verdel, A., Galloo, B., Curtet, S., Brocard, M. P., and Khochbin, S. (2000) *J. Biol. Chem.* **275,** 15594-15599

25. Linseman, D. A., Cornejo, B. J., Le, S. S., Meintzer, M. K., Laessig, T. A., Bouchard, R. J., and Heidenreich, K. A. (2003) *J. Neurochem.* **85,** 1488-1499

26. Soderling, T. R., Chang, B., and Brickey, D. (2001) *J. Biol. Chem.* **276,** 3719-3722

27. Burgin, K. E., Waxham, M. N., Rickling, S., Westgate, S. A., Mobley, W. C., and Kelly, P. T. (1990) *J. Neurosci.* **10,** 1788-1798

28. Kato, T., Sano, M., Miyoshi, S., Sato, T., Hakuno, D., Ishida, H., Kinoshita-Nakazawa, H., Fukuda, K., and Ogawa, S. (2000) *Circ. Res.* **87,** 937-945

29. Condon, J. C., Pezzi, V., Drummond, B. M., Yin, S., and Rainey, W. E. (2002) *Endocrinology* **143,** 3651-3657

30. See, V., Boutillier, A. L., Bito, H., and Loeffler, J. P. (2001) *FASEB J.* **15,** 134-144

31. Yu, Y. T., Breitbart, R. E., Smoot, L. B., Lee, Y., Mahdavi, V., and Nadal-Ginard, B. (1992) *Genes Dev.* **6,** 1783-1798

32. Shore, P., and Sharrocks, A. D. (1995) *Eur. J. Biochem.* **229,** 1-13

33. Molkentin, J. D., and Olson, E. N. (1996) *Proc. Natl. Acad. Sci. USA* **93,** 9366-9373

34. Martin, J. F., Miano, J. M., Hustad, C. M., Copeland, N. G., Jenkins, N. A., and Olson, E. N. (1994) *Mol. Cell. Biol.* **14,** 1647-1656

35. Leifer, D., Krainc, D., Yu, Y. T., McDermott, J., Breitbart, R. E., Heng, J., Neve, R. L., Kosofsky, B., Nadal-Ginard, B., and Lipton, S. A. (1993) *Proc. Natl. Acad. Sci. USA* **90,** 1546-1550

36. Leifer, D., Golden, J., and Kowall, N. W. (1994) *Neuroscience* **63,** 1067-1079

37. Leifer, D., Li, Y. L., and Wehr, K. (1997) *J. Mol. Neurosci.* **8,** 131-143

38. Black, B. L., and Olson, E. N. (1998) *Annu. Rev. Cell Dev. Biol.* **14,** 167-196

39. Puri, P. L., and Sartorelli, V. (2000) *J. Cell Physiol.* **185,** 155-173

40. McKinsey, T. A., Zhang, C. L., and Olson, E. N. (2001) *Curr. Opin. Genet. Dev.* **11,** 497-504

41. Kolodziejczyk, S. M., Wang, L., Balazsi, K., DeRepentigny, Y., Kothary, R., and Megeney, L. A. (1999) *Curr. Biol.* **9,** 1203-1206

42. Passier, R., Zeng, H., Frey, N., Naya, F. J., Nicol, R. L., McKinsey, T. A., Overbeek, P., Richardson, J. A., Grant, S. R., and Olson, E. N. (2000) *J. Clin. Invest.* **105,** 1395-1406

43. Zhang, C. L., McKinsey, T. A., Chang, S., Antos, C. L., Hill, J. A., and Olson, E. N. (2002) *Cell* **110,** 479-488

44. Han, J., and Molkentin, J. D. (2000) *Trends Cardiovasc. Med.* **10,** 19-22

45. Chin, E. R., Olson, E. N., Richardson, J. A., Yang, Q., Humphries, C., Shelton, J. M., Wu, H., Zhu, W., Bassel-Duby, R., and Williams, R. S. (1998) *Genes Dev.* **12,** 2499-2509

46. Dunn, S. E., Simard, A. R., Bassel-Duby, R., Williams, R. S., and Michel, R. N. (2001) *J. Biol. Chem.* **276,** 45243-45254

47. Xu, Q., Yu, L., Liu, L., Cheung, C. F., Li, X., Yee, S. P., Yang, X. J., and Wu, Z. (2002) *Mol. Biol. Cell* **13,** 1940-1952

48. Kao, H. Y., Verdel, A., Tsai, C. C., Simon, C., Juguilon, H., and Khochbin, S. (2001) *J. Biol. Chem.* **276,** 47496-47507

49. Chawla, S., Vanhoutte, P., Arnold, F. J., Huang, C. L., and Bading, H. (2003) *J. Neurochem.* **85,** 151-159

50. Linseman, D. A., Phelps, R. A., Bouchard, R. J., Le, S. S., Laessig, T. A., McClure, M. L., and Heidenreich, K. A. (2002) *J. Neurosci.* **22,** 9287-9297

51. Borodinsky, L. N., Coso, O. A., and Fiszman, M. L. (2002) *J. Neurochem.* **80,** 1062-1070

52. Silva, A. J., Stevens, C. F., Tonegawa, S., and Wang, Y. (1992) *Science* **257,** 201-206

53. Beaman-Hall, C. M., Hozza, M. J., and Vallano, M. L. (1992) *J. Neurochem.* **58,** 1259-1267

54. Borodinsky, L. N., O'Leary, D., Neale, J. H., Vicini, S., Coso, O. A., and Fiszman, M. L. (2003) *J. Neurochem.* **84,** 1411-1420

55. Shackelford, D. A., Yeh, R. Y., Hsu, M., Buzsaki, G., and Zivin, J. A. (1995) *J. Cereb. Blood Flow Metab.* **15,** 450-461

56. Churn, S. B., Limbrick, D., Sombati, S., and DeLorenzo, R. J. (1995) *J. Neurosci.* **15,** 3200-3214

57. Babcock, A. M., Liu, H., Paden, C. M., Churn, S. B., and Pittman, A. J. (1999) *J. Neurosci. Res.* **56,** 36-43

58. Babcock, A. M., Everingham, A., Paden, C. M., and Kimura, M. (2002) *J. Neurosci. Res.* **67,** 804-811

59. Okamoto, S., Li, Z., Ju, C., Scholzke, M. N., Mathews, E., Cui, J., Salvesen, G. S., Bossy-Wetzel, E., and Lipton, S. A. (2002) *Proc. Natl. Acad. Sci. USA* **99,** 3974-3979

FIGURE LEGENDS

FIG. 1. **A truncated mutant of MEF2A acts as a dominant-negative transcription factor and inhibits depolarization-mediated survival of CGNs.** *A*, CGNs (day 7 *in vitro*) were transiently co-transfected with a MEF2-responsive luciferase reporter plasmid and pCMV-β-gal in the presence of either empty vector (pcDNA3.1) or a truncated mutant of MEF2A lacking the transcriptional activation domain (MEF2A131). After transfection, cells were placed in serum-free medium containing either 25 mM KCl (25K) or 5 mM KCl (5K). Luciferase and β-galactosidase activities were determined and luciferase activity was normalized with respect to that of β-galactosidase. Data are expressed as a percentage of the activity in control neurons transfected with empty vector. Results represent the mean±SEM for three independent experiments each performed in duplicate. *Significantly different from the empty vector control in 25K ($p < 0.01$). *B*, On day 4 *in vitro*, CGNs were placed in 25K medium and were infected with either adenovirus expressing green fluorescent protein (Ad-GFP) or expressing a Flag-tagged truncated MEF2A (Ad-Flag-MEF2A131), each at a titer of 100 m.o.i. Cells were incubated for 72 h following infection and immunocytochemistry for the Flag epitope was performed. GFP-positive cells were detected by fluorescence under a FITC filter. Nuclei were stained with DAPI and apoptosis was quantified by counting the percentage of either GFP-positive or Flag-positive cells that had condensed and/or fragmented chromatin. The values shown represent the mean±SEM % apoptosis for three experiments each performed in triplicate. Arrows in the DAPI (*right*) panels point to the corresponding GFP-positive or Flag-positive cells shown in the *left* panels. Scale bar, 10 μm.

FIG. 2. **Overexpression of HDAC5 inhibits MEF2 activity and induces CGN apoptosis in depolarizing medium.** *A*, CGNs (day 7 *in vitro*) were transiently co-transfected with a MEF2-responsive luciferase reporter plasmid and pCMV-β-gal in the presence of either empty vector (pcDNA3.1) or HA-tagged HDAC5. After transfection, cells were placed in serum-free medium containing either 25 mM KCl (25K) or 5 mM KCl (5K). Luciferase and β-galactosidase activities were determined and luciferase activity was normalized with respect to that of β-galactosidase. Data are expressed as a percentage of the activity in control neurons transfected with empty vector. Results represent the mean±SEM for three independent experiments each performed in duplicate. *Significantly different from the empty vector control in 25K ($p < 0.01$). *B*, CGNs were transfected with either empty vector or HA-HDAC5 and then placed in either 25K or 5K medium for an additional 24 h. CGN apoptosis was quantified by DAPI staining of nuclei. HDAC5 expressing cells were identified by immunoreactivity for the HA epitope tag. The values shown represent the mean±SEM % apoptosis for three experiments each performed in triplicate. *Significantly different from the empty vector control in 25K ($p < 0.01$).

FIG. 3. **Cytoplasm-to-nuclear translocation of endogenous HDAC5 is induced in CGNs deprived of depolarizing potassium or incubated with the CaMK inhibitor KN93.** CGNs (day 7 *in vitro*) were incubated for 4 h in serum-free medium containing either 25 mM KCl (25K), 5 mM KCl (5K), or 25K+KN93 (5 μM). Following incubation, cells were fixed in 4% paraformaldehyde, permeabilized with 0.2% Triton X-100, and blocked in 5% BSA. HDAC5 and MEF2D were immunocytochemically localized by incubating the cells with a polyclonal antibody to HDAC5 and a monoclonal antibody to MEF2D followed by Cy3-conjugated and FITC-conjugated secondary antibodies, respectively. Nuclei were identified by DAPI staining.

Digitally deconvolved images were captured using a 63X oil objective. The images shown are representative of results obtained in three independent experiments. The bottom row shows the merged images of the DAPI, FITC, and Cy3 channels. Note that MEF2D was exclusively nuclear under all conditions, whereas the localization of HDAC5 changed from cytoplasmic in 25K to nuclear in the 5K and 25K+KN93 conditions. The nuclear colocalization of HDAC5 with MEF2D and DAPI under the 5K and 25K+KN93 conditions is evident by the resultant white overlapping staining in the merged images. Scale bar, 10 μm.

FIG. 4. **Removal of depolarizing potassium or addition of the CaMK inhibitor KN93 promotes an increased mobility of HDAC5 on polyacrylamide gels and association of HDAC5 with MEF2D.** *A*, CGNs (day 7 *in vitro*) were incubated for 4 h in serum-free medium containing either 25 mM KCl (25K), 5 mM KCl (5K), or 25K+KN93 (5 μM). Following incubation, detergent-soluble cell lysates were subjected to SDS-PAGE on 5% polyacrylamide gels and the proteins were subsequently transferred to PVDF membranes. HDAC5 was detected by immunoblotting (IB) with a polyclonal antibody and a horseradish-peroxidase-conjugated secondary. Immunoreactive proteins were detected by enhanced chemiluminescence. The blot shown is representative of results obtained in three separate experiments. Note that HDAC5 runs as a broad apparent doublet in 25K, whereas under the 5K or 25K+KN93 conditions the upper band of the doublet disappears, indicative of an enhanced mobility of HDAC5 under these conditions. *B*, CGNs were incubated exactly as described in *A* and cell lysates were prepared. MEF2D was immunoprecipitated (IP) from the cell lysates using a polyclonal antibody and immune complexes were resolved on 7.5% gels. The membranes were cut at the 75 kDa standard and the upper portion of the blot was probed for HDAC5 while the lower portion was

probed for MEF2D. The blots shown are indicative of data observed in two independent experiments. Note that HDAC5 was only detectable in MEF2D immune complexes obtained from CGNs incubated in either 5K or 25K+KN93 conditions. HC, immunoglobulin heavy chain from the precipitating antibody.

FIG. 5. **The CaMK inhibitors, KN93 and KN62, block depolarization-mediated MEF2 transcriptional activity and induce apoptosis of CGNs.** *A*, CGNs (day 7 *in vitro*) were transiently co-transfected with a MEF2-responsive luciferase reporter plasmid and pCMV-β-gal. After transfection for 2 h, cells were placed in serum-free medium containing either 25 mM KCl (25K) ± KN93 or KN62 (each at 5 μM) or 5 mM KCl (5K). Luciferase and β-galactosidase activities were determined 4 h later and luciferase activity was normalized with respect to that of β-galactosidase. Data are expressed as a percentage of the activity in control neurons transfected with empty vector. Results represent the mean±SEM for three independent experiments each performed in duplicate. *Significantly different from the 25K control ($p < 0.01$). *B*, CGNs (day 6 *in vitro*) were incubated in either 25K medium ± KN93 or KN62 or 5K medium for 24 h. CGN apoptosis was quantified by Hoechst staining of nuclei. The values shown represent the mean±SEM % apoptosis for three experiments each performed in triplicate. *Significantly different from the 25K control ($p < 0.01$). *C*, CGNs incubated for 24 h in 25K medium alone (*left panels*) or containing KN93 (*right panels*) were fixed in 4% paraformaldehyde, permeabilized with 0.2% Triton X-100, and blocked in 5% BSA. Beta-tubulin and active (cleaved) caspase-3 [Casp-3 (a)] were immunostained by incubating the cells with a monoclonal antibody to tubulin and a polyclonal antibody that specifically recognizes the active fragment of caspase-3, followed by FITC-conjugated and Cy3-conjugated secondary antibodies, respectively.

Nuclei were identified by DAPI staining. Digitally deconvolved images were captured using a 63X oil objective. The images shown are representative of results obtained in three independent experiments. The bottom panels show the merged images of the DAPI, FITC, and Cy3 channels. Arrows point to cells in the KN93 treated culture that demonstrate significant chromatin fragmentation and immunoreactivity for active caspase-3. Also, note the substantial loss of fine microtubule staining in the KN93 treated culture. Scale bar, 10 μm.

FIG. 6. **An antisense oligonucleotide to CaMKIIα decreases CaMKIIα expression and induces nuclear translocation of HDAC5.** *A*, CGNs (day 7 *in vitro*) were incubated in serum-free medium containing 25 mM KCl (25K) and a phosphorothioate, FITC-labeled antisense oligonucleotide to CaMKIIα (CaMKIIα-FITC-as, 1 μM final concentration). After incubation for 8 h, cells were fixed in 4% paraformaldehyde, permeabilized with 0.2% Triton X-100, and blocked in 5% BSA. Expression of endogenous CaMKIIα was then assessed by immunostaining with an isozyme-specific antibody and a Cy3-conjugated secondary. Nuclei were stained with DAPI and CGNs expressing the antisense construct were identified by positive staining in the FITC channel (indicated by the arrows). Note that cells positive for the antisense exhibited substantially less immunoreactivity for CaMKIIα than cells in the same field that did not take up the oligonucleotide. In general, approximately 25% of the entire CGN culture took up the FITC-labeled CaMKIIα antisense. The images shown are indicative of data obtained in two separate experiments. Scale bar, 10 μm. *B*, CGNs incubated exactly as described in *A* were immunostained for HDAC5 using a polyclonal antibody and a Cy3-conjugated secondary. The arrows point to cells that were positive for the CaMKIIα-FITC-as. Note that CGNs expressing the antisense demonstrated nuclear localization of HDAC5, whereas antisense-negative cells in

the same field showed cytoplasmic localization of HDAC5. The lower right panel shows the merged image of the DAPI, FITC and Cy3 channels – note the white overlapping nuclear staining in cells expressing the antisense and showing nuclear HDAC5. The results shown are representative of three independent experiments. Scale bar, 10 μm.

FIG. 7. **CREB phosphorylation in CGNs is not affected by a CaMKIIα antisense oligonucleotide.** *A*, CGNs (day 7 *in vitro*) were incubated for 4 h in serum-free medium containing 25 mM KCl (25K) in the absence or presence of KN93 (5 μM). Cells were fixed in paraformaldehyde and CREB phosphorylated on Ser133 (p-CREB) was identified by staining with a phospho-specific polyclonal antibody and a Cy3-conjugated secondary. Each of the p-CREB images was captured with a 63X oil objective under a Cy3 filter using equal exposure times. Scale bar, 10 μm. *B*, Cells were incubated for 8 h in 25K medium containing a FITC-labeled antisense oligonucleotide to CaMKIIα (CaMKIIα-FITC-as, 1 μM final concentration). Following incubation, cells were immunostained for p-CREB. Arrows point to CGNs that were positive for the FITC-labeled antisense. Note that all of the cells demonstrated similar immunoreactivity for p-CREB regardless of whether or not they expressed the CaMKIIα antisense. The images shown are indicative of three independent experiments. Scale bar, 10 μm.

FIG. 8. **Antisense to CaMKIIα induces caspase-3 activation in CGNs maintained in depolarizing medium.** CGNs (day 7 *in vitro*) were incubated in serum-free medium containing 25 mM KCl (25K) and a phosphorothioate, FITC-labeled antisense oligonucleotide to CaMKIIα (CaMKIIα-FITC-as, 1 μM final concentration). After incubation for 24 h, cells were fixed in 4% paraformaldehyde, permeabilized with 0.2% Triton X-100, and blocked in 5% BSA.

Activation of caspase-3 was assessed by immunostaining with a polyclonal antibody that specifically recognizes the active (cleaved) form of the caspase [Casp-3(a)], followed by a Cy3-conjugated secondary. Nuclei were stained with DAPI and CGNs expressing the antisense construct were identified by positive staining in the FITC channel (indicated by the arrows). Note that cells positive for the antisense exhibited high immunoreactivity for active caspase-3, whereas cells in the same field that did not take up the oligonucleotide showed no staining for active caspase. The images shown are representative of two independent experiments. Scale bar, 10 μm.

FIG. 1.

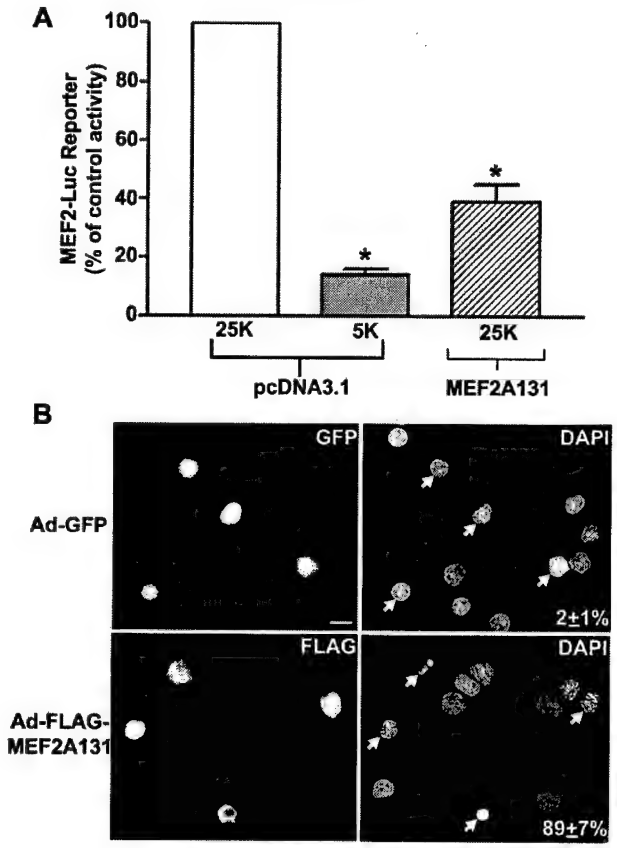
A
MEF2-Luc Reporter
(% of control activity)
100
80
60
40
20
0
*
*
25K
5K
25K
pcDNA3.1
MEF2A131
B
Ad-GFP
GFP
DAPI
2±1%
Ad-FLAG-
MEF2A131
FLAG
DAPI
89±7%

FIG. 2.

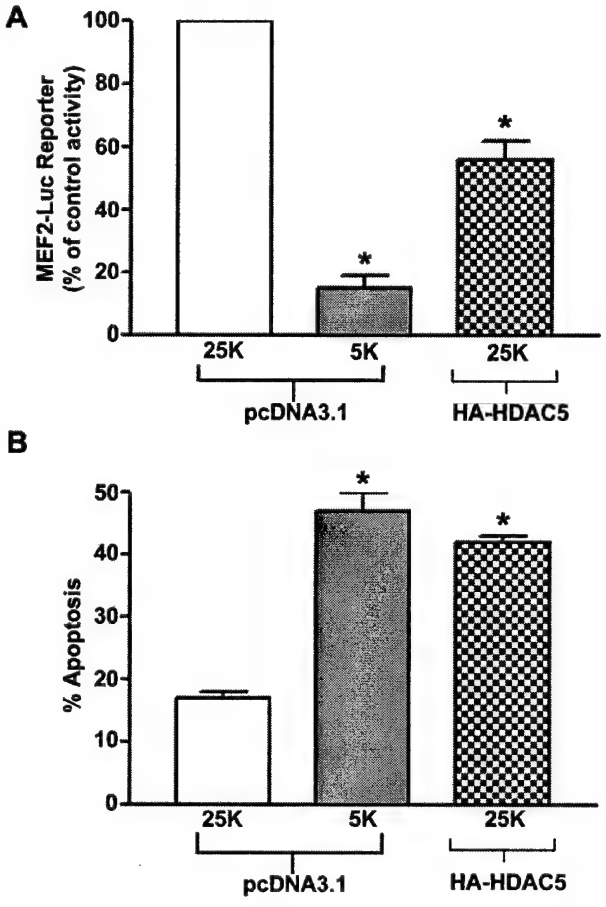
A
MEF2-Luc Reporter
(% of control activity)
100
80
60
40
20
0
*
*
25K
5K
25K
pcDNA3.1
HA-HDAC5
B
% Apoptosis
50
40
30
20
10
0
*
*
25K
5K
25K
pcDNA3.1
HA-HDAC5

FIG. 3.

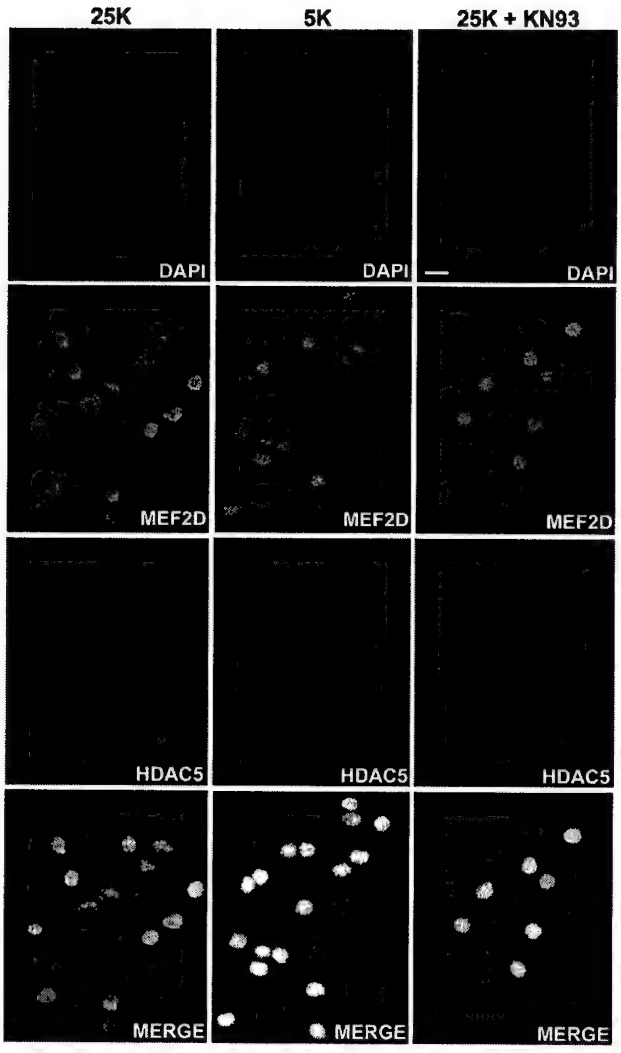
25K
5K
25K + KN93
DAPI
DAPI
DAPI
MEF2D
MEF2D
MEF2D
HDAC5
HDAC5
HDAC5
MERGE
MERGE
MERGE

FIG. 4.

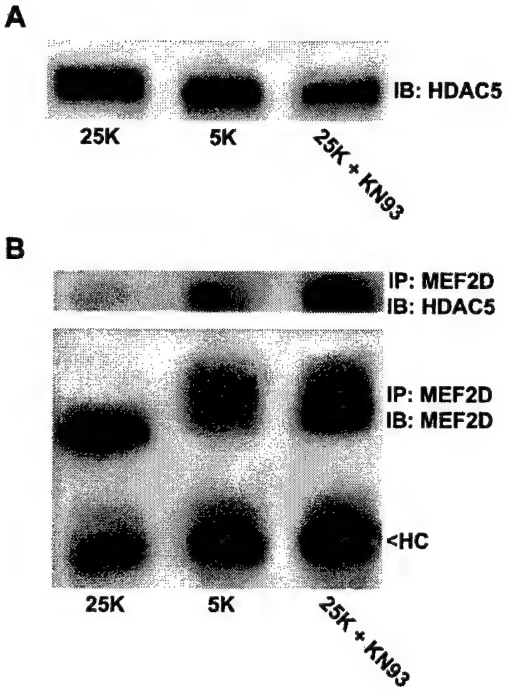
A
IB: HDAC5
25K
5K
25K + KN93
B
IP: MEF2D
IB: HDAC5
IP: MEF2D
IB: MEF2D
<HC
25K
5K
25K + KN93

FIG. 5.

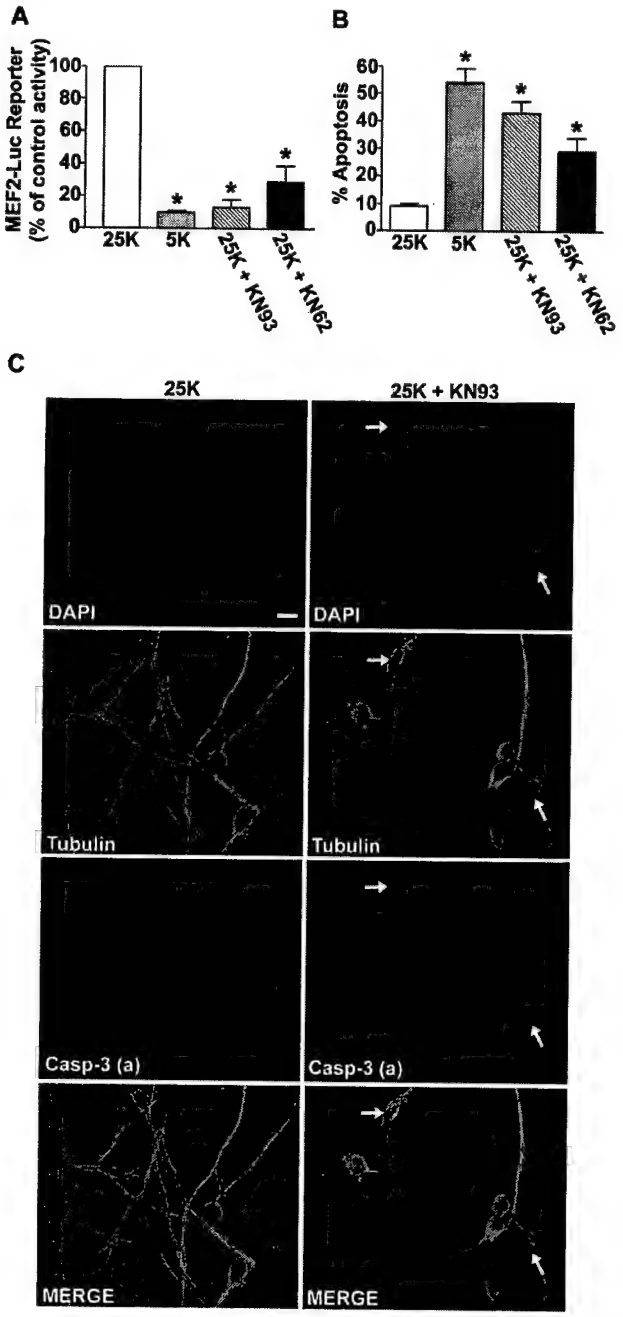
A
MEF2-Luc Reporter (% of control activity)
100
80
60
40
20
0
25K
5K
25K + KN93
25K + KN62
B
% Apoptosis
60
50
40
30
20
10
0
25K
5K
25K + KN93
25K + KN62
C
25K
25K + KN93
DAPI
DAPI
Tubulin
Tubulin
Casp-3 (a)
Casp-3 (a)
MERGE
MERGE

FIG. 6.

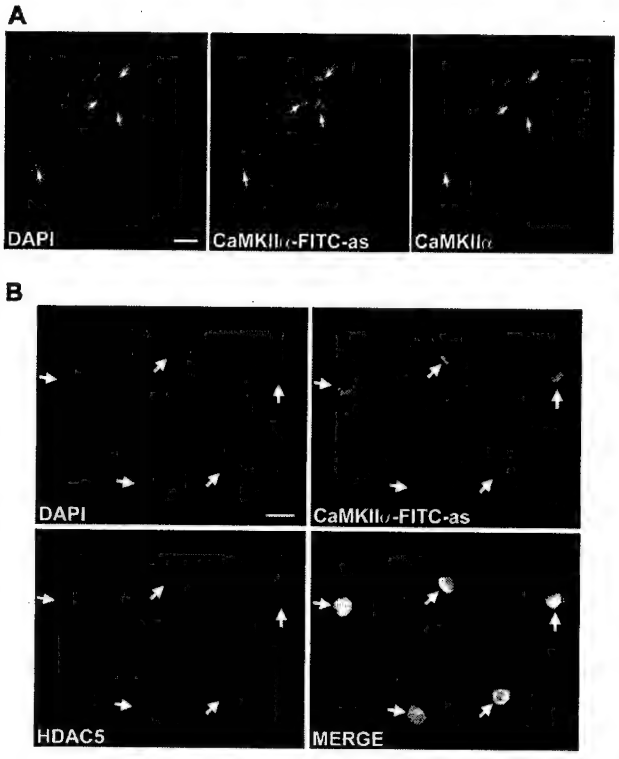
A
DAPI
CaMKIIα-FITC-as
CaMKIIα
B
DAPI
CaMKIIα-FITC-as
HDAC5
MERGE

FIG. 7.

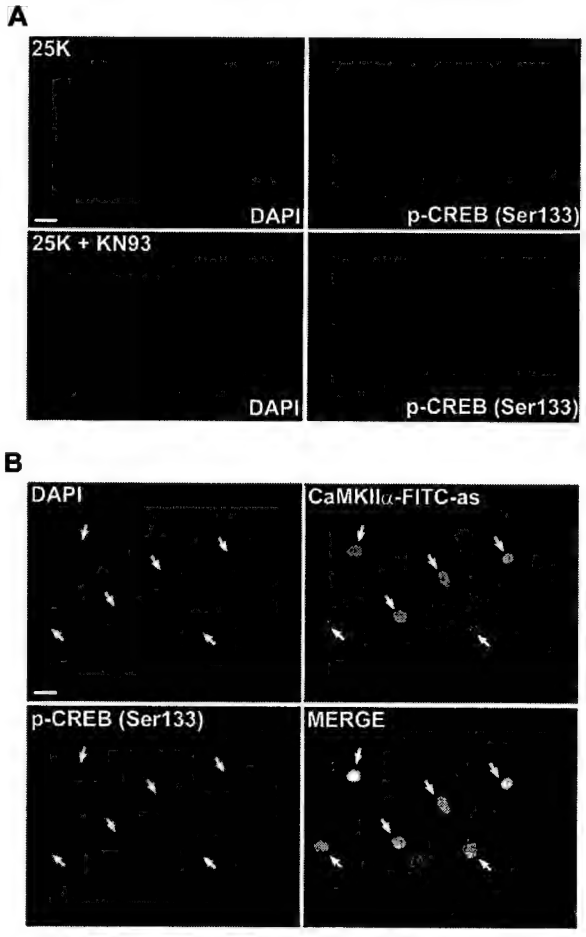
A
25K
DAPI
p-CREB (Ser133)
25K + KN93
DAPI
p-CREB (Ser133)
B
DAPI
CaMKIIα-FITC-as
p-CREB (Ser133)
MERGE

FIG. 8.

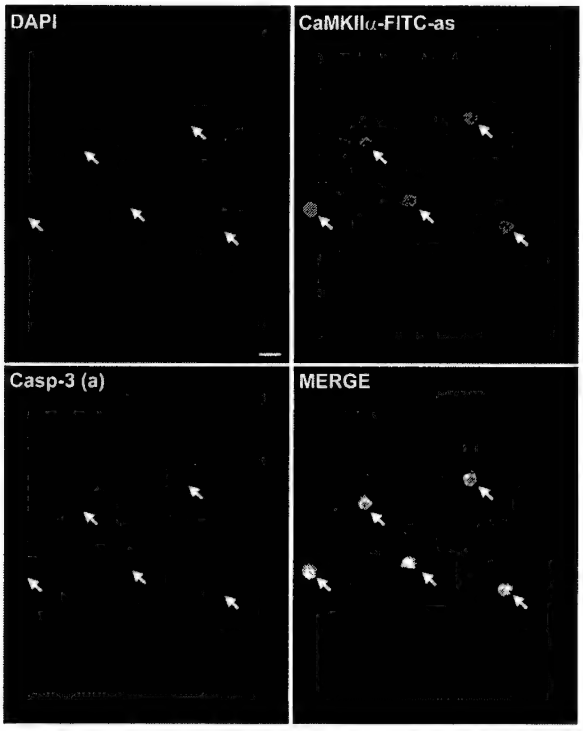

The Journal of Neuroscience, November 1, 2002, 22(21):9287–9297

Insulin-Like Growth Factor-I Blocks Bcl-2 Interacting Mediator of Cell Death (Bim) Induction and Intrinsic Death Signaling in Cerebellar Granule Neurons

Daniel A. Linseman, Reid A. Phelps, Ron J. Bouchard, Shoshona S. Le, Tracey A. Laessig, Maria L. McClure, and Kim A. Heidenreich

Department of Pharmacology, University of Colorado Health Sciences Center and the Denver Veterans Affairs Medical Center, Denver, Colorado 80262

Cerebellar granule neurons depend on insulin-like growth factor-I (IGF-I) for their survival. However, the mechanism underlying the neuroprotective effects of IGF-I is presently unclear. Here we show that IGF-I protects granule neurons by suppressing key elements of the intrinsic (mitochondrial) death pathway. IGF-I blocked activation of the executioner caspase-3 and the intrinsic initiator caspase-9 in primary cerebellar granule neurons deprived of serum and depolarizing potassium. IGF-I inhibited cytochrome *c* release from mitochondria and prevented its redistribution to neuronal processes. The effects of IGF-I on cytochrome *c* release were not mediated by blockade of the mitochondrial permeability transition pore, because IGF-I failed to inhibit mitochondrial swelling or depolarization. In contrast, IGF-I blocked induction of the BH3-only Bcl-2 family member, Bim (Bcl-2 interacting mediator of cell death), a mediator of Bax-dependent cytochrome *c* release. The suppression of Bim expression by IGF-I did not involve inhibition of the c-Jun transcription factor. Instead, IGF-I prevented activation of the forkhead family member, FKHRL1, another transcriptional regulator of Bim. Finally, adenoviral-mediated expression of dominant-negative AKT activated FKHRL1 and induced expression of Bim. These data suggest that IGF-I signaling via AKT promotes survival of cerebellar granule neurons by blocking the FKHRL1-dependent transcription of Bim, a principal effector of the intrinsic death-signaling cascade.

Key words: insulin-like growth factor; cerebellar granule neuron; apoptosis; mitochondria; Bim; forkhead transcription factor

Insulin-like growth factor-I (IGF-I) has significant neurotrophic and neuroprotective effects. IGF-I expression is regulated differentially in various brain regions and is associated temporally with critical stages of CNS development (Rotwein et al., 1988; Bach et al., 1991). Deficits in IGF-I are observed in Alzheimer's disease (Mustafa et al., 1999) and degenerative cerebellar ataxias (Torres-Aleman et al., 1996), and recombinant IGF-I slows disease progression in sporadic amyotrophic lateral sclerosis (Lai et al., 1997). IGF-I decreases neuronal apoptosis and enhances functional recovery in animal models of neurodegeneration including toxin exposure (Fernandez et al., 1998), transient ischemia (Liu et al., 2001), and neurotransplantation (Clarkson et al., 2001). Similarly, IGF-I rescues primary neurons from apoptosis induced by trophic factor withdrawal (Russell et al., 1998), excitotoxicity (Tagami et al., 1997), and oxidative stress (Heck et al., 1999). Thus IGF-I is essential for the survival of CNS neurons *in vivo* and *in vitro*.

Cerebellar granule neurons (CGNs) are critically dependent on IGF-I for their survival (Lin and Bulleit, 1997). In hereditary models of cerebellar Purkinje cell degeneration (pcd; *lurcher*), the primary death of Purkinje neurons induces the subsequent apoptosis of CGNs because of the loss of Purkinje-derived IGF-I (Bartlett et al., 1991; Zhang et al., 1997; Selimi et al., 2000a). Transgenic mice overexpressing IGF-I exhibit a remarkable doubling of CGN number (Ye et al., 1996) and show decreased expression of caspase-3 in cerebellum (Chrysis et al., 2001). These observations illustrate that IGF-I protects CGNs from apoptosis *in vivo*.

Similarly, IGF-I rescues primary CGNs from apoptosis induced by removal of depolarizing potassium and serum (trophic factor withdrawal), an established *in vitro* model of neuronal apoptosis (D'Mello et al., 1993; Galli et al., 1995; Miller et al., 1997a). CGN apoptosis involves activation of the intrinsic (mitochondrial) death pathway (Green, 1998). For example, trophic factor-deprived CGNs demonstrate Bax-dependent cytochrome *c* release from mitochondria (Desagher et al., 1999), and CGNs isolated from Bax knock-out mice are less sensitive to trophic factor withdrawal (Miller et al., 1997b). Moreover, the BH3-only proapoptotic Bcl-2 family member, Bim (Bcl-2 interacting mediator of cell death), is induced in CGNs undergoing apoptosis (Harris and Johnson, 2001; Putcha et al., 2001). BH3-only proteins facilitate intrinsic death signaling in a Bax-dependent manner (Desagher et al., 1999; Zong et al., 2001). Although it is recognized that IGF-I rescues CGNs via phosphatidylinositol 3 kinase (PI3K) and AKT (Dudek et al., 1997; Miller et al., 1997a), the effects of IGF-I on components of the intrinsic death pathway have not been examined.

Here we found that IGF-I suppresses induction of Bim, cytochrome *c* release from mitochondria, and activation of the intrinsic initiator caspase-9 and the executioner caspase-3 in trophic factor-deprived CGNs. Although c-Jun N-terminal protein kinase

Received March 22, 2002; revised Aug. 5, 2002; accepted June 24, 2002.

This work was supported by a Department of Veterans Affairs Merit Award (K.A.H.), Department of Defense Grant DAMD17-99-1-9481 (K.A.H.), National Institutes of Health Grant NS38619-01A1 (K.A.H.), and a Department of Veterans Affairs Research Enhancement Award Program (K.A.H. and D.A.L.). We thank Mary Kay Meintzer for her help with preparation of this manuscript.

Correspondence should be addressed to Dr. Kim A. Heidenreich, Department of Pharmacology (C236), University of Colorado Health Sciences Center, 4200 East Ninth Avenue, Denver, CO 80262. E-mail: Kim.Heidenreich@UCHSC.edu.

 0270-6474/02/229287-11$15.00/0

(JNK)/c-Jun signaling has been implicated in the induction of Bim during neuronal apoptosis (Harris and Johnson, 2001; Whitfield et al., 2001), our data suggest that IGF-I suppresses Bim expression via a distinct mechanism involving inhibition of the forkhead transcription factor FKHRL1. These results indicate that the intrinsic death pathway is a principal target of IGF-I in neurons.

MATERIALS AND METHODS

Materials. Recombinant human IGF-I was provided by Margarita Quiroga (Chiron, Emeryville, CA). Polyclonal antibodies to Bim, Bcl-X_L, caspase-3, caspase-9, cytochrome *c*, and c-Jun were from Santa Cruz Biotechnology (Santa Cruz, CA). Polyclonal antibodies to phospho-c-Jun (Ser^{63}), phospho-AKT (Ser^{473}), and AKT were from Cell Signaling Technologies (Beverly, MA). Polyclonal antibodies to phospho-FKHRL1 (Ser^{253}) and FKHRL1 were from Upstate Biotechnology (Lake Placid, NY). Cy3-conjugated secondary antibodies for immunocytochemistry were purchased from Jackson ImmunoResearch Laboratories (West Grove, PA). Horseradish peroxidase-linked secondary antibodies and reagents for enhanced chemiluminescence detection were obtained from Amersham Biosciences (Piscataway, NJ). JC1, tetramethylrhodamine ethyl ester (TMRE), and MitoTracker Green were from Molecular Probes (Eugene, OR). Wortmannin, Hoechst dye number 33258, and 4′,6-diamidino-2-phenylindole (DAPI) were from Sigma (St. Louis, MO). Adenoviral cytokine response modifier A (CrmA) was obtained from Dr. James DeGregori [University of Colorado Health Sciences Center (UCHSC), Denver, CO]. Adenoviral CMV (negative control adenovirus) was from Dr. Jerry Schaack (UCHSC). Adenoviral kinase-dead K179M mutant (dominant-negative) AKT was obtained from Drs. Prem Sharma and Jerry Olefsky (University of California, San Diego, CA).

Cell culture. Rat CGNs were isolated from 7-d-old Sprague Dawley rat pups (15–19 gm) as described previously (Li et al., 2000). Briefly, neurons were plated on 35-mm-diameter plastic dishes coated with poly-L-lysine at a density of 2.0×10^6 cells/ml in basal modified Eagle's medium containing 10% fetal bovine serum, 25 mM KCl, 2 mM L-glutamine, and 100 U/ml penicillin/100 μg/ml streptomycin (Invitrogen, Grand Island, NY). Cytosine arabinoside (10 μM) was added to the culture medium 24 hr after plating to limit the growth of non-neuronal cells. With the use of this protocol the cultures were ~95–99% pure for granule neurons. In general, experiments were performed after 7 d in culture.

Quantification of apoptosis. Apoptosis was induced by removing serum and decreasing the extracellular potassium concentration from 25 to 5 mM. After 24 hr the CGNs were fixed with 4% paraformaldehyde, and the nuclei were stained with either Hoechst dye or DAPI. Cells were considered apoptotic if their nuclei either were condensed or were fragmented. In general, ~500 cells from at least two fields of a 35 mm well were counted. Data are presented as the percentage of cells in a given treatment group that were scored as apoptotic. Experiments were performed at least in triplicate.

Preparation of CGN cell extracts. After incubation for the indicated times and with the reagents specified in Results, the culture medium was aspirated; the cells were washed once with 2 ml of ice-cold PBS, pH 7.4, placed on ice, and scraped into lysis buffer (200 μl/35 mm well) containing (in mM): 20 HEPES, pH 7.4, 50 NaCl, 1 EGTA, 5 β-glycerophosphate, 30 sodium pyrophosphate, and 1 phenylmethylsulfonyl fluoride plus 1% Triton X-100, 100 μM sodium orthovanadate, 10 μg/ml leupeptin, and 10 μg/ml aprotinin. Cell debris was removed by centrifugation at $6000 \times g$ for 3 min, and the protein concentration of the supernatant was determined by a commercially available protein assay kit (Pierce, Rockford, IL). Aliquots (~150 μg) of supernatant protein were diluted to a final concentration of 1× SDS-PAGE sample buffer, boiled for 5 min, and electrophoresed through 10–15% polyacrylamide gels. Proteins were transferred to polyvinylidene difluoride (PVDF) membranes (Millipore, Bedford, MA) and processed for immunoblot analysis.

Immunoblot analysis. Nonspecific binding sites were blocked in PBS, pH 7.4, containing 0.1% Tween 20 (PBS-T) and 1% BSA for 1 hr at room temperature. Primary antibodies were diluted in blocking solution and incubated with the membranes for 1 hr. Excess primary antibody was removed by washing the membranes three times in PBS-T. Then the blots were incubated with the appropriate horseradish peroxidase-conjugated secondary antibody diluted in PBS-T for 1 hr and subsequently were washed three times in PBS-T. Immunoreactive proteins were detected by enhanced chemiluminescence. In some experiments the membranes were reprobed after stripping in 0.1 M Tris-HCl, pH 8.0, 2% SDS, and 100 mM β-mercaptoethanol for 30 min at 52°C. The blots were rinsed twice in PBS-T and processed as above with a different primary antibody. Autoluminograms shown are representative of at least three independent experiments.

Immunocytochemistry. CGNs were cultured on polyethyleneimine-coated glass coverslips at a density of $\sim 2.5 \times 10^5$ cells per coverslip. After incubation as described in Results, the cells were fixed in 4% paraformaldehyde and were permeabilized and blocked in PBS, pH 7.4, containing 0.2% Triton X-100 and 5% BSA. Cells then were incubated for ~16 hr at 4°C with primary antibody diluted in PBS containing 0.2% Triton X-100 and 2% BSA. The primary antibody was aspirated, and the cells were washed five times with PBS. Then the cells were incubated with a Cy3-conjugated secondary antibody and DAPI for 1 hr at room temperature. CGNs were washed five more times with PBS, and coverslips were adhered to glass slides in mounting medium (0.1% *p*-phenylenediamine in 75% glycerol in PBS). Fluorescent images were captured by using either 63× or 100× oil immersion objectives on a Zeiss Axioplan 2 microscope equipped with a Cooke Sensicam deep-cooled CCD camera and a Slidebook software analysis program for digital deconvolution (Intelligent Imaging Innovations, Denver, CO).

Measurement of mitochondrial swelling. CGNs were incubated as described in Results, and JC1 (final concentration, 2 μg/ml) was added to the cultures 30 min before fixation to stain mitochondria. JC1 fluorescence was captured in paraformaldehyde-fixed cells by using a Cy3 filter under a 100× oil objective. Then the diameters of ~150 mitochondria per treatment condition were measured from digitally deconvolved images obtained from a total of 15–20 CGNs (randomly pooled from four independent experiments).

Assessment of mitochondrial membrane potential. CGNs grown on glass coverslips were incubated as described in Results, and TMRE (500 nM) was added directly to the cells 30 min before the end of the incubation period. After incubation the coverslips were inverted onto slides into a small volume of phenol red-free medium containing TMRE (500 nM). Living cells then were imaged with a Cy3 filter to detect TMRE fluorescence under a 100× oil objective. All images were acquired at equal exposure times for TMRE fluorescence to assess the relative mitochondrial membrane potentials.

Adenoviral infection. Recombinant adenoviruses were purified by cesium chloride gradient ultracentrifugation. The viral titer (multiplicity of infection) was determined by measuring the absorbance at 260 nm (where 1.0 absorbance unit = 1×10^{12} particles/ml), and infectious particles were verified by plaque assay. Adenoviral (Ad)-CMV, Ad-CrmA, or Ad-dominant-negative (DN)-AKT was added to CGN cultures on day 5 at a multiplicity of infection of 50. At 48 hr after infection either CGN apoptosis was induced by removal of serum and depolarizing potassium for 24 hr (for Ad-CMV and Ad-CrmA) or cell lysates were prepared directly for Western blotting for phospho-FKHRL1 and Bim (for Ad-CMV and Ad-DN-AKT).

Data analysis. The results that are shown represent the means ± SEM for the number (*n*) of independent experiments that were performed. Statistical differences between the means of unpaired sets of data were evaluated by one-way ANOVA, followed by a *post hoc* Dunnett's test. A *p* value of <0.01 was considered statistically significant.

RESULTS

IGF-I suppresses CGN apoptosis and activation of caspase-3 and caspase-9

Primary CGNs are dependent on depolarization-mediated calcium influx and serum-derived growth factors for their survival *in vitro* (D'Mello et al., 1993; Galli et al., 1995). The removal of serum and depolarizing potassium induced marked apoptosis of CGNs, characterized morphologically by chromatin condensation and fragmentation (Fig. 1*A*). Quantification of CGN apoptosis was performed by counting the number of cells with condensed and/or fragmented nuclei from several representative fields for each incubation condition. Basal CGN apoptosis was ~10% and increased to ~60% after 24 hr of trophic factor withdrawal (Fig. 1*B*). We used this cell system to investigate the mechanism of IGF-I neuroprotection. As described previously (D'Mello et al., 1993; Galli et al., 1995; Miller et al., 1997a), the addition of IGF-I

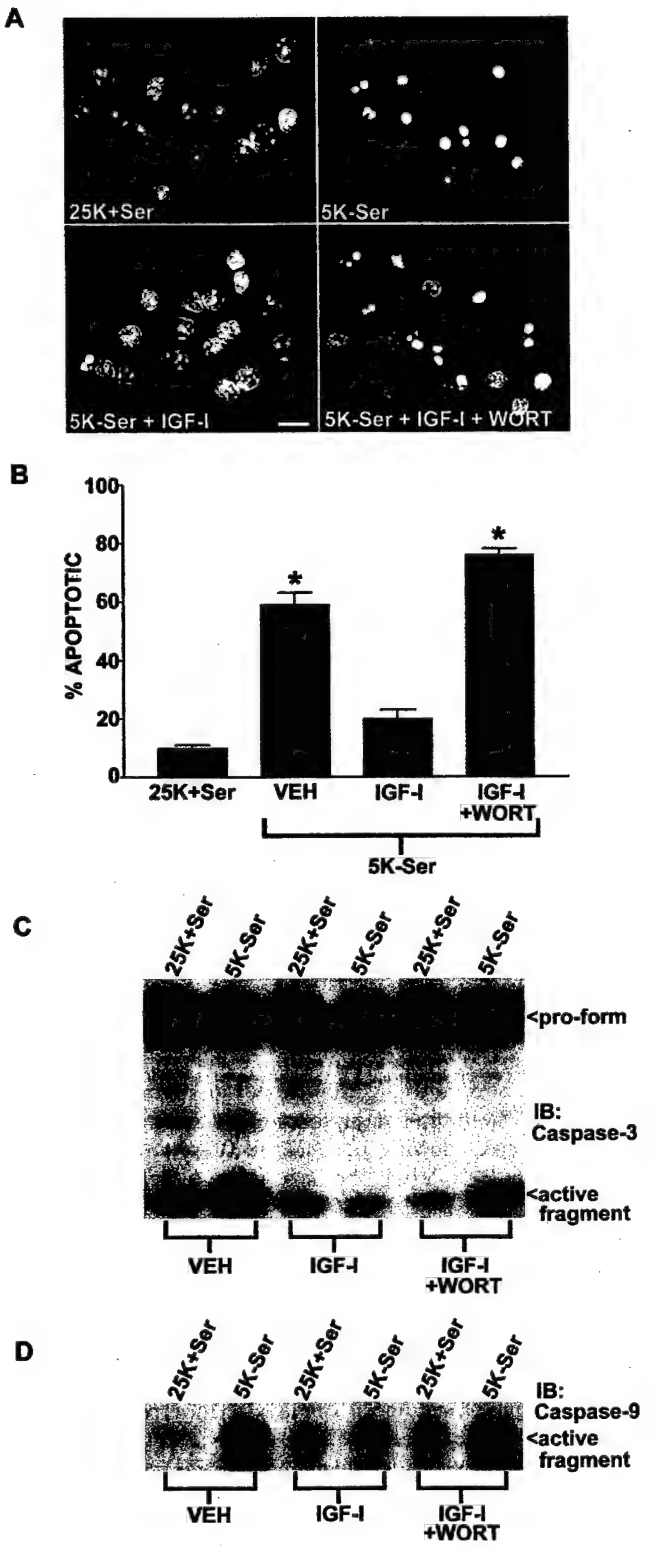

Figure 1. IGF-I inhibits apoptosis and activation of the executioner caspase-3 and the intrinsic initiator caspase-9 in CGNs subjected to trophic factor withdrawal. *A*, CGNs were incubated for 24 hr in either control (*25K+Ser*) or apoptotic (*5K-Ser*) medium containing either PBS vehicle (*VEH*) or IGF-I (200 ng/ml) in the absence or presence of wortmannin (*WORT*; 100 nM). After incubation the CGNs were fixed, and the nuclei were stained with DAPI. Scale bar, 10 μm. *B*, The percentages of apoptotic CGNs observed under the conditions described in *A* were quantified by counting ~500 CGNs per field in two fields per condition. Values represent the means ± SEM for three independent experiments, each performed in triplicate. *Significantly different from the 25K+Ser control ($p < 0.01$). *C*, CGNs were incubated as described in *A*, but for only 6 hr. Detergent-soluble cell lysates were subjected to SDS-PAGE on 15% polyacrylamide gels, and the proteins were transferred to PVDF membranes. Activation of caspase-3 was assessed by immunoblotting (*IB*) with a polyclonal antibody that recognizes both the proform (~32 kDa) and the cleaved form (~19 kDa active fragment) of the enzyme. The blot shown is representative of results obtained in three separate experiments. *D*, CGNs were incubated exactly as described in *C*, and the cell lysates were electrophoresed as described in *C*. Activation of caspase-9 was assessed by Western blotting with a polyclonal antibody that specifically recognizes the cleaved form (active fragment) of the caspase. The blot shown is representative of three independent experiments.

to cerebellar cultures immediately after trophic factor withdrawal resulted in an ~80% reduction in CGN apoptosis (Fig. 1*A*,*B*). The ability of IGF-I to rescue CGNs from apoptosis required the activation of PI3K, as demonstrated by the loss of protection observed in the presence of wortmannin (Fig. 1*A*,*B*). Activation of the executioner caspase-3 has been implicated in the apoptotic death of CGNs (Eldadah et al., 2000). Consistent with this, we observed cleavage of caspase-3 from the proform to an active fragment within 6 hr of serum and potassium deprivation (Fig. 1*C*). Like the results obtained for nuclear condensation and fragmentation, IGF-I inhibited caspase-3 activation in a PI3K-dependent manner (Fig. 1*C*). This latter result suggested that IGF-I blocks proapoptotic signaling events early in the apoptotic cascade, because caspase-3 cleavage commonly is thought to signify commitment to apoptosis.

To identify potential targets of IGF-I action upstream of the executioner caspase-3 in the apoptotic cascade, we focused on components of the intrinsic (mitochondrial) death pathway (Green, 1998). Recent data indicate that the intrinsic death pathway plays a significant role in CGN apoptosis evoked by trophic factor withdrawal (Miller et al., 1997b; Desagher et al., 1999). Immediately upstream of caspase-3 cleavage, activation of the initiator caspase-9 is the most distal event in the intrinsic pathway (Kuida et al., 1998). Recently, caspase-9 activation was shown to be required for caspase-3 cleavage in CGNs deprived of serum and depolarizing potassium (Gerhardt et al., 2001). Consistent with the involvement of caspase-9 in CGN apoptosis, we found that infection of CGNs with adenoviral CrmA, an inhibitor of Group III caspases (including caspase-9), but not Group II caspases (such as caspase-3) (Garcia-Calvo et al., 1998), significantly decreased apoptosis from 72 ± 8% ($n = 3$) to 29 ± 3% ($n = 3$; $p < 0.01$). In contrast, a negative control adenovirus (Ad-CMV) had no effect on CGN apoptosis (70 ± 8%; $n = 3$). After acute serum and potassium deprivation, we observed marked cleavage of caspase-9 consistent with its activation (Fig. 1*D*). As was observed for caspase-3 cleavage, activation of caspase-9 was inhibited significantly by IGF-I in a PI3K-dependent manner (Fig. 1*D*), demonstrating that IGF-I suppresses a key component of the intrinsic death pathway in CGNs.

IGF-I inhibits release of cytochrome *c* from mitochondria and its redistribution to neuronal processes

Caspase-9 is activated after its association with Apaf-1 and cytochrome *c*, which assemble into a large oligomeric complex known as the apoptosome (Zou et al., 1999). Formation of the apoptosome occurs after release of the mitochondrial protein, cytochrome *c*, into the cytoplasm. In CGNs maintained in the pres-

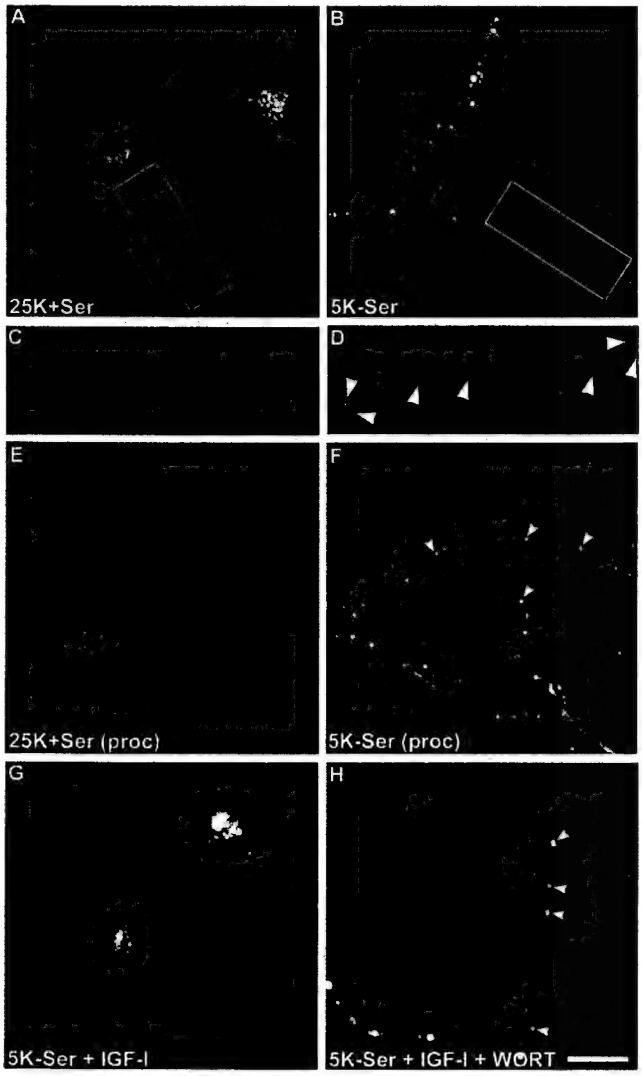

Figure 2. IGF-I blocks cytochrome *c* release from mitochondria and prevents its redistribution to focal complexes localized in neuronal processes. CGNs were incubated for 4 hr in control (*25K+Ser*) or apoptotic (*5K-Ser*) medium containing either PBS vehicle or IGF-I (200 ng/ml) in the absence or presence of wortmannin (*WORT*; 100 nM). After incubation the CGNs were fixed in 4% paraformaldehyde, permeabilized with 0.2% Triton X-100, and blocked with 5% BSA. Cytochrome *c* was localized by incubating the cells with a polyclonal antibody to cytochrome *c* and a Cy3-conjugated secondary antibody. Digitally deconvolved images were captured by using a 63× oil objective. The images shown are representative of results obtained in three separate experiments. Scale bar, 10 μm. *A*, CGNs incubated in control medium demonstrated intense cytochrome *c* staining in the perinuclear region consistent with localization to mitochondria. Very diffuse staining was observed in neuronal processes. *B*, CGNs incubated in apoptotic medium for 4 hr showed a marked redistribution of cytochrome *c*. Note the overall diffuse staining throughout the cytoplasm accompanied by the formation of distinct, brightly fluorescent focal complexes on the cell bodies and processes. *C*, The area demarcated by the *box* in *A* is enlarged to show the diffuse cytochrome *c* staining in a control neuronal process. *D*, The area demarcated by the *box* in *B* is enlarged to show the intense cytochrome *c* staining localized to discrete focal complexes (indicated by the *arrowheads*) in neuronal processes of CGNs deprived of serum and depolarizing potassium. *E*, A region containing multiple processes (*proc*) from control CGNs is shown. Note the overall diffuse cytochrome *c* staining. *F*, A region containing multiple processes from CGNs incubated in apoptotic medium for 4 hr is shown. Note the presence of many distinct focal areas of intense cytochrome *c* staining (indicated by the *arrowheads*). *G*, CGNs incubated in apoptotic medium containing exogenous IGF-I displayed cytochrome *c* localization to mitochondria similar to control CGNs (see *A* for comparison). *H*, CGNs incubated in apoptotic medium containing both IGF-I and wortmannin showed cytochrome *c* staining similar to CGNs incubated in apoptotic medium alone (see *B* for comparison). Focal complexes of cytochrome *c* staining are indicated by the *arrowheads*.

ence of serum and depolarizing potassium, cytochrome *c* was localized predominantly in mitochondria (Fig. 2*A*), with only diffuse staining observed in neuronal processes (Fig. 2*C*,*E*). Removal of serum and depolarizing potassium for 4 hr resulted in a rapid redistribution of cytochrome *c* from mitochondria to a diffuse staining throughout the cytoplasm. This redistribution was accompanied by the formation of many pronounced punctate areas of cytochrome *c* staining (Fig. 2*B*). The latter were observed primarily, although not exclusively, in distinct focal complexes localized to neuronal processes (Fig. 2*D*,*F*). In contrast to cytochrome *c* staining, no detectable redistribution of the mitochondrial marker MitoTracker Green was observed in neuronal processes under apoptotic conditions, indicating that the punctate areas of cytochrome *c* staining were not associated with intact mitochondria (data not shown). Inclusion of IGF-I during trophic factor withdrawal prevented the release and redistribution of cytochrome *c* from mitochondria (Fig. 2*G*). However, the addition of wortmannin in combination with IGF-I restored the release of cytochrome *c* from mitochondria and its redistribution to focal complexes in neuronal processes (Fig. 2*H*), indicating that the effects of IGF-I on cytochrome *c* release were PI3K-dependent. Thus, IGF-I inhibits the release of cytochrome *c* from mitochondria and, in this manner, blocks the subsequent activation of the intrinsic initiator caspase-9.

Mitochondrial swelling and mitochondrial membrane depolarization are not prevented by IGF-I

There are two potential mechanisms underlying cytochrome *c* release from mitochondria that have received considerable attention. The first involves opening of the permeability transition pore (PTP). The PTP is a heteromeric protein complex that includes the voltage-dependent anion channel, the adenine nucleotide translocator, and cyclophilin D as well as several other proteins (for review, see Martinou and Green, 2001). The PTP is localized at contact sites between the inner and outer mitochondrial membranes. Some apoptotic stimuli are capable of opening the PTP, resulting in disruption of the mitochondrial membrane potential (depolarization), a decline in ATP production, and entry of solutes and water into the mitochondrial matrix. Ultimately, mitochondrial swelling and rupture of the outer mitochondrial membrane occur, allowing the leakage of proteins (e.g., cytochrome *c*) from the intermembrane space into the cytoplasm. We used the mitochondrial dye JC1 to visualize mitochondria in CGNs undergoing apoptosis. Although the absolute amount of JC1 accumulated in mitochondria varies with membrane potential, JC1 is extremely photostable and labels all mitochondria to some extent (White and Reynolds, 1996). After incubation with JC1 the CGNs were fixed, and the diameters of labeled mitochondria were measured after digital deconvolution imaging. As shown in Figure 3, serum and potassium deprivation for 4 hr resulted in dramatic swelling of mitochondria in CGNs (Fig. 3*A*, *top panels*). This effect was reversible if serum and depolarizing potassium were restored within the first 2 hr after trophic factor withdrawal (Fig. 3*A*, *bottom right panel*). Inclusion of IGF-I during the apoptotic stimulus did not prevent the swelling of CGN

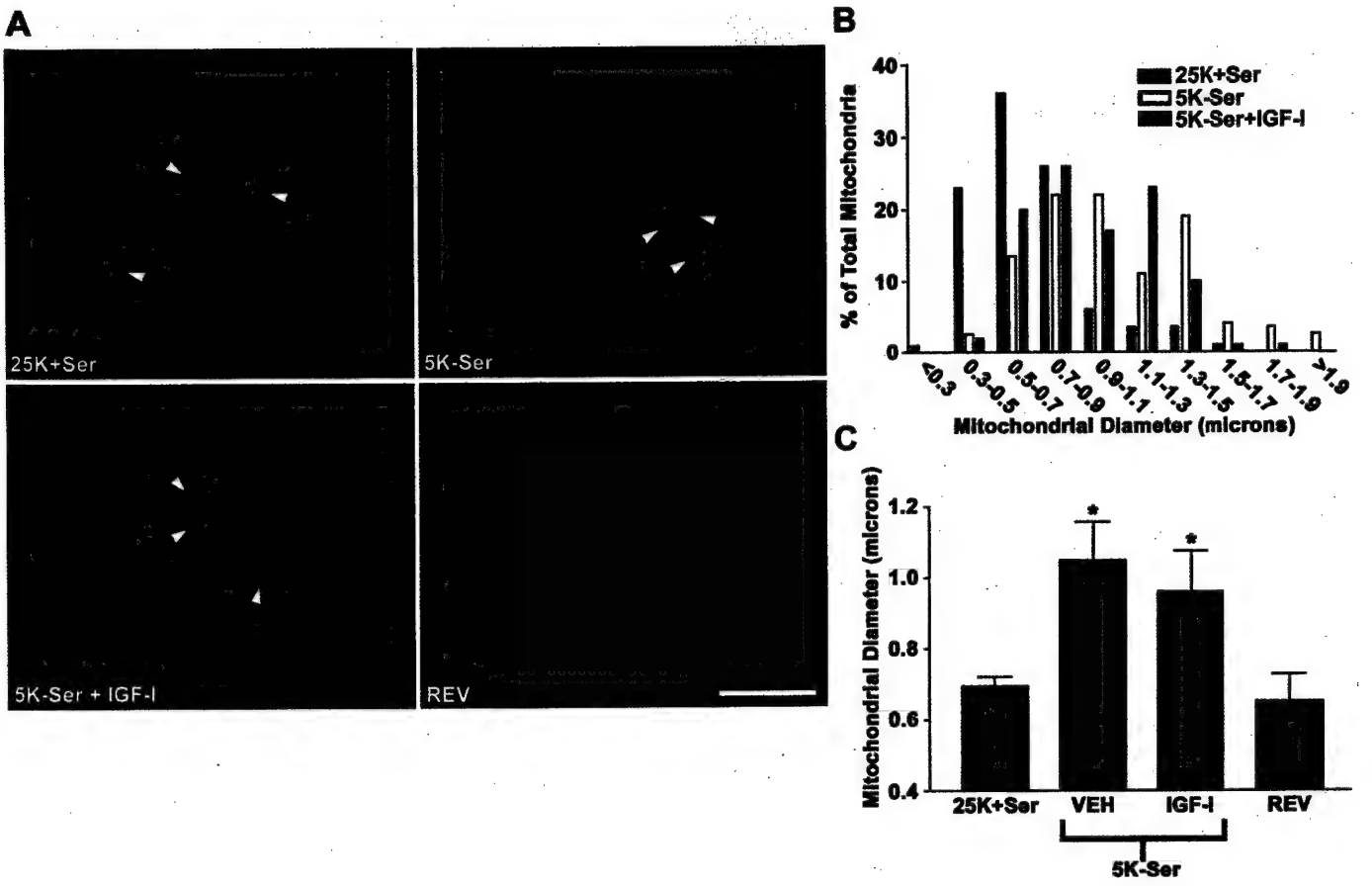

Figure 3. Mitochondrial swelling induced by trophic factor withdrawal is not inhibited by IGF-I. CGNs were incubated for 4 hr in either control (*25K+Ser*) or apoptotic (*5K-Ser*) medium containing either PBS vehicle (*VEH*) or IGF-I (200 ng/ml). To test for reversibility of mitochondrial swelling, we first incubated CGNs for 2 hr in apoptotic medium and then returned them to control medium for an additional 2 hr before staining (*REV*). In preliminary time course experiments a 2 hr incubation in apoptotic medium was found to be sufficient to induce marked mitochondrial swelling (data not shown). At 30 min before fixation, JC1 (final concentration, 2 μg/ml) and Hoechst dye were added to the cultures to stain mitochondria and nuclei, respectively. JC1 fluorescence was captured by using a Cy3 filter under a 100× oil objective. *A*, Representative images of CGNs incubated as described above and stained with Hoechst and JC1. Mitochondria are indicated by the *arrowheads*. Note the dramatic swelling of mitochondria in CGNs incubated in apoptotic medium in either the absence or presence of IGF-I. Mitochondrial swelling was completely reversible if control medium was replaced within 2 hr (*REV*). The images shown are representative of CGNs from four separate experiments. Scale bar, 10 μm. *B*, Distribution of mitochondrial diameters from CGNs observed under the conditions described in *A*. The diameters of ~150 mitochondria per treatment condition were measured from digitally deconvolved images obtained from a total of 15–20 CGNs (randomly pooled from 4 independent experiments). The mitochondrial diameters were categorized into the indicated size groups and graphed as a percentage of the total mitochondria with a given diameter *C*, Quantification of the mean mitochondrial diameters for CGNs observed under the conditions described in *A*. Values represent the means ± SEM mitochondrial diameters obtained from the mitochondria measured in *B*. *Significantly different from the 25K+Ser control; $p < 0.01$.

mitochondria (Fig. 3*A*, *bottom left panel*). The distribution of mitochondrial diameters under control, apoptotic, and apoptotic plus IGF-I conditions is shown in Figure 3*B*, and the mean diameters are shown in Figure 3*C*. Serum and potassium deprivation resulted in a significant 50% increase in the mean mitochondrial diameter in CGNs (0.69 ± 0.03 μm in control vs 1.05 ± 0.11 μm in apoptotic; $p < 0.01$), an effect that was unaltered by IGF-I (0.96 ± 0.12 μm) (Fig. 3*C*). Interestingly, inclusion of IGF-I in trophic factor-deprived CGNs failed to reverse the mitochondrial swelling even after 48 hr of incubation, although apoptosis was still blocked at this time point. However, the readdition of depolarizing potassium for the latter 24 hr of the incubation period did reverse the mitochondrial swelling, indicating that it is a depolarization-sensitive event that is unaffected by IGF-I (data not shown).

Next we analyzed the mitochondrial membrane potential by incubating living CGNs with the membrane potential-sensitive dye TMRE. TMRE is accumulated actively in mitochondria possessing an intact membrane potential but is excluded or lost from mitochondria that are depolarized (Krohn et al., 1999). CGNs maintained in the presence of serum and depolarizing potassium displayed mitochondria that were stained brightly with TMRE, indicative of an intact membrane potential (Fig. 4, *top left panel*). Because these experiments were conducted in living CGNs, we showed that the mitochondrial membrane potential of control CGNs was maintained throughout the duration required to capture all of the images described below (Fig. 4, *bottom right panel*). Serum and potassium deprivation for 4 hr resulted in a marked loss of mitochondrial TMRE staining, consistent with mitochondrial membrane depolarization (Fig. 4, *top right panel*). As was observed for mitochondrial swelling, the addition of IGF-I to trophic factor-deprived CGNs did not prevent the loss of mitochondrial membrane potential (Fig. 4, *bottom left panel*). The above results demonstrate that IGF-I does not block cytochrome

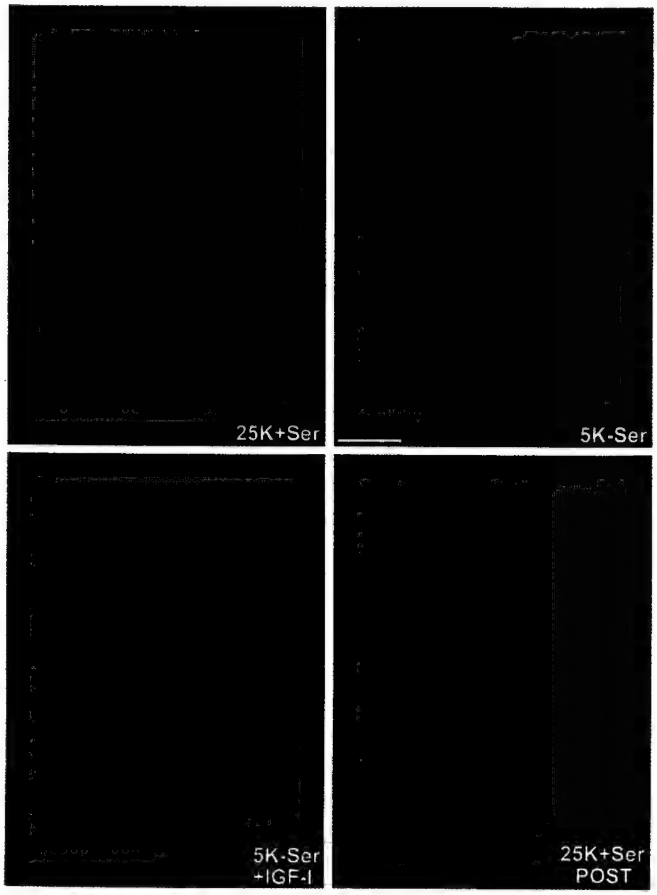

Figure 4. Mitochondrial membrane depolarization elicited by trophic factor withdrawal is not prevented by IGF-I. CGNs grown on glass coverslips were incubated for 4 hr in either control (*25K+Ser*) or apoptotic (*5K-Ser*) medium alone or containing IGF-I (200 ng/ml). At 30 min before the end of the incubation period TMRE and Hoechst were added directly to the cells. After incubation the coverslips were inverted onto slides into a small volume of phenol red-free medium lacking serum or depolarizing potassium but containing TMRE (500 nM). Living cells then were imaged under a 100× oil objective. Nuclear staining with Hoechst is shown in *blue*; TMRE is shown in *red*. Scale bar, 10 μm. CGNs maintained in control medium during the 4 hr incubation period displayed many mitochondria that were stained intensely with TMRE, indicative of an intact membrane potential (*top left panel*). In contrast, CGNs incubated in apoptotic medium in either the absence (*top right panel*) or presence (*bottom left panel*) of IGF-I expressed very little detectable mitochondrial TMRE staining, characteristic of a loss of mitochondrial membrane potential or depolarization. Approximately 5–10 min was required to capture the images described above. Therefore, at the end of the capture duration a final image was acquired of another control CGN to show that the mitochondrial membrane potential was not compromised during the time required to capture the images (*25K+Ser POST*). All of the images shown were acquired at equal exposure times for TMRE fluorescence and are representative of results obtained from three independent experiments, each performed in duplicate.

c release from CGN mitochondria by the inhibition of mitochondrial swelling or depolarization, suggesting that opening of the PTP does not play a significant role in cytochrome *c* release during apoptosis of CGNs.

IGF-I blocks induction of the BH3-only Bcl-2 family member Bim

The second potential mechanism by which cytochrome *c* release is regulated involves the formation of a Bax- or Bak-containing

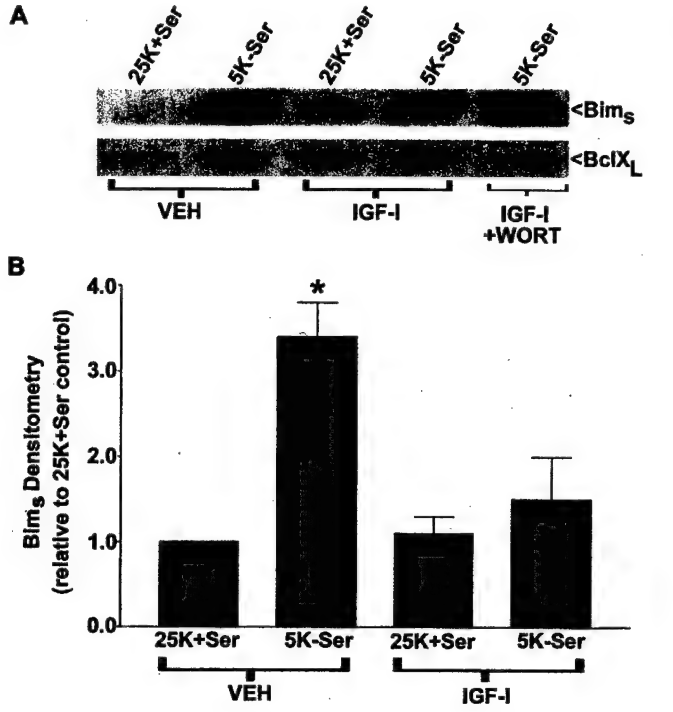

Figure 5. IGF-I inhibits induction of the BH3-only Bcl-2 family member Bim in a PI3K-dependent manner. *A*, CGNs were incubated for 6 hr in either control (*25K+Ser*) or apoptotic (*5K-Ser*) medium containing either PBS vehicle (*VEH*) or IGF-I (200 ng/ml) ± wortmannin (*WORT*; 100 nM). After incubation the cell lysates were subjected to SDS-PAGE on 15% polyacrylamide gels, and the proteins were transferred to PVDF membranes. Bim expression was assessed by immunoblotting with a polyclonal antibody to Bim that specifically recognized an ~15 kDa protein, consistent with the apparent molecular weight of Bim short (*Bim$_s$*). To affirm equal protein loading, we then stripped the blot and reprobed it for the anti-apoptotic Bcl-2 family member Bcl-X_L, which did not demonstrate any significant change in expression under the conditions of this experiment. The blots shown are representative of three separate experiments. *B*, Quantification of Bim$_s$ expression observed under the conditions described in *A* was performed by computer-assisted imaging densitometry. Values represent the means ± SEM for three independent experiments and are expressed relative to the densitometry of Bim$_s$ observed in control CGNs (set to 1.0). *Significantly different from the 25K+Ser control ($p < 0.01$).

"pore" in the outer mitochondrial membrane that permits the passage of proteins (Korsmeyer et al., 2000). Bax and Bak are proapoptotic members of the Bcl-2 family that appear to serve a redundant function in making the mitochondrial membrane permeable to cytochrome *c* (Wei et al., 2001). The BH3-only Bcl-2 family members, including Bad, Bid, Dp5/Hrk, and Bim, have been shown to promote the proapoptotic effects of Bax and Bak while concomitantly suppressing the prosurvival function of Bcl-2 (Desagher et al., 1999; Zong et al., 2001). Recently, Bim was shown to be upregulated after either nerve growth factor (NGF) withdrawal from primary sympathetic neurons or serum and potassium withdrawal from CGNs (Putcha et al., 2001; Whitfield et al., 2001). Moreover, overexpression of Bim or related BH3-only family members promotes apoptosis of CGNs in a Bax-dependent manner (Harris and Johnson, 2001). Immunoblotting for Bim after acute trophic factor withdrawal in CGNs demonstrated a marked increase in the expression of Bim short (Bim$_s$, ~15 kDa) (Fig. 5*A*), the most proapoptotic splice variant of this protein family (O'Connor et al., 1998). Quantification of the change in protein expression by densitometry revealed that serum

and potassium deprivation for 6 hr induced a significant 3.4 ± 0.4-fold increase ($n = 3$; $p < 0.01$) in Bim_s (Fig. 5*B*). Inclusion of IGF-I completely blunted the induction of Bim_s (1.5 ± 0.5-fold increase; $n = 3$) in a PI3K-dependent manner (Fig. 5*A*,*B*). In contrast, the expression of the prosurvival Bcl-2 family member Bcl-X_L was unaffected by either trophic factor withdrawal or IGF-I (Fig. 5*A*). These data indicate that the suppression of Bim is one mechanism by which IGF-I inhibits cytochrome *c* release in CGNs deprived of serum and depolarizing potassium.

IGF-I does not suppress Bim expression by inhibiting c-Jun

Activation of the transcription factor c-Jun is required for apoptosis of primary sympathetic neurons subjected to NGF withdrawal (Eilers et al., 1998) and CGNs undergoing serum and potassium deprivation (Watson et al., 1998). The ability of a dominant-negative mutant of c-Jun to rescue sympathetic neurons from apoptosis recently has been attributed, in part, to its ability to block the induction of Bim (Whitfield et al., 2001). The transcriptional activity of c-Jun is stimulated after its phosphorylation on multiple serine residues (including Ser^{63} and Ser^{73}) by upstream kinases of the JNK family (Minden et al., 1994). Chemical inhibitors of JNK have been shown to inhibit apoptosis of CGNs (Harada and Sugimoto, 1999; Coffey et al., 2002) and to attenuate Bim mRNA expression in CGNs subjected to trophic factor withdrawal (Harris and Johnson, 2001). In the present study we observed that incubation of trophic factor-deprived CGNs with the pyridinyl imidazole JNK/p38 inhibitor SB203580 (Harada and Sugimoto, 1999; Coffey et al., 2002) blunted the phosphorylation of c-Jun on Ser^{63} (Fig. 6*A*) and prevented the increased expression of c-Jun detected by immunoblotting (Fig. 6*B*). Moreover, SB203580 significantly attenuated the induction of Bim_s, consistent with a role for c-Jun in the regulation of Bim expression in CGNs (Fig. 6*C*,*D*). To determine whether IGF-I blocks Bim induction via an inhibition of c-Jun, we analyzed the effects of IGF-I on c-Jun phosphorylation and expression. The addition of IGF-I to CGNs deprived of serum and depolarizing potassium failed to attenuate either the phosphorylation of c-Jun on Ser^{63} (Fig. 6*E*) or the increased expression of c-Jun observed by Western blot (Fig. 6*F*). Thus IGF-I suppresses the induction of Bim in apoptotic CGNs via a mechanism that is independent of the transcription factor c-Jun.

IGF-I prevents dephosphorylation and nuclear translocation of the forkhead transcription factor FKHRL1

Recently, a member of the forkhead family of transcription factors, FKHRL1, was shown to regulate the induction of Bim in lymphocytes undergoing apoptosis in response to cytokine withdrawal (Dijkers et al., 2000). Furthermore, overexpression of a constitutively active mutant of FKHRL1 was sufficient to increase Bim expression in B-cells (Dijkers et al., 2000). The actions of forkhead family members are regulated by phosphorylation on serine and threonine residues. The prosurvival kinase AKT is the main effector of IGF-I that is activated downstream of PI3K, and FKHRL1 has been identified as a principal substrate of AKT in neuronal cells (Brunet et al., 1999; Zheng et al., 2000). Therefore, we first assessed the phosphorylation status of AKT and FKHRL1 in CGNs by immunoblotting with phospho-site-specific antibodies. CGNs cultured in the presence of serum and depolarizing potassium showed marked phosphorylation of AKT on Ser^{473}, indicative of high AKT activity (Fig. 7*A*, *first lane*). In parallel, control CGNs also exhibited high phosphorylation of FKHRL1 on Ser^{253}, one of the sites targeted by AKT (Fig. 7*B*, *first lane*). Removal of serum and depolarizing potassium resulted in a pronounced dephosphorylation (inactivation) of AKT (Fig. 7*A*, *second lane*) and a corresponding loss of FKHRL1 phosphorylation (Fig. 7*B*, *second lane*). The addition of IGF-I to CGNs deprived of serum and depolarizing potassium maintained the phosphorylation of both AKT (Fig. 7*A*) and FKHRL1 (Fig. 7*B*), effects that were blocked by the PI3K inhibitor wortmannin.

Phosphorylation of FKHRL1 on Thr^{32} and Ser^{253} by AKT results in the translocation of FKHRL1 from the nucleus to the cytoplasm where it subsequently is sequestered by 14-3-3 proteins (Brunet et al., 1999). Thus IGF-I signaling via AKT has the potential to regulate negatively the transcriptional activity of FKHRL1 by excluding it from the nucleus. We next examined the cellular localization of FKHRL1 in CGNs. FKHRL1 was localized predominantly to the cytoplasm in CGNs maintained in the presence of trophic factors (Fig. 7*C*, *top left panel*). After acute trophic factor withdrawal FKHRL1 underwent a dramatic translocation to the nucleus (Fig. 7*C*, *top right panel*). The nuclear translocation of FKHRL1 was prevented completely by IGF-I (Fig. 7*C*, *bottom left panel*) in a PI3K-dependent manner (Fig. 7*C*, *bottom right panel*). Collectively, these results demonstrate that, under conditions in which IGF-I blocks Bim induction (Fig. 5), it concurrently sustains high AKT activity, robust FKHRL1 phosphorylation, and the exclusion of FKHRL1 from the nucleus. These findings are consistent with a role for FKHRL1 in the regulation of Bim expression in CGNs. Moreover, these data suggest a novel mechanism by which IGF-I suppresses Bim induction in trophic factor-deprived CGNs by blocking the actions of FKHRL1.

Adenoviral-mediated expression of dominant-negative AKT results in dephosphorylation of FKHRL1 and induction of Bim

To assess more directly the role of AKT in the regulation of FKHRL1 activity and Bim expression, we infected CGNs with an adenovirus expressing a kinase-dead dominant-negative mutant of AKT (Ad-DN-AKT). As described above, CGNs cultured in the presence of serum and depolarizing potassium showed marked phosphorylation of AKT on Ser^{473}, indicative of high endogenous AKT activity (Fig. 7*A*, *first lane*). Under these conditions the adenoviral-mediated expression of DN-AKT resulted in a marked dephosphorylation of FKHRL1 on the AKT target site Ser^{253} (Fig. 8*A*) when compared with CGNs infected with a negative control adenovirus (Ad-CMV). Moreover, the dephosphorylation of FKHRL1 induced by DN-AKT was associated with a coordinated increase in the expression of Bim_s (Fig. 8*B*). These data further support a mechanism by which IGF-I/AKT signaling blocks Bim induction at the level of the FKHRL1 transcription factor.

DISCUSSION

IGF-I promotes the survival of CGNs both *in vitro* and *in vivo* (Ye et al., 1996; Lin and Bulleit, 1997). In the current study we have investigated the neuroprotective mechanism of IGF-I in CGNs by systematically analyzing its effects on components of the intrinsic death-signaling cascade. First we found that IGF-I suppressed activation of the executioner caspase-3 in CGNs subjected to trophic factor withdrawal. This effect was blocked by the PI3K inhibitor wortmannin, consistent with a role for PI3K/AKT signaling in the IGF-I-mediated survival of CGNs. Previously, ribozyme-mediated downregulation of caspase-3 was shown to

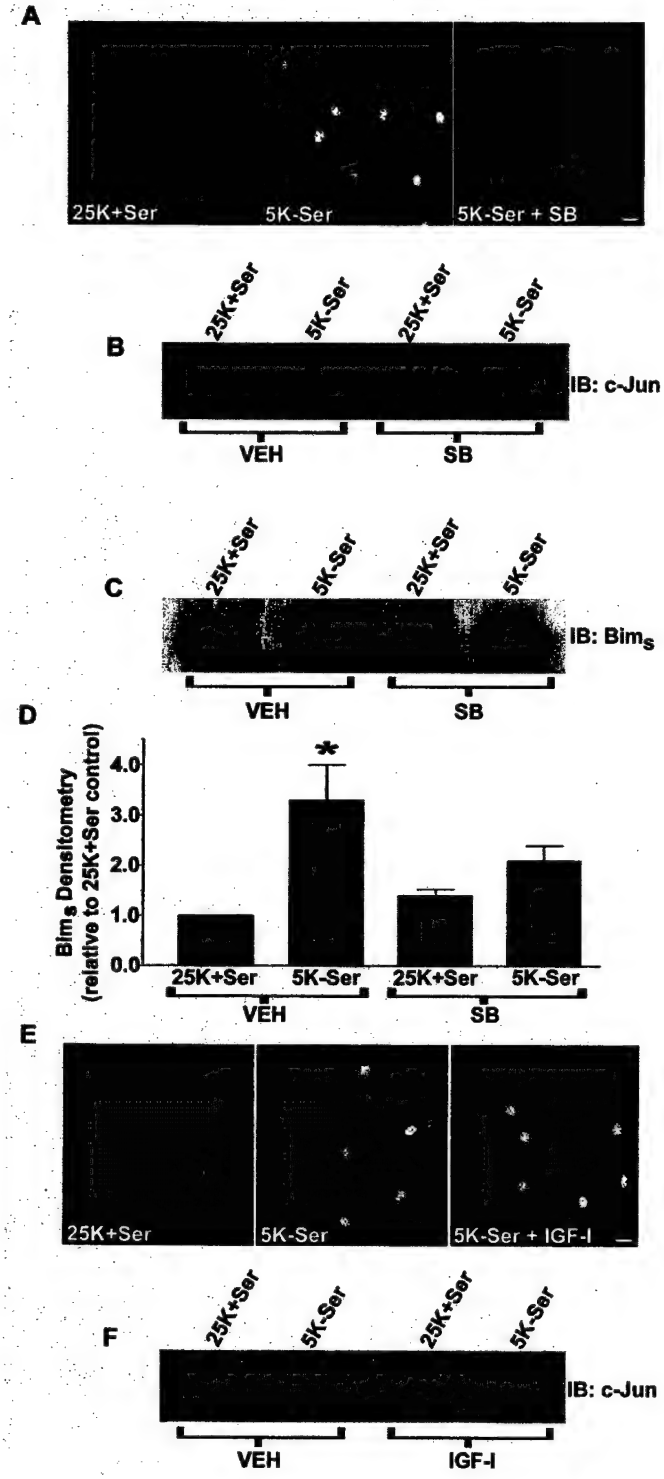

Figure 6. Inhibition of c-Jun signaling attenuates the induction of Bim. IGF-I does not block c-Jun activation in trophic factor-deprived CGNs. *A*, CGNs were incubated for 4 hr in either control (*25K+Ser*) or apoptotic (*5K-Ser*) medium in the absence or presence of the JNK/p38 inhibitor SB203580 (*SB*; 20 μM). After incubation the cells were fixed, and c-Jun phosphorylated on Ser[63] was detected exclusively in the nuclear compartment by using a phospho-specific polyclonal antibody. The images shown are representative of results obtained in three independent experiments. Scale bar, 10 μm. *B*, CGNs were incubated for 4 hr in either control (*25K+Ser*) or apoptotic (*5K-Ser*) medium in the presence of either DMSO vehicle (*VEH*; 0.2%) or SB (20 μM), and cell lysates were subjected to SDS-PAGE on 10% polyacrylamide gels. Proteins were transferred to PVDF membranes and immunoblotted (*IB*) with a polyclonal antibody to c-Jun. The blot shown is representative of three separate experiments. *C*, CGNs were incubated as described in *B*, but for 6 hr, and the cell lysates were electrophoresed on 15% polyacrylamide gels and probed for Bim$_S$. *D*, Densitometric analysis of Bim$_S$ from three independent experiments performed as described in *C*. The densitometry of Bim$_S$ detected in control (*25K+Ser*) CGNs was set at 1.0, and all other values were calculated relative to the control. *Significantly different from the 25K+Ser control ($p < 0.01$). *E*, CGNs were incubated for 4 hr in either control (*25K+Ser*) or apoptotic (*5K-Ser*) medium in the presence of either PBS vehicle (*VEH*) or IGF-I (200 ng/ml). After incubation the nuclear c-Jun phosphorylated on Ser[63] was detected by using a phospho-specific polyclonal antibody. The images shown are representative of three experiments. Scale bar, 10 μm. *F*, CGNs incubated as described in *E* were lysed, and extracted proteins were immunoblotted for c-Jun. The blot shown is illustrative of results obtained from three separate experiments.

inhibit CGN apoptosis (Eldadah et al., 2000), supporting involvement of this executioner caspase in the mechanism of cell death. Comparable with our results, IGF-I has been shown to attenuate caspase-3 activation in other models of neuronal apoptosis via a PI3K/AKT-dependent mechanism (Van Golen and Feldman, 2000; Barber et al., 2001). We also found that IGF-I blocked activation of the intrinsic initiator caspase-9 in a PI3K-dependent manner. Recently, selective peptide inhibitors of caspase-9 were shown to prevent caspase-3 activation in CGNs, demonstrating that caspase-9 activation occurs upstream of the executioner during CGN apoptosis (Gerhardt et al., 2001). Moreover, we found that adenoviral CrmA, an inhibitor of caspase-9, protected CGNs from apoptosis. Similar to our data, IGF-I has been shown to prevent caspase-9 activation in rat retinal ganglion cells after optic nerve transection (Kermer et al., 2000). Collectively, these data suggest a common mechanism by which IGF-I blocks activation of the executioner caspase-3 in neurons via inhibition of the upstream intrinsic initiator caspase-9.

Because caspase-9 is activated after its recruitment into the apoptosome, we analyzed the effects of IGF-I on cytochrome *c* release from mitochondria. Acute trophic factor withdrawal from CGNs induced a rapid redistribution of cytochrome *c* from mitochondria to focal complexes localized in neuronal processes. The precise nature of these complexes is currently under investigation, but it is possible that these cytochrome *c*-rich structures represent large aggregates of apoptosomes. This would allow for a localized activation of caspases in neuronal processes where many structural targets of these proteases exist (e.g., cytoskeletal proteins). We currently are attempting to colocalize Apaf-1 and caspase-9 by immunocytochemical methods to these cytochrome *c*-containing complexes. Regardless of their exact content, IGF-I essentially abolished the formation of these complexes and maintained cytochrome *c* in mitochondria. The effects of IGF-I on cytochrome *c* redistribution were prevented by wortmannin, consistent with a previously recognized role for PI3K/AKT in the inhibition of cytochrome *c* release (Kennedy et al., 1999). The above results suggest that IGF-I inhibits the activation of caspase-9 by preventing the release of cytochrome *c* and the subsequent formation of apoptosomes.

We next examined the role of the mitochondrial PTP in mediating the release of cytochrome *c* during CGN apoptosis. In trophic factor-deprived CGNs marked mitochondrial swelling and depolarization were observed, indicative of PTP opening. Although IGF-I has been shown to prevent mitochondrial depolarization in neuroblastoma cells exposed to hyperosmotic conditions (Van Golen and Feldman, 2000), we did not observe any

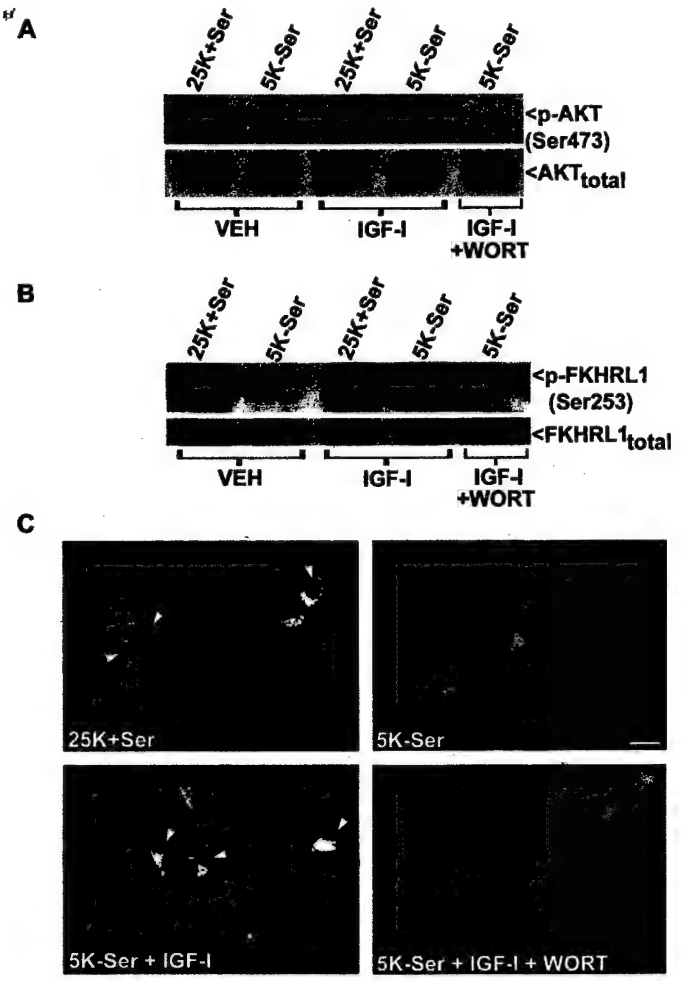

Figure 7. IGF-I sustains the phosphorylation of AKT and FKHRL1 and prevents the nuclear localization of FKHRL1 in CGNs deprived of trophic support. *A*, CGNs were incubated for 4 hr in either control (*25K+Ser*) or apoptotic (*5K-Ser*) medium containing either PBS vehicle (*VEH*) or IGF-I (200 ng/ml) ± wortmannin (*WORT*; 100 nM). After incubation the cell lysates were subjected to SDS-PAGE on 10% polyacrylamide gels, and the proteins were transferred to PVDF membranes. Membranes were probed with a phospho-specific antibody that detects *active* AKT that was phosphorylated on Ser^{473} (*p-AKT*). Then the blots were stripped and reprobed for total AKT to demonstrate equal loading. The blots shown are typical of results obtained in three separate experiments. *B*, CGNs were treated exactly as described in *A*, and the cell lysates were immunoblotted for *inactive* FKHRL1 that was phosphorylated on Ser^{253} (p-FKHRL1) by using a phospho-specific antibody. Then the membranes were stripped and reprobed for total FKHRL1 to verify equal loading. The blots shown are illustrative of three independent experiments. *C*, CGNs incubated as described in *A* were fixed and then incubated with a polyclonal antibody to FKHRL1, followed by a Cy3-conjugated secondary antibody. Fluorescent digitally deconvolved images were acquired by using a 63× oil objective. The *arrowheads* indicate nuclei that are relatively devoid of FKHRL1 immunoreactivity. The images shown are representative of three separate experiments. Scale bar, 10 μm.

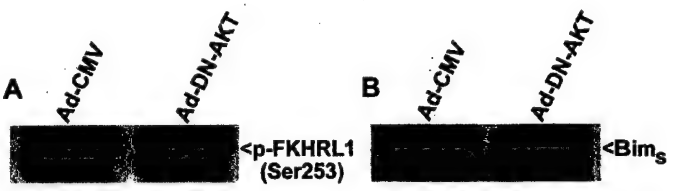

Figure 8. Adenoviral dominant-negative AKT induces dephosphorylation of FKHRL1 and increases Bim expression. On day 5 in culture the CGNs were infected with either a negative control adenovirus (*Ad-CMV*) or adenovirus expressing kinase-dead (dominant-negative) AKT (*Ad-DN-AKT*), each at a multiplicity of infection of 50. At 48 hr after infection the cell lysates were subjected to SDS-PAGE on either 7.5% (*p-FKHRL1*) or 15% (Bim_s) polyacrylamide gels, and the proteins were transferred to PVDF membranes. *A*, The membrane was probed with a phospho-specific antibody to *inactive* FKHRL1 phosphorylated on Ser^{253} (*p-FKHRL1*). *B*, The blot was probed with a polyclonal antibody that detects the short isoform of Bim (Bim_s).

effect of IGF-I on either mitochondrial swelling or depolarization in CGNs. Although IGF-I clearly blocked apoptosis in trophic factor-deprived CGNs, the observation that it failed to prevent mitochondrial swelling indicates that the neurons still have damaged mitochondria in the presence of IGF-I. This finding suggests that a slower nonapoptotic death process was unmasked in CGNs by blocking the more rapid apoptotic death with IGF-I. The characterization of a nonapoptotic death pathway in CGNs will require further investigation. Nonetheless, because IGF-I blocked cytochrome *c* release under conditions in which it failed to affect mitochondrial swelling or depolarization, we conclude that opening of the PTP is insufficient to promote cytochrome *c* release in trophic factor-deprived CGNs. These results are in agreement with those previously reported for hippocampal neurons exposed to staurosporine in which cytochrome *c* release and caspase-3 activation preceded mitochondrial depolarization (Krohn et al., 1999). Collectively, these results indicate that opening of the PTP may not be a principal mechanism for cytochrome *c* release in neurons.

The proapoptotic Bcl-2 family member Bax has been implicated in cytochrome *c* release and the apoptosis of CGNs *in vitro* and *in vivo* (Miller et al., 1997b; Desagher et al., 1999; Selimi et al., 2000b). The proapoptotic function of Bax is attenuated by anti-apoptotic members of the Bcl-2 family (Bcl-2, Bcl-X_L) that heterodimerize with Bax and sequester it away from mitochondria (Otter et al., 1998). Conversely, BH3-only Bcl-2 family members promote the proapoptotic effects of Bax by binding to Bcl-2, thus freeing Bax to incorporate into the mitochondrial membrane (Zong et al., 2001). In addition, BH3-only proteins also have been shown to interact with Bax and induce a conformational change that facilitates its incorporation into mitochondria (Desagher et al., 1999). These findings illustrate that BH3-only proteins serve several key functions in the Bax-dependent release of cytochrome *c* and initiation of the intrinsic death pathway.

The BH3-only protein Bim was shown recently to be induced both in sympathetic neurons subjected to NGF withdrawal and in trophic factor-deprived CGNs (Putcha et al., 2001; Whitfield et al., 2001). Sympathetic neuron apoptosis was attenuated by injection of Bim antisense oligonucleotides (Whitfield et al., 2001), and neurons from Bim knock-out mice were less sensitive to apoptosis than neurons from wild-type mice (Putcha et al., 2001). In addition, overexpression of Bim induced apoptosis in sympathetic neurons (Whitfield et al., 2001) and in CGNs in a Bax-dependent manner (Harris and Johnson, 2001). Multiple isoforms of Bim have been identified that apparently arise by alternative splicing (O'Connor et al., 1998). In the works cited above (Putcha et al., 2001; Whitfield et al., 2001), Bim_{EL} was induced during neuronal apoptosis, whereas we observed the induction of Bim_s in CGNs subjected to trophic factor withdrawal. These isoform-specific differences may be a result of the specific antibodies used to detect Bim. The polyclonal antibody used in

the current study detected primarily a single ~15 kDa protein in CGN lysates and in human embryonic kidney 293 cell lysates (data not shown), consistent with the apparent molecular weight of Bim_S. We observed an approximately threefold induction of Bim_S protein after acute trophic factor withdrawal that was prevented completely by inclusion of IGF-I in a PI3K-dependent manner. These results suggest that IGF-I suppresses the intrinsic death pathway upstream of Bim synthesis. Consistent with this conclusion, Harris and Johnson (2001) have shown recently that IGF-I was unable to rescue CGNs from apoptosis induced by overexpression of the BH3-only protein Dp5/Hrk. Thus our data are the first to identify the upregulation of Bim as a major target of IGF-I action in neurons undergoing apoptosis.

Bim expression is regulated by multiple transcription factors. In NGF-deprived sympathetic neurons dominant-negative c-Jun partially attenuated the induction of Bim mRNA and Bim_{EL} protein, inhibited cytochrome *c* release, and rescued sympathetic neurons from apoptosis (Whitfield et al., 2001). c-Jun also has been implicated in the apoptosis of CGNs (Watson et al., 1998), and an inhibitor of the JNK signaling pathway (CEP-1347) was shown recently to blunt partially the induction of Bim mRNA in CGNs subjected to trophic factor withdrawal (Harris and Johnson, 2001). In agreement with JNK/c-Jun involvement in the induction of Bim_S in CGNs undergoing apoptosis, the p38/JNK inhibitor SB203580 significantly attenuated both the activation of c-Jun and the increase in Bim_S expression. However, IGF-I failed to inhibit c-Jun activation under conditions in which it significantly blocked the induction of Bim_S. These results indicate that c-Jun plays a role in the regulation of Bim expression during CGN apoptosis, but IGF-I suppresses the induction of Bim via a mechanism that does not involve modulation of JNK/c-Jun signaling. This conclusion is in agreement with the work of Whitfield et al. (2001), who proposed that JNK/c-Jun signaling cooperates with a distinct JNK/c-Jun-independent pathway to stimulate the expression of Bim in sympathetic neurons deprived of NGF.

In this context the forkhead transcription factor FKHRL1 has been shown recently to regulate Bim expression in hematopoietic cells (Dijkers et al., 2000). Cytokine withdrawal from a pro-B cell line induced activation (dephosphorylation) of FKHRL1, induction of Bim, and apoptosis (Dijkers et al., 2000). Moreover, expression of a constitutively active mutant of FKHRL1, in which three putative AKT phosphorylation sites are mutated to alanine, induced Bim expression, cytochrome *c* release, and apoptosis in hematopoietic cells (Dijkers et al., 2002). Given that FKHRL1 has been shown to be a substrate for AKT in neurons (Zheng et al., 2000), the AKT-mediated inactivation of FKHRL1 may be one mechanism by which IGF-I inhibits apoptosis. Indeed, overexpression of a constitutively active FKHRL1 triple phosphorylation site mutant is sufficient to induce the apoptosis of CGNs (Brunet et al., 1999). In the present study we showed that trophic factor withdrawal from CGNs led to an inactivation of AKT, a corresponding activation of FKHRL1, and translocation of FKHRL1 to the nucleus. All of these effects, along with the induction of Bim, were prevented by IGF-I in a PI3K-dependent manner. In addition, adenoviral expression of a dominant-negative mutant of AKT was sufficient to activate FKHRL1 and induce Bim expression in CGNs maintained in the presence of serum and depolarizing potassium. Taken together, our data suggest that IGF-I attenuates the induction of Bim in trophic factor-deprived CGNs via a PI3K/AKT-mediated inactivation of the FKHRL1 transcription factor.

In summary, our results demonstrate that suppression of the intrinsic death signaling cascade is a principal mechanism underlying the neuroprotective effects of IGF-I. IGF-I blocks Bim induction, cytochrome *c* release, and activation of the intrinsic initiator caspase-9 and the executioner caspase-3 in CGNs deprived of trophic support. Moreover, IGF-I inhibits the actions of FKHRL1, a transcriptional regulator of Bim, suggesting a novel c-Jun-independent mechanism for the modulation of Bim in neurons.

REFERENCES

Bach MA, Shen-Orr Z, Lowe Jr WL, Roberts Jr CT, LeRoith D (1991) Insulin-like growth factor-I mRNA levels are developmentally regulated in specific regions of the rat brain. Brain Res Mol Brain Res 10:43–48.

Barber AJ, Nakamura M, Wolpert EB, Reiter CE, Seigel GM, Antonetti DA, Gardner TW (2001) Insulin rescues retinal neurons from apoptosis by a phosphatidylinositol 3-kinase/Akt-mediated mechanism that reduces the activation of caspase-3. J Biol Chem 276:32814–32821.

Bartlett WP, Li XS, Williams M, Benkovic S (1991) Localization of insulin-like growth factor-1 mRNA in murine central nervous system during postnatal development. Dev Biol 147:239–250.

Brunet A, Bonni A, Zigmond MJ, Lin MZ, Juo P, Hu LS, Anderson MJ, Arden KC, Blenis J, Greenberg ME (1999) Akt promotes cell survival by phosphorylating and inhibiting a Forkhead transcription factor. Cell 96:857–868.

Chrysis D, Calikoglu AS, Ye P, D'Ercole AJ (2001) Insulin-like growth factor-I overexpression attenuates cerebellar apoptosis by altering the expression of Bcl family proteins in a developmentally specific manner. J Neurosci 21:1481–1489.

Clarkson ED, Zawada WM, Bell KP, Esplen JE, Choi PK, Heidenreich KA, Freed CR (2001) IGF-I and bFGF improve dopamine neuron survival and behavioral outcome in parkinsonian rats receiving cultured human fetal tissue strands. Exp Neurol 168:183–191.

Coffey ET, Smiciene G, Hongisto V, Cao J, Brecht S, Herdegen T, Courtney MJ (2002) c-Jun N-terminal protein kinase (JNK) 2/3 is specifically activated by stress, mediating c-Jun activation, in the presence of constitutive JNK1 activity in cerebellar neurons. J Neurosci 22:4335–4345.

Desagher S, Osen-Sand A, Nichols A, Eskes R, Montessuit S, Lauper S, Maundrell K, Antonsson B, Martinou JC (1999) Bid-induced conformational change of Bax is responsible for mitochondrial cytochrome *c* release during apoptosis. J Cell Biol 144:891–901.

Dijkers PF, Medema RH, Lammers JW, Koenderman L, Coffer PJ (2000) Expression of the pro-apoptotic Bcl-2 family member Bim is regulated by the forkhead transcription factor FKHR-L1. Curr Biol 10:1201–1204.

Dijkers PF, Birkenkamp KU, Lam EW, Thomas NS, Lammers JW, Koenderman L, Coffer PJ (2002) FKHR-L1 can act as a critical effector of cell death induced by cytokine withdrawal: protein kinase B-enhanced cell survival through maintenance of mitochondrial integrity. J Cell Biol 156:531–542.

D'Mello SR, Galli C, Ciotti T, Calissano P (1993) Induction of apoptosis in cerebellar granule neurons by low potassium: inhibition of death by insulin-like growth factor-I and cAMP. Proc Natl Acad Sci USA 90:10989–10993.

Dudek H, Datta SR, Franke TF, Birnbaum MJ, Yao R, Cooper GM, Segal RA, Kaplan DR, Greenberg ME (1997) Regulation of neuronal survival by the serine-threonine protein kinase Akt. Science 275:661–665.

Eilers A, Whitfield J, Babij C, Rubin LL, Ham J (1998) Role of the Jun kinase pathway in the regulation of c-Jun expression and apoptosis in sympathetic neurons. J Neurosci 18:1713–1724.

Eldadah BA, Ren RF, Faden AI (2000) Ribozyme-mediated inhibition of caspase-3 protects cerebellar granule cells from apoptosis induced by serum-potassium deprivation. J Neurosci 20:179–186.

Fernandez AM, de la Vega AG, Torres-Aleman I (1998) Insulin-like growth factor-I restores motor coordination in a rat model of cerebellar ataxia. Proc Natl Acad Sci USA 95:1253–1258.

Galli C, Meucci O, Scorziello A, Werge TM, Calissano P, Schettini G (1995) Apoptosis in cerebellar granule cells is blocked by high KCl, forskolin, and IGF-1 through distinct mechanisms of action: the involvement of intracellular calcium and RNA synthesis. J Neurosci 15:1172–1179.

Garcia-Calvo M, Peterson EP, Leiting B, Ruel R, Nicholson DW, Thornberry NA (1998) Inhibition of human caspases by peptide-based and macromolecular inhibitors. J Biol Chem 273:32608–32613.

Gerhardt E, Kugler S, Leist M, Beier C, Berliocchi L, Volbracht C, Weller M, Bahr M, Nicotera P, Schulz JB (2001) Cascade of caspase activation in potassium-deprived cerebellar granule neurons: targets for treatment with peptide and protein inhibitors of apoptosis. Mol Cell Neurosci 17:717–731.

Green DR (1998) Apoptotic pathways: the roads to ruin. Cell 94:695–698.

Harada J, Sugimoto M (1999) An inhibitor of p38 and JNK MAP kinases prevents activation of caspase and apoptosis of cultured cerebellar granule neurons. Jpn J Pharmacol 79:369–378.

Harris CA, Johnson Jr EM (2001) BH3-only Bcl-2 family members are coordinately regulated by the JNK pathway and require Bax to induce apoptosis in neurons. J Biol Chem 276:37754–37760.

Heck S, Lezoualc'h F, Engert S, Behl C (1999) Insulin-like growth factor-1-mediated neuroprotection against oxidative stress is associated with activation of nuclear factor κB. J Biol Chem 274:9828–9835.

Kennedy SG, Kandel ES, Cross TK, Hay N (1999) Akt/protein kinase B inhibits cell death by preventing the release of cytochrome *c* from mitochondria. Mol Cell Biol 19:5800–5810.

Kermer P, Ankerhold R, Klocker N, Krajewski S, Reed JC, Bahr M (2000) Caspase-9: involvement in secondary death of axotomized rat retinal ganglion cells *in vivo*. Brain Res Mol Brain Res 85:144–150.

Korsmeyer SJ, Wei MC, Saito M, Weiler S, Oh KJ, Schlesinger PH (2000) Pro-apoptotic cascade activates BID, which oligomerizes BAK or BAX into pores that result in the release of cytochrome *c*. Cell Death Differ 7:1166–1173.

Krohn AJ, Wahlbrink T, Prehn JH (1999) Mitochondrial depolarization is not required for neuronal apoptosis. J Neurosci 19:7394–7404.

Kuida K, Haydar TF, Kuan CY, Gu Y, Taya C, Karasuyama H, Su MS, Rakic P, Flavell RA (1998) Reduced apoptosis and cytochrome *c*-mediated caspase activation in mice lacking caspase-9. Cell 94:325–337.

Lai EC, Felice KJ, Festoff BW, Gawel MJ, Gelinas DF, Kratz R, Murphy MF, Natter HM, Norris FH, Rudnicki SA (1997) Effect of recombinant human insulin-like growth factor-I on progression of ALS. A placebo-controlled study. The North America ALS/IGF-I study group. Neurology 49:1621–1630.

Li M, Wang X, Meintzer MK, Laessig T, Birnbaum MJ, Heidenreich KA (2000) Cyclic AMP promotes neuronal survival by phosphorylation of glycogen synthase kinase 3β. Mol Cell Biol 20:9356–9363.

Lin X, Bulleit RF (1997) Insulin-like growth factor-I (IGF-I) is a critical trophic factor for developing cerebellar granule cells. Brain Res Dev Brain Res 99:234–242.

Liu XF, Fawcett JR, Thorne RG, Frey II WH (2001) Non-invasive intranasal insulin-like growth factor-I reduces infarct volume and improves neurologic function in rats following middle cerebral artery occlusion. Neurosci Lett 308:91–94.

Martinou JC, Green DR (2001) Breaking the mitochondrial barrier. Nat Rev Mol Cell Biol 2:63–67.

Miller TM, Tansey MG, Johnson Jr EM, Creedon DJ (1997a) Inhibition of phosphatidylinositol 3-kinase activity blocks depolarization- and insulin-like growth factor-I-mediated survival of cerebellar granule cells. J Biol Chem 272:9847–9853.

Miller TM, Moulder KL, Knudson CM, Creedon DJ, Deshmukh M, Korsmeyer SJ, Johnson Jr EM (1997b) Bax deletion further orders the cell death pathway in cerebellar granule cells and suggests a caspase-independent pathway to cell death. J Cell Biol 139:205–217.

Minden A, Lin A, Smeal T, Derijard B, Cobb M, Davis R, Karin M (1994) c-Jun N-terminal phosphorylation correlates with activation of the JNK subgroup but not the ERK subgroup of mitogen-activated protein kinases. Mol Cell Biol 14:6683–6688.

Mustafa A, Lannfelt L, Lilius L, Islam A, Winblad B, Adem A (1999) Decreased plasma insulin-like growth factor-I level in familial Alzheimer's disease patients carrying the Swedish APP 670/671 mutation. Dement Geriatr Cogn Disord 10:446–451.

O'Connor L, Strasser A, O'Reilly LA, Hausmann G, Adams JM, Cory S, Huang DC (1998) Bim: a novel member of the Bcl-2 family that promotes apoptosis. EMBO J 17:384–395.

Otter I, Conus S, Ravn U, Rager M, Olivier R, Monney L, Fabbro D, Borner C (1998) The binding properties and biological activities of Bcl-2 and Bax in cells exposed to apoptotic stimuli. J Biol Chem 273:6110–6120.

Putcha GV, Moulder KL, Golden JP, Bouillet P, Adams JA, Strasser A, Johnson Jr EM (2001) Induction of Bim, a proapoptotic BH3-only Bcl-2 family member, is critical for neuronal apoptosis. Neuron 29:615–628.

Rotwein P, Burgess SK, Milbrandt JD, Krause JE (1988) Differential expression of insulin-like growth factor genes in rat central nervous system. Proc Natl Acad Sci USA 85:265–269.

Russell JW, Windebank AJ, Schenone A, Feldman EL (1998) Insulin-like growth factor-I prevents apoptosis in neurons after nerve growth factor withdrawal. J Neurobiol 36:455–467.

Selimi F, Doughty M, Delhaye-Bouchaud N, Mariani J (2000a) Target-related and intrinsic neuronal death in *lurcher* mutant mice are both mediated by caspase-3 activation. J Neurosci 20:992–1000.

Selimi F, Vogel MW, Mariani J (2000b) Bax inactivation in *lurcher* mutants rescues cerebellar granule cells but not Purkinje cells or inferior olivary neurons. J Neurosci 20:5339–5345.

Tagami M, Yamagata K, Nara Y, Fujino H, Kubota A, Numano F, Yamori Y (1997) Insulin-like growth factors prevent apoptosis in cortical neurons isolated from stroke-prone spontaneously hypertensive rats. Lab Invest 76:603–612.

Torres-Aleman I, Barrios V, Lledo A, Berciano J (1996) The insulin-like growth factor-I system in cerebellar degeneration. Ann Neurol 39:335–342.

Van Golen CM, Feldman EL (2000) Insulin-like growth factor-I is the key growth factor in serum that protects neuroblastoma cells from hyperosmotic-induced apoptosis. J Cell Physiol 182:24–32.

Watson A, Eilers A, Lallemand D, Kyriakis J, Rubin LL, Ham J (1998) Phosphorylation of c-Jun is necessary for apoptosis induced by survival signal withdrawal in cerebellar granule neurons. J Neurosci 18:751–762.

Wei MC, Zong WX, Cheng EH, Lindsten T, Panoutsakopoulou V, Ross AJ, Roth KA, MacGregor GR, Thompson CB, Korsmeyer SJ (2001) Proapoptotic BAX and BAK: a requisite gateway to mitochondrial dysfunction and death. Science 292:727–730.

White RJ, Reynolds IJ (1996) Mitochondrial depolarization in glutamate-stimulated neurons: an early signal specific to excitotoxin exposure. J Neurosci 16:5688–5697.

Whitfield J, Neame SJ, Paquet L, Bernard O, Ham J (2001) Dominant-negative c-Jun promotes neuronal survival by reducing Bim expression and inhibiting mitochondrial cytochrome *c* release. Neuron 29:629–643.

Ye P, Xing Y, Dai Z, D'Ercole AJ (1996) *In vivo* actions of insulin-like growth factor-I (IGF-I) on cerebellum development in transgenic mice: evidence that IGF-I increases proliferation of granule cell progenitors. Brain Res Dev Brain Res 95:44–54.

Zhang W, Ghetti B, Lee WH (1997) Decreased IGF-I gene expression during the apoptosis of Purkinje cells in *pcd* mice. Brain Res Dev Brain Res 98:164–176.

Zheng WH, Kar S, Quirion R (2000) Insulin-like growth factor-1-induced phosphorylation of the forkhead family transcription factor FKHRL1 is mediated by Akt kinase in PC12 cells. J Biol Chem 275:39152–39158.

Zong WX, Lindsten T, Ross AJ, MacGregor GR, Thompson CB (2001) BH3-only proteins that bind pro-survival Bcl-2 family members fail to induce apoptosis in the absence of Bax and Bak. Genes Dev 15:1481–1486.

Zou H, Li Y, Liu X, Wang X (1999) An APAF-1·cytochrome *c* multimeric complex is a functional apoptosome that activates procaspase-9. J Biol Chem 274:11549–11556.

Abstract View

NEUROTROPHINS AND DEATH RECEPTORS REGULATE AUTOPHAGIC DEATH IN CEREBELLAR PURKINJE NEURONS

M.L. Florez-McClure[1*]; D.A. Linseman[1,2]; C.T. Chu[3]; R.J. Bouchard[2]; T.A. Laessig[2]; S.S. Le[2]; K.A. Heidenreich[1,2]

1. Pharmacology, Univ Colorado Hlth Sci Ctr, Denver, CO, USA2. Denver VAMC, Denver, CO, USA
3. Neuropathology, Univ Pitt Sch Med, Pittsburgh, PA, USA

Cerebellar neuronal cultures obtained from early postnatal rats are recognized as an *in vitro* model system to investigate the regulation of neuronal survival and death. Granule neurons make up approximately 95% of the cerebellar cell cultures and undergo a classical apoptotic mode of cell death following the removal of serum and depolarizing potassium. In contrast, Purkinje neurons, which make up 3% of the cerebellar culture, undergo a non-apoptotic, autophagic death following serum withdrawal. The Purkinje cell death is characterized morphologically by extensive cytoplasmic vacuolation and by a notable lack of nuclear condensation. The vacuoles that form are positively stained with the acidic pH-sensitive dye, lysosensor blue, and monodansylcadaverine, a marker of autophagic vacuoles. Transmission electron microscopy confirmed that these vacuoles were autophagic in nature. In this model, exogenous nerve growth factor (NGF) inhibited the vacuolation and death of Purkinje neurons induced by serum withdrawal. Conversely, addition of NGF-neutralizing antibodies induced the vacuolation and death of Purkinje neurons. Finally, the autophagic death of Purkinje neurons induced by either serum withdrawal or NGF-neutralizing antibodies was significantly inhibited by adenoviral expression of a dominant-negative Fas-associated death domain (FADD) protein. These data suggest a model in which neurotrophin and death receptor signaling pathways converge to regulate the autophagic death of Purkinje neurons. The potential roles of high vs. low affinity NGF receptors, TrkA and p75ntr, respectively, in modulating Purkinje neuron survival are currently being investigated.

Support Contributed By: VA Merit and REAP Awards (KAH and DAL); NIH Grant NS38619-01A1 (KAH); DOD Grant AIBS#980281 (KAH); NRSA Fellowship NS045560-01 (MLM)

Close

8th International Conference on Neural Transplantation and Repair, Keystone, CO (2002)

EXTRINSIC AND INTRINSIC DEATH SIGNALING IN CEREBELLAR NEURONAL APOPTOSIS: THE IGF-I CONNECTION

Linseman DA, McClure ML, Phelps RA, Bouchard RJ, Laessig TA, Le SS, Ahmadi F, Heidenreich KA
University of Colorado Health Sciences Center, Department of Pharmacology, 4200 East Ninth Avenue, Denver CO 80262 and Denver Veterans Affairs Medical Center

Primary cerebellar granule neurons die by apoptosis when deprived of serum and depolarizing potassium. Here, we investigated the role of extrinsic (death receptor-mediated) and intrinsic (mitochondrial-dependent) death signals in cerebellar neuron apoptosis. Expression of adenoviral, epitope-tagged, dominant-negative Fas-associated death domain protein (ΔFADD) decreased granule neuron apoptosis by approximately 75%. Immunocytochemical staining for the epitope tag revealed that <5% of granule neurons expressed ΔFADD. In contrast, ΔFADD expression was observed in >95% of Purkinje neurons. Purkinje neurons were calbindin-positive and made up ~2% of the cerebellar neuron culture. Granule neuron survival was dependent on proximity to ΔFADD-expressing Purkinje neurons and was inhibited by an insulin-like growth factor-I (IGF-I) receptor blocking antibody. Utilizing exogenous IGF-I, we identified the intrinsic death pathway as a principal target of IGF-I action in granule neurons. IGF-I blocked activation of both the executioner caspase-3 and the intrinsic initiator caspase-9. Upstream of caspase-9, IGF-I inhibited release of cytochrome C from mitochondria and prevented its redistribution to focal complexes localized in neuronal processes. Finally, IGF-I blocked nuclear translocation of the forkhead transcription factor, FKHRL1, and attenuated induction of its transcriptional target, the BH3-only Bcl-2 family member Bim. The results indicate that blockade of extrinsic death signaling in Purkinje neurons rescues neighboring granule neurons by sustaining the secretion of Purkinje-derived IGF-I. In turn, IGF-I exerts its neuroprotective effect in granule neurons by suppressing the intrinsic death cascade. Thus, IGF-I acts as a key intercellular mediator between cerebellar Purkinje neurons and granule neurons to promote neuron survival. *Supported by a United States Army Medical Research Grant DAMD17-99-1-9481 (K.A.H.), a Veterans Affairs Merit Award (K.A.H.), and a Veterans Affairs Research Enhancement Award Program (K.A.H. and D.A.L.).*

Society for Neuroscience 2003

BAX TRANSLOCATION TO MITOCHONDRIA IS TRIGGERED BY PERMEABILITY TRANSITION PORE OPENING IN CEREBELLAR GRANULE NEURONS UNDERGOING APOPTOSIS

T.A. Precht[1]; R.A. Phelps[1]; D.A. Linseman[1,2]; B.D. Butts[1]; R.J. Bouchard[2]; S.S. Le[2]; T.A. Laessig[2]; K.A. Heidenreich[1,2]

1. Pharmacology, Univ Col Hlth Sci Ctr, Denver, CO, USA

2. Denver VAMC, Denver, CO, USA

Cerebellar granule neurons (CGNs) require depolarization for their survival. When deprived of this stimulus, CGNs die via a mitochondrial apoptotic cascade involving Bim induction, cytochrome C release, and caspase-9 and -3 activation (Linseman et al., J Neurosci 2002, 22: 9287-97). Opening of the mitochondrial permeability transition pore (mPTP), characterized by mitochondrial depolarization and swelling, is an early event in apoptosis. However, the precise role of mPTP opening is presently unclear. Here, we show that an inhibitor of mPTP opening, cyclosporin A (CyA), blocks cytochrome C release from mitochondria in CGNs deprived of depolarizing K+. While CyA had no effect on Bim induction, it prevented the cytosol-to-mitochondrial translocation of a GFP-Bax fusion protein expressed in CGNs. These data suggested that mPTP opening acts as an initiating event to stimulate Bax translocation to mitochondria. To determine if this is the principal function of mPTP opening during CGN apoptosis, we constructed a GFP-Bax point mutant (T182A) that constitutively localizes to mitochondria and induces apoptosis in transfected HEK cells. Expression of this Bax mutant in CGNs resulted in cytochrome C release and caspase-9 and -3 activation that occurred in the absence of mPTP opening. Moreover, CGN apoptosis induced by the Bax (T182A) mutant was insensitive to inhibition by CyA. These results demonstrate that constitutive localization of Bax to mitochondria circumvents the requirement for mPTP opening and is sufficient to induce apoptosis. Collectively, these data indicate that the major role of mPTP opening in CGN apoptosis is to trigger Bax translocation to mitochondria, ultimately leading to cytochrome C release and caspase activation.

Support Contributed By: VA Merit and REAP Awards (KAH and DAL); NIH and DOD Grants (KAH)

Society for Neuroscience 2003

INHIBITION OF RAC GTPASE INDUCES BIM AND ACTIVATES A MITOCHONDRIAL APOPTOTIC CASCADE IN CEREBELLAR GRANULE NEURONS

S.S. Le[2]; R.J. Bouchard[2*]; T.A. Laessig[2]; B.D. Butts[1]; R.A. Phelps[2]; K.A. Heidenreich[1,2]; D.A. Linseman[1,2]

1. Pharmacology, Univ Col Hlth Sci Ctr, Denver, CO, USA2. Denver VAMC, Denver, CO, USA

Cerebellar granule neurons (CGNs) require depolarization and serum for their survival and undergo a mitochondrial apoptotic death when deprived of this trophic support (J Neurosci 2002, 22: 9287-97). In addition to synaptic activity and growth factors, neuronal survival also depends on signaling from cell-matrix contacts. Rho family GTPases are key transducers of extracellular matrix survival signals. We recently showed that CGN survival is compromised by inactivation of Rac/Cdc42 GTPases (J Biol Chem 2001, 276: 39123-31). Here, we investigate the death pathway activated in CGNs by inhibition of Rac using either C. difficile toxin B (a specific inhibitor of Rho, Rac, and Cdc42) or an adenoviral dominant-negative Rac mutant (from H. Udo and E. Kandel, Columbia University, NY). Inhibition of Rac in CGNs cultured in the presence of serum and depolarization induced cytochrome C release from mitochondria and activation of the initiator caspase-9 and the executioner caspase-3. Rac inhibition also led to phosphorylation of c-Jun, induction of the BH3-only protein Bim, and translocation of Bax to mitochondria. An inhibitor of JNK (SB203580) blocked c-Jun phosphorylation and attenuated Bim induction, cytochrome C release, and caspase activation induced by loss of Rac function. The mitochondrial apoptotic cascade activated by Rac inhibition is indistinguishable from that induced after trophic factor deprivation, indicating that loss of distinct pro-survival signals promotes execution of a common death pathway in CGNs. Moreover, these data are the first to implicate Rho family GTPases in the regulation of Bim and Bax. Identification of the Rac-dependent signals that modulate these pro-apoptotic Bcl-2 family members is key to understanding how Rac influences CGN survival.

Support Contributed By: VA Merit and REAP Awards (DAL and KAH); NIH and DOD Grants (KAH)

Society for Neuroscience 2003

GLYCOGEN SYNTHASE KINASE-3β PROMOTES BAX TRANSLOCATION TO MITOCHONDRIA DURING APOPTOSIS OF CEREBELLAR GRANULE NEURONS

B.D. Butts[1]; D.A. Linseman[1,2]; T.A. Precht[1]; R.A. Phelps[2]; T.A. Laessig[2]; R.J. Bouchard[2]; S.S. Le[2]; K.L. Tyler[2*]; K.A. Heidenreich[1,2]

1. Pharmacology, Univ Col Hlth Sci Ctr, Denver, CO, USA2. Denver VAMC, Denver, CO, USA

Cerebellar granule neurons (CGNs) deprived of depolarizing extracellular K+ and serum die via an intrinsic apoptotic pathway involving Bax-dependent release of cytochrome C from mitochondria and subsequent caspase activation. Translocation of Bax from the cytosol to mitochondria is an early event in CGN apoptosis, but the mechanisms regulating this process are unclear. Here we show that upon induction of apoptosis in CGNs, a transiently expressed GFP-Bax_{alpha} fusion protein undergoes translocation to mitochondria coincident with activation of glycogen synthase kinase-3β (GSK-3β), a Ser/Thr kinase that plays a pro-apoptotic role in CGNs. Both peptide (insulin-like growth factor-I) and non-peptide, small molecule (substituted oxothiadiazolidinones) inhibitors of GSK-3β attenuated GFP-Bax_{alpha} translocation to mitochondria in trophic factor-deprived CGNs. In a separate set of experiments, transient co-transfection of HEK cells with GFP-Bax_{alpha} and a constitutively-active mutant of GSK-3β (Ser9Ala) enhanced GFP-Bax_{alpha} localization to mitochondria. Examination of the Bax_{alpha} amino acid sequence revealed a putative GSK-3β consensus phosphorylation site, S*XXXT, at Ser163 that is highly conserved in multiple species including rat, mouse, bovine, and human. Mutation of Ser163 to Ala in GFP-Bax_{alpha} impaired its localization to mitochondria in HEK cells even when co-transfected with active GSK-3β. Similarly, a naturally occurring splice variant, Bax_{sigma}, which lacks a 13 amino acid region including the putative GSK-3β consensus site, also failed to localize to mitochondria when co-transfected with active GSK-3β into HEK cells. These data reveal a novel role for GSK-3β in regulating Bax translocation to mitochondria during neuronal apoptosis.
Support Contributed By: VA Merit and REAP Awards (KAH and DAL); NIH and DOD Grants (KAH)

Society for Neuroscience 2003

CAMKII PROMOTES CEREBELLAR GRANULE NEURON SURVIVAL BY BLOCKING HDAC REPRESSION OF MEF2 TRANSCRIPTIONAL ACTIVITY

D.A. Linseman[1,2]; C.M. Bartley[1]; S.S. Le[2]; T.A. Laessig[2]; R.J. Bouchard[2]; K.A. Heidenreich[1,2]

1. Pharmacology, Univ Col Hlth Sci Ctr, Denver, CO, USA

2. Denver VAMC, Denver, CO, USA

Cerebellar granule neuron (CGN) survival depends on activity of the myocyte enhancer factor-2 (MEF2) transcription factors that are regulated by depolarization. The mechanism by which Ca2+ influx regulates MEF2 activity in CGNs is presently unclear. Here, we show that depolarization-mediated MEF2 activity and CGN survival are compromised by overexpression of the MEF2 repressor histone deacetylase-5 (HDAC5). Furthermore, induction of CGN apoptosis by removal of depolarizing K+ induced rapid cytoplasm-to-nuclear translocation of endogenous HDAC5. This effect was mimicked by addition of the calcium/calmodulin-dependent kinase (CaMK) inhibitor KN93 to depolarizing medium. Removal of depolarizing K+ or KN93 addition increased the electrophoretic mobility of HDAC5, consistent with its dephosphorylation. Moreover, HDAC5 co-precipitated with MEF2D under these conditions. The nuclear translocation of HDAC5 induced by KN93 caused a marked loss of MEF2 transcriptional activity. MEF2 inactivation was followed by caspase-3 activation, microtubule disruption, and chromatin fragmentation. To selectively decrease CaMKII activity, CGNs were incubated with a FITC-labeled antisense oligonucleotide to CaMKIIα. This antisense decreased CaMKIIα protein expression and induced nuclear shuttling of HDAC5 in CGNs maintained in depolarizing medium. Selectivity of the CaMKIIα antisense was demonstrated by its lack of effect on CaMKIV-mediated CREB phosphorylation. Finally, antisense to CaMKIIα induced caspase-3 activation and apoptosis, whereas a missense control oligo had no effect on CGN survival. These results indicate that depolarization-mediated Ca2+ influx acts through CaMKII to inhibit the MEF2 repressor HDAC5, thereby sustaining high MEF2 activity in CGNs maintained under depolarizing conditions.

Support Contributed By: VA Merit and REAP Awards (KAH and DAL); NIH and DOD Grants (KAH)